# PLAQUE EROSION AND MURINE PLAQUE STABILITY: A BIOMECHANICAL EXAMINATION OF EXCEPTIONS TO THE PHENOMENON OF PLAQUE RUPTURE

A Dissertation
Presented to
The Academic Faculty

by

Ian Christopher Campbell

In Partial Fulfillment
of the Requirements for the Degree
Doctor of Philosophy in the
Wallace H. Coulter Department of Biomedical Engineering

Georgia Institute of Technology
May 2013

**PLAQUE EROSION AND MURINE PLAQUE STABILITY: A BIOMECHANICAL EXAMINATION OF EXCEPTIONS TO THE PHENOMENON OF PLAQUE RUPTURE**

Approved by:

John N. Oshinski, Co-Advisor
Department of Medicine
*Emory University*

W. Robert Taylor, Co-Advisor
Department of Medicine
*Emory University*

Don P. Giddens
Wallace H. Coulter Department of Biomedical Engineering
*Georgia Institute of Technology and Emory University*

Alessandro Veneziani
Department of Mathematics and Computer Science
*Emory University*

Renu Virmani
CVPath Institute, Inc.
*Gaithersburg, MD*

Raymond P. Vito
George W. Woodruff School of Mechanical Engineering
*Georgia Institute of Technology*

Date Approved: December 17, 2012

*Dedicated to Cindy*

# ACKNOWLEDGEMENTS

This dissertation was completed thanks to the generosity, support, kindness, and advice of a multitude of people. I cannot properly thank them enough for their help or for being part of my life. A few people deserve special recognition:

First and foremost, I would like to thank Cindy for all her patience and support, particularly in the final months of grad school. Her ability to make me laugh and help me relax after long days in lab was my favorite escape. Without Cindy, most of my meals these past few months would have come from packages wrapped in cellophane or advertising a prize inside. She helped me eat real food, have a happy home, and stay positive.

Next, I would like to thank my co-advisors, Bob Taylor and John Oshinski. I couldn't have asked for a better advisor in either individual, but I hit the jackpot when I got both. Bob and John are by no means the same, but they are both fantastically brilliant people who genuinely care about the well-being and intellectual advancement of their trainees. I felt like more a member of their families than like an employee, and I can only hope that someday I'm even half as good an advisor as they were. Their perspectives on how to tackle my research challenges differed at times, but together their solutions led to an excellent final product. They were incredibly patient with me, and neither even flinched when I asked to take a summer off of grad school to dabble in science writing.

I was very fortunate to be a member of two labs, not only because I got twice as many free lunches, but also because I had double the labmates. The Oshinski and Taylor labs are full of some of the smartest, most fun, and interesting people I've ever been lucky enough to spend time with. I need to thank every single member of these labs, past and present, for their advice and moral support during my dissertation research. A few individuals in particular made direct contributions to this work. Jonathan was instrumental in developing many of my image processing and data analysis techniques. No matter what kind of puzzle I was trying to solve, he could find an algorithm to fit the bill and then write code that was orders of magnitude faster than my own implementation. Luke also provided considerable wisdom when formulating my computational modeling approaches and was

generous enough to share his codes with me. Daiana taught me everything I could ever hope to know about mice and was extraordinarily patient during my project. Not only did she precisely harvest dozens upon dozens of mouse aortas, she also helped me pressure-fix human coronary arteries for hours at 2 in the morning when she could have been home sleeping. Giji helped me with my histology numerous times and was always willing to make time in her schedule to stain something for me or help me troubleshoot a protocol.

To each of the members of my thesis committe, I am forever thankful that they were willing to take time out of their busy schedules to advise me on my research. In addition to providing expertise during my thesis updates, each was willing to meet with me individually. Dr. Giddens always had great advice about how to approach my CFD models and whether my approaches were appropriate. Dr. Veneziani was always willing to sit down with me and discuss numerical methods and finite element approaches. My simulations probably would have taken 10 extra years without his advice. Dr. Virmani provided me with almost all the human data for my study and was extraordinarily generous to host me at the CVPath Institute on multiple occasions. I learned more about the pathology of atherosclerosis by sitting down at a microscope with her for 10 minutes than from reading a dozen papers. Dr. Vito was also extremely willing to sit down with me to break down modeling assumptions and help me improve my approach. I cannot thank each of you enough.

My thesis committee members provided me with more than just their own wisdom. Their lab members were also incredibly patient and helpful to me, and I would like to thank many of them. Dan Karolyi in Dr. Giddens' lab taught me how to use Fluent and got me started with CFD. Tiziano Passerini and Marina Piccinelli in Dr. Veneziani's lab both gave me so much great advice and computational support with my data processing approaches. At the CVPath Institute, Frank Kolodgie helped me interpret histological slides. Lila Adams and Heddie Avallone were both profoundly patient, teaching me sectioning and immunohistochemistry during a marathon 2-week visit to CVPath.

Others who weren't directly involved in my labs or in my thesis committee's labs were also critical players in helping me with my dissertation. Steven Marzec provided the highest-quality computer support I've ever come across. He was always willing to help me with even the slightest technical speed bump without breaking a smile. Lu Hilenski was instrumental in all of my confocal microscopy acquisition and provided fantastic advice to boot. Brad Kairdolf and Mike Mancini both

sacrificed huge amounts of their time helping me optimize solvents and characterize hydroxyapatite microparticles. Angela Lin helped me acquire all of my MicroCT data and interpret it. Hong Yi performed all of my electron microscopy. Luca Antiga at Orobix taught a fantastic course on VMTK software and was very generous to host me for a day to help improve my CFD post-processing approach. Aloke Finn, Michael McDaniel, Habib Samady, and S. Tanveer Rab, all interventional cardiologists, provided fantastic advice when formulating my hemodynamics of erosion project and were instrumental in acquiring all of my patient data.

When teaching during graduate school, I had two excellent mentors. Essy Behravesh at Georgia Tech and Doug Falls at Emory. Both provided great advice and support when navigating the new world of lecturing and grading. My teaching skills are much stronger today because of their support.

I was extremely fortunate to take a small hiatus during grad school thanks to the AAAS Mass Media Fellowship. All of the staff at AAAS and my sponsoring organization, IEEE-USA, were incredibly supportive. At The Oregonian, the daily newspaper where I worked for a summer, all of the journalists and editors were so patient with me despite having no prior newsroom experience. I would like to particularly thank Joany Carlin, Scott Learn, and Joe Rojas-Burke for all of their mentoring, support, and encouragement.

I would also like to thank my sponsoring organizations. I received an American Heart Association predoctoral fellowship and a National Science Foundation Graduate Research Fellowship during my time as a grad student, and none of this work would have been possible without their financial support.

Last, but certainly not least, I would like to thank all of my friends, roommates, and family for supporting me throughout my thesis work. I couldn't begin to name them all individually, but opportunities to chat and laugh over a beer were essential to get myself through this work.

Research is never done in a box (metaphorically speaking, of course. Most of this dissertation work was literally completed inside of a cubicle). Without help from everybody mentioned here, I could never have finished this project. I am eternally grateful for all of your support.

# TABLE OF CONTENTS

# LIST OF TABLES

# LIST OF FIGURES

## LIST OF SYMBOLS OR ABBREVIATIONS

| | |
|---|---|
| **AHA** | American Heart Association. |
| **AngII** | Angiotensin II. |
| **ANOVA** | Analysis of Variance. |
| **ApoE** | Apolipoprotein E. |
| **CFD** | Computational Fluid Dynamics. |
| **CRP** | C-reactive Protein. |
| **CT** | Computed Tomography. |
| **DOCA** | Deoxycorticosterone Acetate. |
| **EDTA** | Ethylenediaminetetraacetic Acid. |
| **EEL** | External Elastic Lamina. |
| **FEA** | Finite Element Analysis. |
| **FSI** | Fluid-Structure Interaction. |
| **FVA** | Finite Volume Analysis. |
| **GPCR** | G-Protein Coupled Receptor. |
| **H&E** | Hematoxylin and Eosin. |
| **HF** | High-Fat. |
| **IACUC** | Institutional Animal Care and Use Committee. |
| **IEL** | Internal Elastic Lamina. |
| **IHC** | Immunohistochemistry. |
| **IVUS** | Intra-Vascular Ultrasound. |
| **LAD** | Left Anterior Descending. |
| **LCx** | Left Circumflex. |
| **LDL** | Low Density Lipoprotein. |
| **LDLr** | Low Density Lipoprotein Receptor. |
| **MMA** | Methyl Methacrylate. |
| **MMP** | Matrix Metalloproteinase. |
| **MRA** | Magnetic Resonance Angiography. |

| | |
|---|---|
| **MRI** | Magnetic Resonance Imaging. |
| **NADPH** | Nicotinamide Adenine Dinucleotide Phosphate. |
| **NF-$\kappa$B** | Nuclear Factor-Kappa B. |
| **OCT** | Optical Coherence Tomography. |
| **OSI** | Oscillatory Shear Index. |
| **PCMR** | Phase-Contrast Magnetic Resonance. |
| **RCA** | Right Coronary Artery. |
| **RNA** | Ribonucleic Acid. |
| **SEM** | Standard Error of the Mean. |
| **SMA** | Smooth Muscle Actin. |
| $\tau$ | Wall Shear Stress. |
| **TCFA** | Thin-Cap Fibroatheroma. |
| **ThCFA** | Thick-Cap Fibroatheroma. |
| **TIMP** | Tissue Inhibitor of Metalloproteinase. |
| **TKR** | Tyrosine Kinase Receptor. |
| **TOF** | Time of Flight. |
| **TUNEL** | Terminal Deoxynucleotidyl Transferase dUTP Nick End Labeling. |
| **VH** | Virtual Histology. |
| **WSS** | Wall Shear Stress. |
| **XO** | Xanthine Oxidase. |

# SUMMARY

Atherosclerotic plaque disruption leading to thrombosis has traditionally been studied as a rupture of a thin fibrous cap over a lipid-laden necrotic core. However, two noteworthy categories of plaques that do not rupture have presented themselves: 1) in mice, plaque rupture is rare if not absent, and 2) in humans, some plaques erode and form a thrombus without rupturing. Current understanding of the biomechanical differences between plaques that rupture and those that do not is incomplete. In this research, we used patient-specific computational biomechanics tools to study differences among these groups.

Lesion-specific solid mechanical modeling of murine plaques revealed that the relative distribution of stresses differs considerably between mice and man. In human vulnerable plaques, peak stresses are on the thin fibrous cap over a necrotic core, but in mice the highest stresses are in the media and adventitia, away from the plaque. Whereas atherosclerotic human arteries usually experience neointima formation around the entire circumference of the vessel, mouse plaques tend to be punctate and adjacent lesion-free regions. The difference in mechanical environment suggests that plaque rupture, if possible in mice, is likely not driven by mechanics in the same manner as humans.

Similar mechanical modeling of human ruptured and eroded plaques and comparison to histological staining revealed that ruptured plaques exhibit increased levels of inflammatory markers in response to strain in ruptured plaques, but no such response was observed in plaque erosion. This suggests that treatment of inflammation, a current paradigm for care of atherosclerotic patients, may not be an effective approach to mediate plaque erosion. Computational fluid dynamics modeling of patients with plaque erosion revealed no relation between wall shear stress magnitude or direction, further suggesting that the mechanism of plaque erosion differs considerably from that of plaque rupture. Together, these findings suggest that biomechanics can help explain why not all plaques rupture and that different clinical approaches are necessary to address different phenotypes of lesions.

# CHAPTER I

# INTRODUCTION AND BACKGROUND

## *1.1 Introduction*

Heart disease and its associated comorbidities are the leading killer in the modern world. Today, almost twice as many women die of heart disease than from all kinds of cancer combined [1]. Atherosclerosis is no modern phenomenon: analysis of Egyptian mummies from thousands of years ago when diet and exercise patterns differed considerably from modern routines reveals evidence of advanced lesions [2]. The disease is essentially unavoidable: early-stage lesions can be found in many individuals starting as early as infancy [3]. When a plaque progresses to an advanced stage, it could cause a blood clot called a thrombus to form and occlude blood flow. Despite decades of research into cardiovascular disease, we still cannot accurately predict when a heart attack or stroke will occur, and patients who have had events are at high risk for recurrence [4]. There is ongoing need for a better understanding of how plaques progress to form a thrombus and predict events before they occur in diseased individuals.

Among the most common techniques to study this disease are the atherosclerosis-prone mouse models. These animals rapidly and reliably form atherosclerotic plaques under specific conditions, although rodents are naturally resistant to vascular disease. Despite their prevalence in the atherosclerosis literature for studying processes of atherogenesis and atherosclerotic burden, no rodent model has been shown conclusively to reproduce spontaneous plaque rupture, the process that causes heart attack or stroke. Existing reports of spontaneous rupture are controversial [5–7], and without confirmed reports of this event, the models may not be ideal for studying endpoints of atheroscelerosis.

## *1.2 Layers of arteries*

Arteries are made of three layers: the intima, media, and adventitia. In healthy individuals, the intima is a monolayer of endothelial cells lining the lumen of the blood vessel [8]. Endothelial cells present an anti-thrombogenic surface to the blood pool such that blood can flow and transport

nutrients without clotting under normal circumstances [9]. In atherosclerosis, a "neointima" layer expands below the endothelial monolayer [10]. Outside the intima is the media, a ring of smooth muscle cells that gives blood vessels most of their compliance, as well as the ability to dilate or contract. Outside the media is the adventitia, a ring of fibrous tissue, mostly collagen, that gives the vessel support and a surface by which to tether onto neighboring tissue. The adventitia is a the location where some inflammation is initiated and the source of approximately half the cells comprising the neointima [11]. Between each of the three layers in humans is an elastic lamina, a fenestrated tube of elastin that further adds to the vessel's compliance and separates the different tissue layers [12]. In other animals such as rodents, multiple elastic laminae are present inside the media, although the exact reason for this is not well understood.

## *1.3 Progression of Atherosclerosis*

Atherosclerosis is a complex pathology, with multiple risk factors and several stages of progression. All blood vessels become more fibrous with age, a process called arteriosclerosis [10], but atherosclerosis is a specific process of lesion formation that occurs preferentially in specific sites: mostly the coronary arteries, inner curvature of the aortic arch, carotid bifurcation, and around the renal arteries in the descending aorta [13]. Two classification schemes dominate existing literature: the American Heart Association (AHA) and widely accepted Virmani schemes [3, 14, 15]. The former was developed by a council of researchers in 1994 and contains 6 stages. The latter is a revised scheme based on more modern histological findings. Both are useful for understanding the disease.

### 1.3.1 The American Heart Association classification scheme

The American Heart Association classification describes a range of developmental steps from the initiation of lesions to development to advanced stages [3, 14]. At Stage I, lesions are initiated. The mechanism for this is not precisely known, but it is thought to involve endothelial injury, cholesterol accumulation in the matrix of vessel walls, or adventitial inflammation [11]. Immune cells called monocytes enter the region and differentiate into macrophages. Some engulf plasma-derived oxidized LDL in the wall and become engorged with lipid droplets [16]. These cells, called foam cells, are clustered within a distinct region. AHA Type I lesions occur mostly in infants and very young

children, though they can be found in some adults in regions not typically predisposed to lesion formation.

The next stage of atherosclerosis is production of fatty streaks, classified AHA Type II, also known as xanthomas (defined as "focal accumulations of fat-laden macrophages") [15]. Foam cells form larger clusters than in stage I, and smooth muscle cells here also contain lipid droplets. The AHA subclassifies these into progression-prone (Type IIa) and progression-resistant (Type IIb) lesions. The two subclasses are morphologically different: progression-prone lesions contain more smooth muscle and foam cells. Type IIb lesions are not considered likely to advance, although fluid dynamics are the greatest determinant of lesion progression (see section 1.8). Type II lesions typically emerge around puberty in humans.

In AHA Type III lesions, there is pronounced pathological intimal thickening. These are also called intermediate lesions or "preatheromas". Here, the lipid droplets in smooth muscle cells have progressed to form pools of extracellular lipid, substituting the extracellular matrix that normally holds these cells together. The lipid pools are not yet organized into the large, confluent lipid core, but have more lipid than Type II lesions. Additionally, free cholesterol is present. Type III lesions are typically found in young adults. They may progress to Type IV.

At Type IV, also known as an "atheromatous plaque", lipid pools merge to form a large confluent lipid core [14]. Atheromas are usually located where intimal thickening occurred in stages I-III, leading to an eccentric lesion. Smooth muscle cells disperse and get replaced by fibrous tissue. Because the wall is so thick at this stage, blood vessels called *vasa vasorum* expand and become more developed within the wall of the artery to better supply nutrients to the tissue.

From Type IV, the plaque may or may not progress into one of three subclassifications of Type V lesions. Type Va (or sometimes simply Type V) is the fibroatheromaa type IV plaque that has added more fibrous tissue while retaining a large lipid core. Multiple cores separated by fibrous tissue are possible. Type Vb (also called Type VII) lesion are calcified, and Type Vc (or Type VIII) lesions have most of the lipid replaced by fibrous tissue.

The final stage recognized in the AHA scheme is Type VI, although it should be noted that few plaques progress to this stage, and some that do may heal and return to Type V. Type VI is a plaque with histological evidence of plaque disruption: hematoma (Type VIa), hemorrhage (Type VIb), and

thrombus (Type VIc). When *vasa vasorum* becomes disrupted, hematoma or hemorrhage result. A thrombus is a blood clot in the lumen that partially or completely occludes blood flow. Type VI plaques are frequently subclinical but are thought to be the most common cause of myocardial infarction and stroke.

### 1.3.2 The Virmani classification scheme

To reflect shortcomings of the AHA classification scheme, Virmani and colleagues developed another scheme to describe atherosclerotic lesions [15]. For example, the AHA scheme does not differentiate between plaques based on fibrous cap thickness, although this feature can greatly affect the clinical relevance of the lesion. Therefore, they modified the AHA scheme according to the following criteria.

First is the initial xanthoma, similar to Type I plaques. These are characterized by lipid-laden macrophage accumulations and frequently regress. Next comes intimal thickening, which is mostly fibrous neointima tissue buildup from the site of xanthoma. Minimal cell replication occurs at this stage, although it is worth noting that most smooth muscle cells are clones of one another at this point. Eventually, intimal thickening becomes pathological when lipid and foam cells begin to accumulate alongside this fibrous tissue.

The most important features of the Virmani classification scheme are in fibroatheromas. Although the AHA types IV and Va plaques both describe fibroatheromas, these imply a series of events in fibrous cap formation and lipid core expansion that may not be correct in the scheme of plaque progression. Therefore, the Virmani scheme adds the thin-cap fibroatheroma (TCFA) as a new category not recognized in the AHA scheme where the fibrous cap is $< 65$ μm thick. These plaques are known to be likely to rupture and are sometimes called "vulnerable plaques" [17]. If a fibroatheroma contains a necrotic core that is thicker than this threshold, it is called a thick-cap fibroatheroma (ThCFA).

### 1.3.3 Composition of plaques

Atherosclerotic plaques are composed of a complex milieu of inflammatory cells, synthetic smooth muscle cells, collagen, proteoglycans, oxidized lipid, and calcification, among other things. Although lesions are extremely heterogeneous, specific regions of the plaque tend to be composed

of specific components. Fibrous tissue, which comprises a large portion of the neointima of most plaques, is mainly formed from synthetic smooth muscle cells that have abandoned their contractile phenotype and migrated out of the media. Multiple types of collagen, including Types I and III, make up this fibrous layer. Fibrous tissue also may accumulate in response to vascular injury through a process called intimal hyperplasia, but this is a different phenomenon than atherosclerosis.

During pathological intimal thickening, lipid, particularly oxidized low-density lipoprotein (LDL), begins to accumulate within the vessel wall [16, 18]. This tends to accumulate in neointimal lipid pools, which are proteoglycan-rich regions interspersed with lipid that have a gelatinous texture. This lipid may be consumed by macrophages, but many macrophages become engorged with LDL they cannot process and die. This, in turn, attracts more macrophages to the region, and after enough foam cells die, the region becomes a necrotic core [19]. A necrotic core is a mixture of lipid once contained within living foam cells and other necrotic tissue. At the periphery of the necrotic core may be more, living macrophages or even smooth muscle cells building fibrous tissue around the necrotic core. Microcalcifications may form when cells die, leaving behind accumulated calcium from their mitochondria [20].

## *1.4 Endpoints of atherosclerosis*

### 1.4.1 Vulnerable plaques

The so-called "vulnerable plaque" (Figure 1.1), stage IV or Va in the AHA scheme and called the thin-cap fibroatheroma in the Virmani scheme, is currently thought to be the most important stage for preventing morbidity and mortality [17]. A vulnerable plaque is not necessarily dangerous on its own, but it can sometimes progress to a ruptured plaque for reasons that are not well understood. Many vulnerable plaques will never progress to rupture, but because we cannot yet predict exactly which plaques will cause clinical events, identification of a vulnerable plaque is typically grounds for immediate medical intervention. Identification of a vulnerable plaque in vivo is a process still in its infancycurrent techniques are mostly invasive and still imperfect [4].

In a TCFA, a thin fibrous cap (defined as being $< 65$ μm) must be present over a lipid-rich necrotic core [21, 22]. If this fibrous cap breaks open, the plaque will have ruptured. Although a vulnerable plaque may progress to fatal rupture, it is not necessarily a "large" plaque. Many

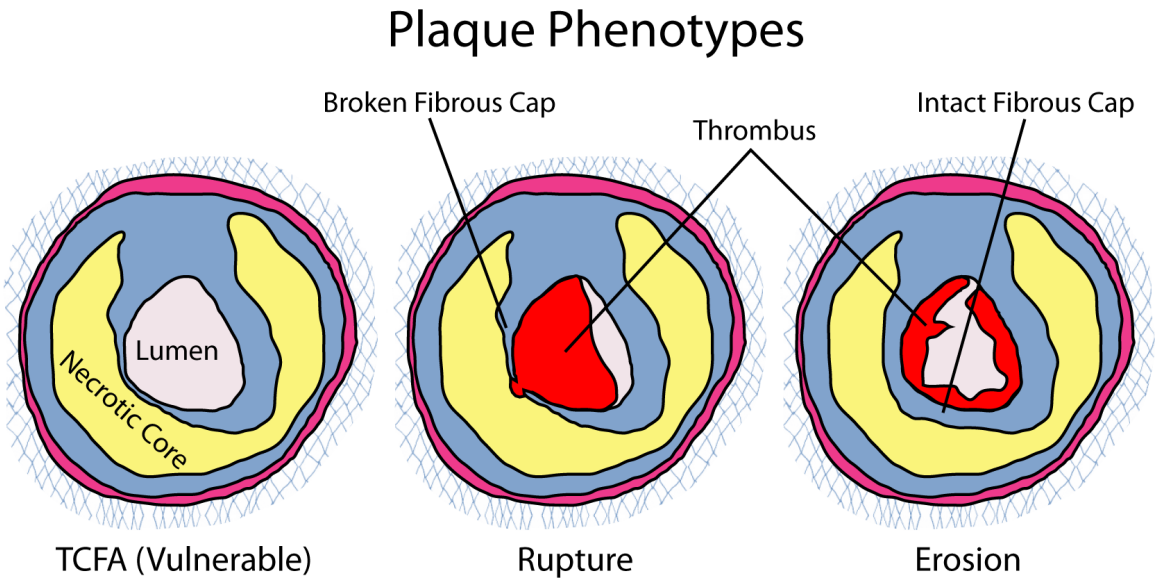


Figure 1.1: Atherosclerotic plaques can be classified into three groups. Left, an undisrupted vulnerable thin-cap fibroatheroma (TCFA) plaque exists within the vessel wall but has no thrombus associated with it. If a fibrous cap over a necrotic core breaks open and a thrombus forms, the plaque has ruptured (middle). If a thrombus forms over an atherosclerotic plaque without breakage of the fibrous cap, erosion has occurred (right)

highly stenotic plaques are quite stable, whereas minimally stenotic plaques can often be vulnerable [23]. Although vulnerable plaques are an advanced stage of atherosclerosis clinically speaking, one should not conflate or confuse "advanced" with "large". This makes their identification difficult using techniques such as angiograms, which are only sensitive to visible stenosis. Other causes of thrombosis such as plaque erosion and calcified nodules likely have their own vulnerable phenotypes, but how these would be classified is not currently known (for example, eroded plaques could be classified as AHA Types IV, Va, or Vc).

### 1.4.2 Plaque Rupture

If a plaque breaks open, a blood clot called a thrombus can form and occlude blood flow, leading to a heart attack or stroke [13]. For a plaque to rupture, the fibrous cap over a necrotic core fissures, exposing the necrotic core (a thrombogenic substance) to the blood pool [24]. Plaques currently thought most likely to progress to rupture are the thin-cap fibroatheroma phenotype [17]. The rupture site is usually directly on the thin fibrous cap or on the shoulders of the plaque, the region where the fibrous cap ends and connects to the rest of the vessel wall [25]. This is frequently an

acute event, although often ruptures can heal without causing morbidity or mortality [26]. Layered plaques due to healed rupture are frequently observed in pathology studies [6]. The exact frequency of non-fatal rupture is not known, but when a non-occlusive thrombus forms, it can heal as smooth muscle cells enter the thrombus and begin synthesizing fibrous tissue. This leaves behind a fibrous, and often highly stenotic, region with layers of fibrin and platelets from the original thrombus in between.

Inflammation is a key factor in the development of atherosclerotic plaques [27]. Not only are inflammatory cells essential for the formation of a necrotic core, but they also affect vascular remodeling and predispose certain lesions to rupture. The necrotic core is formed by foam cells, which migrate into the neointima of vessels and release their lipid-laden contents upon death. The definition of rupture requires a necrotic core, so lesions without one cannot rupture. Inflammatory cells don't just form this core, however. They also attack or induce apoptosis in synthetic smooth muscle cells forming the fibrous neointima [28, 29]. Without these cells, a fibrous cap thins and weakens, creating a mechanical environment ideal of rupture to occur. For more on the role of mechanics in plaque rupture, see section 1.9.2.

### 1.4.3 Plaque Erosion

In contrast to plaque rupture, plaque erosion is a relatively recently-discovered phenomenon [30]. Here, a thrombus forms directly over an atherosclerotic plaque, but the plaque remains undisrupted [31]. This thrombus formation may not be an acute event, and instead may accumulate over a period of weeks to form a mural thrombus [32, 33]. Despite identification, the mechanism for plaque erosion is not well understood. Its prevalence seems to be highest in women and in young men who are traditionally considered to be at lower risk for heart disease [17]. For many of these patients, the first symptom of coronary disease is death. This pathology was first noted in 1994 by van der Wal and colleages and then characterized more comprehensively by Virmani and colleagues in 1996 [30, 34]. These initial descriptions are relatively recent, in part because many early studies of heart disease specifically included only male coronary specimens in order to rule out hormonal effects. An unintended consequence of this selection in these early studies was the omission of plaque erosion candidates from study groups.

Plaque erosion is named such because a likely mechanism is endothelial denudation, where the endothelial cells "erode" away for currently unknown reason and expose the collagen and extracellular matrix beneath the cellsa thrombogenic surface [35, 36]. These cells may be lost due to localized apoptosis, but the specific mechanism for induction of denudation in erosion is a topic of current research [37]. In rabbits, localized incubation of the femoral artery with staurosporin induces apoptosis. This leads to denudation and thrombosis, offering a putative animal model for later stages of plaque erosion [37]. However, the mechanism for spontaneous apoptosis over plaques in humans is not clearly known.

Hypocholorous acid made by macrophages is also known to induce endothelial apoptosis in high concentrations, or to trigger endothelial cells to release tissue factor under lower concentrations [38]. Endothelial cells may also be lost as result of destruction of the basement membrane of these cells by proteinases such as MMPs or cathepsins [39, 40]. It has been noted that hyaluronan and proteoglycans like versican tend to be present at sites of plaque erosion. These extracellular matrix proteins may offer an optimal substrate for aggregation of thrombus [36]. Other possible causes of denudation may include vasospasm or highly shearing flow [41, 42]. Plaque erosion may also be, at least in part, a consequence of blood clotting disorders (which increase likelihood of thrombus formation). Proposed mechanisms include elevated levels of circulating tissue factors or suppressed fibrinolytic mechanisms [27, 43].

### 1.4.4 Calcified Nodule

A much less common but still noteworthy cause of coronary thrombosis is that of a calcified nodule . Much as in stage Vb of the development of atherosclerosis intra-plaque macrocalcification forms. If this calcification erupts from the plaque, it presents a thrombogenic surface to the blood pool. One study identified these as being mostly located in the mid-right coronary artery and suggested that torsional stress might play a role [15].

## *1.5 Vessel remodeling*

As an atherosclerotic lesion grows, it adds thickness to the wall of the artery. There are two phases to this process, termed Glagov remodeling [44]. First, the vessel experiences "outward remodeling" where the plaque thickens by increasing its exterior diameter rather than its interior diameter. The

cross section of the lumen is approximately preserved even as the wall thickens in this phase. The media frequently breaks down and becomes fibrous tissue as this happens. Next, after the plaque burden has reached about 40% (meaning 40% of the area inside the exterior border of the vessel is made up of plaque and media), the vessel undergoes "inward remodeling". Inward remodeling is when the plaque actually protrudes into the lumen.

When the lumen diameter is changed, we call this a stenosis. Whereas in outward remodeling a plaque exists but does not impede blood flow, stenotic inward remodeling can actually change blood flow [45]. Any constriction of flow results in a pressure drop across the obstacle. Not only is pressure lost but also this region accrues unique hemodynamic properties, discussed in section 1.8. In short, wall shear stress increases across the stenosis, and if the stenosis is severe enough, reversed flow could result downstream [13].

### *1.6 Thrombosis*

A thrombus is a blood clot. The process of forming a thrombus is called thrombosis, and if the thrombus embolizes (breaks off and is carried in the blood stream), it could travel downstream and obstruct a smaller vessel [35]. The human arterial tree is a series of vessels whose diameter decreases distally, so an embolized thrombus could obstruct any variety of small vessels depending on its site of origin and local hemodynamics [13]. Frequent sites of concern include the brain (where the embolism causes a stroke), the heart (a myocardial infarction) or the lung (a pulmonary embolus).

Alternately, a thrombus can stay in situ and create a stenosis or obstruction. Any occlusion of blood flow can result in decreased nutrient transport or, if upstream pressure is high enough, a jet that causes downstream endothelial damage or hemolysis [9]. Thrombus formation can be acute (forming in seconds to minutes) or chronic (days to weeks) depending on circumstances surrounding thrombus formation.

After a thrombus forms, it can heal or form an "organized thrombus" made of layers of smooth muscle cells, proteoglycans, and fibrin [15,32]. This can result in formation of additional neointima and further narrowing of the lumen.

### 1.6.1 Virchow's triad

Typically, a thrombus forms for 3 reasons, described by Virchow's triad. These factors are hypercoaguability, stasis, or endothelial damage. The first is not typically related to atherosclerosisaltered blood composition like increased activity of clotting factors is usually the cause. Stasis of blood (or turbulence, another possibility) are only indirectly related to atherosclerosis. If a plaque is severely stenotic and creates an eddy region downstream, blood stasis is possible [46, 47]. Similarly, a severely stenotic vessel due to atherosclerosis could result in turbulent flow, but this too is a rare situation [35, 48].

The third piece of the triad, endothelial damage, is the most closely associated with atherosclerosis. When a plaque ruptures, it exposes collagen fibrils from the newly-broken fibrous cap [13]. It also allows necrotic core to come into contact with the blood pool, providing a thrombogenic seed point [43]. In plaque erosion, endothelial cells may be lost, and the underlying collagen and elastin serves as a site for thrombus formation [36, 49].

### 1.6.2 Plaque imaging

Because atherosclerosis is such a significant cause of morbidity and mortality, there is significant interest in detection of plaques both for study and for prevention and treatment. Numerous imaging techniques exist, each with unique benefits and drawbacks.

### 1.6.3 Angiography

Perhaps the simplest and most prevalent technique to assess atherosclerotic burden of patients is a technique called angiography. Angiography literally means imaging of blood vessels and could describe a multitude of techniques, but when used alone the term is implied to mean a projectional radiography image of blood vessels. In angiography, a patient receives a dose of radio-opaque contrast agent, and then an x-ray image of blood vessels is acquired. This could be captured on film as a still image (as was done historically) or via fluoroscopy, where a movie of blood vessels is obtained with a fluoroscope. In modern practice, fluoroscopy is typically performed in catheterization labs where a catheter is threaded into the system of interest (for example, the coronary arteries, the cerebral circulation, or the aorta) and a time-lapse image of blood flow is acquired by injecting a

known dosage of a contrast agent into the circulation. One can roughly estimate blood velocity from fluoroscopy by timing the distance an injection of contrast travels.

In these images, physicians are looking for any narrowing of the vessel lumen that would indicate the presence of a stenosis [50]. The contrast agent used only enters the bloodstream and does not get absorbed into the wall, so physicians use angiography to image the cross-sectional diameter and path of blood vessels. Because of Glagov remodeling, many clinically relevant lesions can be missed by angiography [50]. If a vessel is only remodeling outward and yet has formed a thin-cap fibroatheroma, the patient could conceivably experience plaque rupture from a lesion invisible to angiography.

Similarly, an angiography image can only visualize vessels perpendicular to the path of the x-ray beams. Because many plaques are eccentric, one view could reveal no evidence of lesion and yet an orthogonal view could reveal significant stenosis. For this reason, most clinicians obtain a minimum of two unique views of vessels (called bi-plane angiography) [51]. Using more advanced technology, clinicians can now use "rotational angiography" where an x-ray angiography system on a C-arm can collect multiple views of the vessels and then reconstruct the vessels in 3D. This is similar to the idea behind CT imaging, although CT uses radon transforms of x-ray scattering to perform its reconstruction and rotational angiography uses a large number of planar x-ray images to perform its reconstructions. Both techniques deliver a radiation dose to the patient and therefore must be used sparingly.

### 1.6.4 Intravascular techniques

One of the most popular current techniques in cardiovascular diagnostics is intravascular imaging. Here, a patient is sedated in the catheterization lab of a hospital, and a clinician feeds a wire through the subject's arteries from an access port, typically the femoral artery. On the tip of the wire the clinician can thread interventional or diagnostic devices and guide them to the desired site using fluoroscopy. Although any contact of the wire against the artery wall carries a risk of inducing endothelial denudation or vasospasm, this approach successfully resolves myocardial infarctions and strokes in most emergency situations.

Two catheter-based imaging techniques are most popular today: intravascular ultrasound (IVUS)

and optical coherence tomography (OCT). IVUS is the most widely used in the United States at present, though OCT is a technique currently making advances. IVUS uses ultrasound to bounce high-frequency audio waves off the walls of blood vessels and collect back at the catheter tip [50]. Operating like radar, these waves reflect off both the surface of the lumen and off internal reflectors inside the vessel wall, allowing the clinician to image both the lumen and the thickness of the wall by timing how long it takes waves to bounce back. IVUS returns a single cross-section of the vessel at a time corresponding to the axial location of the probe, so clinicians do a "pullback" where they feed the IVUS catheter to the farthest desired location along the artery then acquire images as they pull the catheter back toward the access port.

Traditional IVUS imaging returns the magnitude of the ultrasound pulse, providing a black-and-white image of the vessel borders and information about strong reflectors like stents or calcification. By also tracking the phase of backscattered waves, some systems provide "virtual histology" (VH) revealing the spatial composition of the wall. Tissues such as lipid, fibrous, and calcification alter the phase of the wave differently during each reflection [32,52]. Use of VH is becoming widespread and is commercially available in FDA-approved systems such as those marketed by Volcano Corporation (San Diego, CA). Additional techniques like near-infrared spectroscopy can be combined with IVUS to interrogate the structure of the plaque [53].

One shortcoming of IVUS is its low spatial resolution, which cannot determine fibrous cap thickness precisely. Especially given the threshold in the literature of 65 μm for fibrous cap thickness with respect to vulnerability to plaque rupture, VH-IVUS cannot accurately study this parameter with current spatial resolutions in the neighborhood of 200 μm. If VH-IVUS detects necrotic core adjacent to the lumen, one can only assume it is overlaid by a fibrous cap thinner than this spatial threshold [54]. However, OCT provides considerably higher resolution (approximately 10-20 μm) and can be used to measure the cap thickness of TCFAs [54]. OCT maps vessels using the same pullback technique as IVUS, but it cannot penetrate very far beneath the lumen, behind a thrombus, or through blood (saline must be injected before performing OCT). Typically, signal loss is so great that the exterior of the vessel cannot even be resolved; OCT uses visible light pulses to return its signal, which simply cannot travel through dense tissue more than a handful of microns thick. For this same reason, OCT cannot distinguish thrombus from tissue like smooth muscle; a mural

thrombus prevents imaging almost any of the tissue beneath it.

A third catheter-based probe in use today is called "thermography", which measures the temperature of the wall to create a map of lesions [55]. The principle behind thermography is the notion that inflammation causes atherosclerosis, and inflammation also warms tissue. The utility of this technique is still under investigation, as the local temperature gradient due to an inflamed plaque is currently below the level of sensitivity of probes. Additionally, the act of dragging a thermal probe along the wall of blood vessels carries its own risk of endothelial denudation or even inducing plaque rupture. This technique would be unable to detect lesions not heated by inflammation, meaning many lesions could be missed.

### 1.6.5 Histology

Perhaps the highest-resolution technique to study blood vessels is histology. By viewing stained tissue under a microscope, one can resolve features with submicron resolution. Histology is an ex vivo technique, so it can only be performed on biopsy or autopsy tissue specimens. By staining tissue with chromagens and/or antibodies, one can resolve detailed information on the presence and distribution of proteins and compounds present in the tissue.

In order to stain tissues for microscopy, it must first be mounted. Thick sections of tissue are often not optically transparent, making transillumination of stained features difficult. Confocal microscopy can optically section tissue to resolve some internal features, but light still cannot penetrate through dense, thick structures. Therefore, to see inside of a harvested tissue, it is often prepared by embedding in a mounting medium then sectioned using a microtome, often at single-digit micron thicknesses, onto a glass slide.

Tissue can either be fixed or prepared fresh after harvest. Tissue fixed with agents like formalin can be stored for long periods of time at room temperature, but not all antibodies can operate on fixed tissue. Enzymatic assays like zymography also cannot be performed on fixed tissue. Fresh tissue, on the other hand, must be analyzed immediately upon harvest or frozen for storage at -80°C. Frozen tissue is often prepared by embedding it in optimal cutting temperature (OCT, not to be confused with the vascular imaging technique of the same acronym) medium then sectioning in a cryostat. Frozen tissue sections are often the most compatible with commercial antibodies but

experience considerable morphological distortion during sectioning. For whole-vessel imaging of fresh tissue, en face preparations are common, where a vessel is sliced axially then flattened such that the endothelium is exposed in a single plane.

For fixed tissue, paraffin wax embedding is common because of the ease of processing, but not all commercial antibodies are compatible with paraffin embedding. Methyl methacrylate (MMA) resin embedding is a more technically-complex technique that requires sectioning with a diamond-blade microtome. The hard resin enables even sectioning through solid structures like vascular calcification, and many antibodies compatible with paraffin sections will work with MMA [56–58]. Both paraffin and MMA embedding protocols typically require sending tissue through graded alcohols, a process that dehydrates tissue for storage but also dissolves away any lipid and prevents direct detection of lipids. Glycol methacrylate (GMA) is another plastic resin that does not denature enzymes, but its use is technically complex, it is incompatible with many standard staining protocols, and over time cures into a hard, un-sectionable block.

A large number of "special stains" are common in vascular research that exploit natural affinity of specific tissue types for certain dyes. Perhaps the most universal stain is hematoxylin and eosin (H&E), where nuclei are stained purple with hematoxylin and cytoplasm is stained pink with eosin. Gross vascular tissue composition is often identified using Movat's pentachrome or Masson's trichrome stains, which use multiple simultaneous dyes to color different components of vasculature. Picrosirus red stains collagen pink, enabling identification of necrotic cores in atherosclerotic plaques because of dull yellow staining in these regions. Under polarized light, the birefringent properties of picrosirius red reveal large collagen fibers (Type I) in yellow/orange and thin fibers (reticular fibers, Type III) in green. Other stains reveal specific tissue types, such as Von Kossa's calcium stain which identifies calcium in black or Verhoeff's elastin stains that identifies elastic lamina in black.

Immunohistochemistry (IHC) uses antibodies to detect and stain specific proteins. A primary antibody is incubated on the tissue of interest such that it binds to its specific antigen. After washing of excess primary antibody, a secondary antibody specific to an antigen on the primary antibody (and hopefully not to any other antigens in the tissue) such as the Fc region is then incubated. Finally, a fluorophore or chromagen is bound to the secondary antibody using a technique such as

forming an avidin-biotin complex (although many other conjugation systems exist as well). In order to improve primary antibody binding, particularly on fixed tissue, one must sometimes perform antigen retrieval using pretreatment techniques like placing in boiling ethylenediaminetetraacetic acid (EDTA), or digestion in proteinase K. These techniques improve staining efficiency but may introduce tissue artifacts. The mechanisms of some antigen retrieval techniques, although effective, are not completely understood.

In any type of histology, it is particularly important to include appropriate positive and negative controls. These steps, sometimes inappropriately omitted, are critical to ensure the stain in question is both specific and successful. Control slides typically contain identically-embedded sections of tissue from well-characterized tissue types. Positive control slides ensure that the stain is functioning and that it appears in expected tissue regions. Negative control slides ensure that positive staining is not also observed in regions where it should not exist, perhaps because of nonspecific staining of the chromagen/fluorophore directly to the tissue itself.

### 1.6.6 Other techniques

Magnetic resonance imaging (MRI) is a popular technique to acquire vascular anatomy and an associated flow field. MR angiography (MRA) can use a variety of scan sequences to image blood vessels, with each type of scan offering benefits and drawbacks [59]. For example, 3D time-of-flight (3D-TOF) MRA is a popular technique that allows imaging of the blood pool because blood returns a bright signal [60]. This is useful for determining the lumen of blood vessels, although 3D-TOF sequences are not well suited for imaging the wall itself and cannot resolve blood not leaving the plane of the image (for example, through swirling flow). Conversely, black-blood sequences return poorer resolution of the lumen border but allow viewing of the thickness of the blood vessel itself. Multi-sequence techniques have been proposed that attempt to return not only information on the lumen and wall thickness but even the composition of the wall itself [61, 62]. These techniques are controversial.

To improve visibility of blood in MR scans, contrast agents like gadolinium are often injected. Gadolinium alters the relaxation time of atoms in the blood and enhances vasculature. At the frontier of vascular MR imaging is the use of paramagnetic nanoparticles as a contrast agent [25]. These

particles, wherever present, alter the local brightness of an MR signal and offer promise to detect features of atherosclerotic plaques. Other molecular contrast agents have been proposed that will bind to thrombus for non-invasive detection [63].

Another benefit of MRI, besides that it provides zero ionizing radiation dose to the patient, is that it can image blood velocity, a useful tool for researchers studying both anatomy and blood flow. Using phase-contrast MR (PCMR), a patient's vessel anatomy can be acquired with MRA, and then in the same scan session the corresponding velocity field can be obtained as well [49, 64]. PCMR can only acquire blood flow in a single direction through a single slice at a time, though, so a researcher interested in the full 3D path of blood in a single slice would need 3 scans to acquire x, y, and z-components of velocity. This can be time-intensive since the patient must remain still in the scanner, but the advantage is accurate registration of velocity data with respect to anatomy.

Computed tomography (CT) imaging can provide an even higher resolution angiogram than MRI, although CT uses x-rays for imaging and thus carries a radiation dosage to the patient. Also, no PCMR equivalent exists for CT, so there is no way to measure flow using the technique in patients receiving a CT angiogram. A benefit of CT is a purported ability to identify and look inside soft plaques.

## *1.7 Animal models of atherosclerosis*

Because much work is yet to be done to understand the pathogenesis of atherosclerosis and develop treatments, animal models are an attractive tool because they recapitulate some of the processes of atherosclerosis under controlled circumstances. In humans, imaging plaques is challenging, as each technique carries limitations, and many experimental studies such as inducing plaque rupture would be simply unethical.

A variety of animal models have been developed, and these too carry benefits and limitations. Mice and rats are among the most popular models in use today. Because rodents are naturally resistant to atherosclerosis, additional measures must be taken to induce atherosclerosis, including genetic modification, diet, and pharmaceutical modifiers [65, 66]. Rabbits, dogs, pigs, and primates are all employed in research as well, but logistical, financial, and ethical burdens increase in larger animals [67, 68].

### 1.7.1 Mouse models

Mice are perhaps the most popular animal model of atherosclerosis, since they rapidly and reliably form plaques under certain conditions. More varieties of genetically modified mice are available than for any other animal species at this time, and the two most ubiquitous mouse model strains are the apolipoprotein E ($ApoE^{-/-}$) and low density lipoprotein receptor ($LDLr^{-/-}$) knock-out strains. The $LDLr^{-/-}$ mouse is a more moderate model: it will not form plaques unless also fed a high-fat diet [66]. The $ApoE^{-/-}$ mouse is a more aggressive model which will spontaneously develop lesions without the addition of a high fat diet.

Multiple diets exist for these mice. Beyond the regular chow diet, the Western diet and the Paigen diet (also called atherogenic diet) prevail in the literature [65, 69]. These differ in their lipid composition. Diets can also be supplemented with simultaneous subcutaneous infusion of Angiotensin II (AngII) via osmotic minipump, which makes the mice hypertensive [69]. AngII alone has been shown to increase the severity and distribution of lesions [70]. Other important factors that affect lesions in mice are age (older mice have greater plaque burden), gender ($ApoE^{-/-}$ female mice have more severe lesions than males), and stress (stressful conditions like electric shocks have been shown to increase lesion severity) [65, 66, 68, 69].

Additionally, because of the role of fluid dynamics in developing atherosclerosis (see section 1.8), lesions can be induced by introducing a stenosis. Several techniques have been proposed, including an external gradually narrowing cast and a nitinol shape-memory clip [71, 72]. Downstream of a stenosis, lesions increase, even in locations not typically prone to atherosclerosis. With any type of manmade device introduced into a body, care must be taken to separate effects of the device from effects of immune response to a foreign body.

Although mice are frequently studied as an analog of human atherosclerosis, considerable differences exist between the two species [73]. Besides the fact that the two species are genetically distinct (and thus produce different proteins), there are also discrepancies in size (a human aorta is more than an order of magnitude larger than a mouse's), the location of atherosclerotic plaques (coronary lesions are not as common in mice as in men), posture (humans are upright and mice are prone, leading to different fluid flow patterns and aortic curvature), and timescale of atherosclerosis

(human lesions develop over decades whereas murine lesions develop over weeks).

One of the most noteworthy consequences of these differences is the difference in plaque rupture between species. In humans, plaque rupture is of serious concern, but in mice, there is considerable debate as to whether plaques ever rupture at all, let alone the physiological relevance of this rupture to humans [5, 6, 74]. Some postulate that plaques do rupture frequently in mice, attributing their layered appearance as evidence of past ruptures [7]. Others dismiss reports of rupture in mice, suggesting most reports can be attributed to sectioning artifact or intraplaque hemorrhage [75, 76]. Nonetheless, the debate continues, and the consequence of this uncertainty is that many studies report "rupture" as well as "vulnerable" and "unstable" lesions in mice despite imprecision of these terms [77].

## *1.8 Fluid dynamics and atherosclerosis*

### 1.8.1 Wall shear stress

Throughout the history of atherosclerosis research, multiple hypotheses have been presented to explain why humans get atherosclerosis. Early hypotheses included immune function and dietary cholesterol, but in the 1980s, Giddens and colleagues came up with a new hypothesis that prevails to this day [78]. It had been noted that lesions only form in specific locations such as in the coronary arteries or the carotid bulb [9]. These locations are consistent between individuals, and there are other locations such as the internal mammary artery which almost never carry any atherosclerotic burden [79, 80].

Giddens' group proposed that the fluid dynamics of circulating blood could explain the localization of plaques, and this explanation is supported by considerable evidence to this day [81]. All of the primary locations for plaques tend to be on the inner edge of curving vessels or immediately downstream of vessel bifurcations [82]. As blood flows through a vessel, the frictional force of the flowing blood exerts wall shear stress (WSS) against the endothelium [13].

Wall shear stress (WSS) for a Newtonian fluid is defined as

$$\tau = \mu \frac{dv}{dr}\Big|_{r=R}. \tag{1.1}$$

where $\tau$ is WSS, $\mu$ is the dynamic viscosity of blood, $\frac{dv}{dr}$ is the strain rate (near-wall velocity gradient), and $R$ is the vessel radius.

Today, we now know that low WSS is correlated with atherogenesis, and high WSS tends to be atheroprotective [42, 83, 84]. WSS magnitude is not the only condition to note, however. Directionality also seems to play a roleoscillatory flows may have high instantaneous WSS, but if the flow reverses for enough of the cardiac cycle, it could have low mean magnitude [42]. Thus, current thinking is that both low magnitude unidirectional and low average magnitude oscillatory WSS are atherogenic.

A stenosis typically creates complex fluid flow conditions, and thus may create a feedback loop for plaque formation. As a stenosis narrows an artery, wall shear stress increases across the neck of the stenosis. Downstream, low WSS appears, and if the stenosis is severe enough, oscillatory flow may even appear [85]. This may provide a mechanism for plaques to grow from their downstream edge and minimize continually increasing the degree of stenosis inward rapidly. In endothelial cells, apoptosis tends to be higher in regions of low WSS and lower in regions of high WSS [86]. However, plaques are typically well-bounded and don't grow forever, so WSS alone cannot explain atherogenesis.

At the inner edge of curving vessels such as the inner curvature of the aortic arch, low and possibly even oscillatory WSS dominates, whereas the outer curvature experiences higher WSS as flow rounds the bend and runs into the outer curvature. At bifurcations, depending on the geometry such as angle and diameter of the vessel, oscillatory flow such as that observed in the carotid bulb is often expected on the outer edge immediately distal to the bifurcation.

### 1.8.2 Other metrics

To measure oscillation, a metric called oscillatory shear index (OSI) has been proposed, although different groups have different specific definitions [81, 87, 88]. Despite technical differences, the common theme for all definitions is that OSI measures how much the flow reverses direction over each cardiac cycle. We prefer the definition of Moore et al. because of its range from 0 to 1 (enabling easy logical interpretation as a percent) and its dependence on local mean flow direction (removing the need to prescribe a "forward" flow direction) [89]. It is defined as:

$$\overrightarrow{\mathrm{OSI}} = \frac{\int_0^T |\overrightarrow{\mathrm{WSS}} \cdot \vec{\mathrm{n}}| H(\overrightarrow{\mathrm{WSS}} \cdot \vec{\mathrm{n}}) dt}{\int_0^T |\overrightarrow{\mathrm{WSS}} \cdot \vec{\mathrm{n}}| dt} \tag{1.2}$$

where

$$\vec{\mathrm{n}} = \int_0^T \frac{\overrightarrow{\mathrm{WSS}}}{|\overrightarrow{\mathrm{WSS}}|} dt \tag{1.3}$$

is the mean shear direction, $\overrightarrow{\mathrm{WSS}}$ is the wall shear stress vector, and $H(x)$ is the Heaviside unit function.

OSI is a metric of interest because it helps identify regions where flow is changing direction. Whereas in laminar, unidirectional flows, low mean WSS implies low blood velocity close to the wall, mean WSS could be low despite high instantaneous blood velocities if the flow reverses direction. Regions of low WSS and oscillatory flow are associated with progression of atherosclerosis, but mean WSS alone is not the sole factor affecting vascular disease [9]. Experiments have shown a different phenotype of lesions in mice between low unidirectional and oscillatory flow conditions, and a variety of inflammatory proteins, reactive oxygen species, and micro-RNAs have all been shown to be differentially regulated by laminar and oscillatory shear in vascular cells [71, 90].

Other metrics have been proposed that may also explain the localization and progression of atherosclerosis [91]. Rather than investigating the raw magnitude of WSS, the spatial and/or temporal gradient of WSS may be more important because these measure how WSS changes relative to a local baseline. Additionally, measures such as relative residence time, vorticity, and helicity could play a role in plaque progression and disruption, although such a link is not yet well established [91, 92].

### 1.8.3 Mathematical and computational methods

Fluid flows are governed by a mathematical framework called the Navier-Stokes equations [93]. These describe how any fluid moves, although they are a series of differential equations that cannot be easily solved except under idealized situations; an analytic solution of the full Navier-Stokes equations is the topic of the Clay Mathematics Institute's Millenium Prize for outstanding problems in mathematics.

Instead, to study subject-specific flows, we use a technique called Computational Fluid Dynamics (CFD) that approximates a solution to the Navier-Stokes equations, given geometric and fluid property bounding conditions. CFD is a powerful technique, but it requires careful selection of numerical algorithms to accurately recapitulate the situation at hand. Many of the factors driving these selections are tradeoffs between physiological accuracy and computational efficiency. For example, the numerical method for solving the equations could use a direct approach (solving the matrix equations using linear algebra techniques) or an iterative approach (approximating the solution with multiple guesses). Many vascular CFD problems require an iterative solver because the computational cost of an explicit (direct) solution method is infeasible.

A common assumption in CFD is to represent blood as a Newtonian fluid. Blood is composed of liquid plasma, as well as solid components like red blood cells, platelets, and dissolved proteins. Red and white blood cells are not distributed homogeneously throughout liquid bloodclose to the wall, plasma skimming results in a locally nearly cell-free zone. Factors like shear thickening can also affect apparent viscosity, and the Fahraeus-Lindquist effect (apparent viscosity goes down with vessel diameter) dominates in narrow vessels like capillaries. Thus, blood is probably best represented as a Casson fluid. However, it is mathematically much simpler and computationally more efficient to represent blood as a Newtonian fluid. Studies have shown that approximating blood as a Newtonian fluid alters WSS calculations by about 10% whereas geometric uncertainty affected it by four times that amount [94].

Other efficiency and accuracy assumptions to consider in CFD include discretization of the model. Patient-specific vascular flows can be digitized into a finite-volume mesh comprising the flow field. If the mesh is too coarse, the final solution will not be accurate (or will not solve at all). However, finer meshes require more memory and simulation time for CFD to complete, so a tradeoff must be reached. Typically, mesh resolution will reach a point of diminishing returns where a higher resolution significantly increases the need for solution resources without a comparable increase in solution accuracy. Therefore, CFD operators will often perform a mesh-convergence study by simulating the same problem with meshes of different resolution to ensure that their solution is not affected by mesh resolution. Similarly, temporal resolution must be considered in unsteady flow simulations: iterating through time too quickly will decrease the accuracy of the solution, but too

slowly will create an unnecessary processing burden.

### 1.8.4 Boundary conditions

One decision necessary when setting up a vascular CFD simulation is how to mathematically represent blood flowing in and out of the vessel. At the inlet, a number of possibilities exist. Even in patient-specific CFD simulations, true patient-specific inlet velocities are often not known. For example, if vascular geometry was determined by CT, then no flow information could possibly be obtained by that modality. PCMR techniques can acquire patient-specific velocity profiles, but the spatial and temporal resolution is almost certainly below the spacing of the mesh and timestep. Usually, some sort of velocity waveform (velocity versus time) must be applied to a CFD model, but this typically represents mean velocity in the vessel and does not carry information about the spatial distribution of velocity. Thus, a cross-sectional velocity profile must be applied.

Four idealized velocity profiles are prevalent in fluid dynamics literature. The blunt flow profile, where every point in a single cross-section has a uniform velocity, is typically applied in flow extensions. Flow extensions allow the flow to develop such that it enters the region of interest in a more plausible manner while maintaining the ease of implementation of a blunt flow profile. As the no-slip condition for viscous fluids dictates that velocity must be zero at the wall, a blunt flow profile clearly violates this assumption. Therefore, analysis of hemodynamic parameters should only be performed outside the blunt flow region. Slightly downstream of a blunt flow velocity profile one will find a plug flow profile, a nearly uniform distribution of velocity profiles across the cross-section except at the walls, where velocity ramps down to zero. Plug flow represents flow that is not fully developed and may be an appropriate approximation for the coronary arteries.

When flow can be assumed to be fully developed, it may be approximated with a parabolic (Poiseuille) or Womersley velocity profile [95, 96]. Poiseuille flow is defined for steady flow simulations through a cylinder, neither of which assumption is directly applicable to pulsatile, patient-specific flows through a blood vessel (which is cylindrical but not a mathematically perfect cylinder). Womersley flow solves this pulsatility problem by introducing a Fourier series of Bessel functions to represent a temporally-fluctuating velocity field. Each of these four simplified inlet velocity profiles

carries a set of assumptions, and CFD operators must weigh the pros and cons of using each technique if a patient-specific velocity profile is not known. In our own studies of the carotid artery, we found that the relative effect of each type of profile is much less than the influence of the variation in geometry from patient-to-patient [97].

Another boundary condition to consider is the outlet. Velocity profiles are not usually prescribed at the outlet because this would over-constrain the system and be nearly impossible to solve the Navier-Stokes equations. Instead, pressure is typically prescribed at the outlet. If patient-specific pressure is known, this can be applied, or a target flow rate can be approximated by dynamically adjusting the pressure at each outlet. Otherwise, a pressure outlet may be set as "traction free", meaning the pressure is zero. Other boundary condition possibilities include Windkessel models or higher-order circuit analogies, which prescribe dynamic pressures by defining a resistance and capacitance to approximate downstream blood vessels.

### 1.8.5 Fluid-structure interaction

The next generation of CFD is called fluid-structure interaction (FSI, also standing for fluid-solid interaction depending on who you ask). Whereas CFD only simulates the fluid side of things, we know that blood vessels are compliant and that arteries distend in response to pressure. CFD can include moving walls to simulate this pulsatility, but encoding this motion requires adjustment of the mesh at each timestep. This mesh adjustment process can be extremely complex, particularly in patient-specific models, and prescribing physiologically-relevant moving walls as pre-determined input geometry is very difficult. FSI improves this process by dynamically computing the moving wall by adding a viscoelastic or other solid mechanical model to dynamically adjust the geometry on top of the CFD. Implementations of FSI are computationally expensive and carry a greater burden of assumptions than CFD or computational solid mechanics alone, so this field is still maturing.

### 1.8.6 Fluid dynamics and plaque rupture

WSS may not only govern plaque development, but it may also play a role in atherosclerosis endpoints. Several case reports suggest that plaque rupture occurs directly at the site of greatest WSS [98, 99]. Although isolated case reports cannot explain a mechanism for this (and may be polluted by publication bias), such interplay between fluid flow and thrombosis is not unexpected.

Shearing blood exerts a force on vessel walls in addition to forces from blood pressure, so if a fibrous cap is already weakened, extra WSS could lead to plaque rupture. While WSS is known to help predict sites of plaque formation, its utility in predicting which of those plaques will actually rupture is not well established.

## *1.9 Solid mechanics and atherosclerosis*

Another factor of note in atherosclerosis is that of solid mechanics. Solid mechanics is the study of forces and stresses, and a pressurized blood vessel has complex solid mechanics. Atherosclerotic plaques are made up of numerous componentsthey are a heterogeneous material. Each subcomponent has its own material propertiesitems like calcification are much stiffer than lipid [100]. Biological materials are viscoelastic, meaning that their properties depend on the rate at which they are loaded as well as the composition of the material itself [101]. They typically exhibit nonlinear material properties and anisotropy, meaning that they have different material properties in different directions [102]. Given the composition of blood vessels including collagen and elastin fibers, such a relationship is unsurprising.

### 1.9.1 Residual stresses

Vessel remodeling, particularly at different rates between layers of vessels, results in residual stress accumulation within the wall [101]. The effects of residual stress are readily apparent in opening angle assays [103]. If a ring of an excised artery is sliced axially, it will open up and form a C-shaped piece when viewed from end. If the artery were stress-free, it would remain stationary upon slicing, but differences in levels of residual stress between the intima, media, and adventitia causes this opening. Fung and colleagues postulated that the opening angle assay reveals a stress-free conformation of the vessel, but inhomogeneity of the vessel suggests that some residual stress likely remains even in a sliced vessel [101,104]. Thus, an artery in vivo not only experiences stresses resulting from blood pressure, but also residual stresses innate to the tissue.

### 1.9.2 Plaque rupture

When the local stress exceeds the ultimate stress threshold of a material, the vessel breaks, resulting in a fissure [24]. This is how plaque rupture is thought to occur. Although plaque rupture is a

complex, multifactorial process with plenty of biological risk factors, overall it is a mechanical event: a material is breaking. Within existing literature, a threshold of >300 kPa will result in plaque rupture, but this specific threshold is not well supported by evidence. It was proposed in an early computational study then propagated by the process of citation until it became prevalent in the literature despite minimal evidence from direct measurement [105]. Regardless of the exact magnitude of the ultimate stress of plaque components, plaque rupture occurs because of a local maximum of stress on the thin fibrous cap or plaque shoulders [106].

Multiple factors contribute to the mechanical environment that results in rupture [26, 106, 107]. The blood pressure of a vessel is what exerts most mechanical force on the plaque (the other being residual stresses innate to the growing vessel). Higher blood pressures result in higher stresses in the wall. Hypertension (high blood pressure) is generally a chronic condition, so blood vessels often remodel themselves to redistribute the resulting internal stresses [108, 109].

Another major factor contributing to rupture is the geometry of the plaque. Plaques are made of multiple tissues, including smooth muscle cells, macrophages, lipid, collagen, and elastin. The exact shape, size, and distribution of these tissues, each of which has different mechanical properties, will affect the stresses in the wall [23]. This is the reason that the thin-cap fibroatheroma is thought to be the most vulnerable to rupture whereas a thick-cap fibroatheroma is not.

Several studies have investigated the effects of geometry [110]. It has been shown that showed that the size of the necrotic core, the thickness of the fibrous cap, the presence of necrotic cores and calcifications, as well as the shape and location of the necrotic core all modulate the mechanical environment with implications for plaque rupture [23, 110–112]. Another factor that could increase likelihood of rupture is fatigue, where a tissue becomes weakened after repeated bending over millions of cardiac cycles [107].

### 1.9.3 Microcalcifications

An emerging concept in vascular biomechanics is that of microcalcifications [113]. These small calcifications (single micron or smaller diameter) form when macrophages release calcium deposits, typically on the outside edge of necrotic cores. Nucleation for microcalcifications are thought to come from the mitochondria of dying cells, most likely smooth muscle cells in atherosclerotic

plaques [20]. Macrocalcifications tend to form as "clouds" of microcalcifications around necrotic core that eventually expand to build on top of the core. Whether this process is one of active or passive calcium deposition is not currently known.

Weinbaum et al. proposed recently that microcalcifications may play a role in plaque rupture as well. They hypothesized that microcalcifications within the thin fibrous cap of plaques creates a local stress concentration, which leads to fissuring and rupture [113]. This may explain why some TCFAs rupture and others do not: microcalficiations are not universally present, especially in the fibrous cap [114]. Although the microcalcification hypothesis has theoretical backing, further study is still needed.

### 1.9.4 Biological responses to mechanics

Biomechanics, particularly solid mechanics, are not only important for determining how tissue breaks. They also impact how tissues develop, remodel, and die. Tissues actively respond to mechanical inputs through the process of mechanotransduction, such as when vessels remodel in response to local mechanics. Constituents of the cytoskeleton tethered to membrane-bound proteins like integrins, or mechanosensitive surface receptors themselves deform in response to mechanical loading or shear force across the cell. These, in turn, upregulate intracellular processes to produce specific proteins. For example, matrix metalloproteinases (MMPs) that remodel extracellular matrix are known to be upregulated in regions of high mechanical stress [39,56,115,116]. The transcription factor nuclear factor kappa-B (NF-$\kappa$B) is also upregulated by local elevation of mechanical stress (as well as in response to cytokines and oxidized LDL, among other things). NF-$\kappa$B is known to upregulate production of a large number of inflammatory proteins [117]. Mechanotransduction through integrins, nicotinamide adenine dinucleotide phosphate (NADPH) oxidase, xanthine oxidase (XO), G-protein coupled receptors (GPCRs), tyrosine kinase receptors (TKRs), and others, many proteins involved in the progression of atherosclesis are directly and indirectly regulated by mechanics [52].

### 1.9.5 Computational solid mechanics

Like fluid dynamics, solid mechanics are governed by a series of constitutive equations based upon fundamental mechanics like forces and momentum. Similar to CFD, studying patient-specific geometries using these equations is impractical since blood vessels never perfectly align with Cartesian

or cylindrical coordinates. Therefore, computational solid mechanics techniques are used to estimate local mechanics. Typically, finite element analysis (FEA) or a similar technique, finite volume analysis (FVA) are used to break a region down into numerous small mesh elements and then solve the governing equations at each element relative to its neighbors. A mesh face element is typically a triangle or quadrilateral with 3 or 4 nodes at each corner, respectively, and a mesh volume element is a polyhedron such as a tetrahedron (triangular faces, 4 total nodes) or a hexahedron (quadrilateral faces, 8 total nodes). Higher-order elements may subdivide each edge of planar or volume elements with additional nodes. Additional nodes add mesh resolution at the cost of increased computational expense.

Like CFD, many assumptions are required for solid mechanical modeling of biological tissues. Perhaps the single most important factor is the set of material properties applied to each tissue. Biological tissues are non-linear, viscoelastic, heterogeneous, nearly incompressible, and anisotropic. These properties are difficult to simulate on a lesion-specific basis, so tradeoffs must be weighed when formulating a solid mechanical model.

A variety of mathematical descriptions of the non-linear properties of vascular tissues exist. These are typically described by their strain-energy functions, and a number of possible constitutive formulations for hyperelasticity exist [12]. Most vascular and atherosclerotic tissues can be approximated with a bi-linear model, however, as tissues tend to accrue very little stress for low magnitudes of strain until a breakpoint is reached around 40 mm Hg of pressure, at which point stress increases nearly linearly with increasing strain [100]. Anisotropy of these tissues dictates that material properties have different effective magnitudes along different axes. Anisotropy is dictated by factors like fiber direction, such as alignment of collagen fibers, sarcomeres, or elastic lamina.

Tissues are primarily composed of water, which is incompressible within the normal physiologic range. Although this would imply that the tissues themselves are essentially incompressible, many FEA solvers cannot tolerate this condition. Thus, a Poisson's ratio of around $\nu$=0.49 is typically assumed. Atherosclerotic plaques are heterogeneousthey are not made of a single tissue type. Thus, FEA models must either actively delineate different homeogeneous material properties for different elements (and thus define whether any sliding can occur between adjacent regions) or use a rule-of-mixtures approach to approximate material properties for elements containing multiple materials

[56, 101].

When formulating a problem for FEA, one must define the problem's geometry as well as its boundary conditions. Sufficient boundary conditions must be defined to constrain the system. For example, in a 2D planar loading problem, at least one node's displacement must be constrained in each dimension lest the model float freely in space and have too many degrees of freedom to successfully solve. Nodal rotation boundary conditions may be assigned as well. However, constraining too many nodes may over-define the system and become difficult if not impossible to reach a solution. Forces may be applied either at a specific point as a concentrated load or distributed along an edge or face (in 3D). When relevant, other boundary conditions such as thermal, voltage, or magnetic properties of the system may be applied as well.

In FEA simulations experiencing large deformations or employing non-linear material properties, the problem is said to be non-linear, and requires additional consideration to reach an accurate solution. Among the most popular approaches for solving non-linear problems is the Newton-Raphson procedure. Here, loads are incrementally applied to the system, effectively creating a transient loading problem. For problems not modeling viscoelastic effects or creep, the speed of loading will not affect the solution, and thus this technique simplifies the solution process. Much like CFD, each step must be solved individually for the simulation to progress to the next. Convergence criteria must be defined for any iterative procedure such that the model may progress to its next step.

## *1.10 Summary*

Atherosclerosis is a multifactorial disease that leads to a considerable portion of all deaths annually. A complex combination of biology and mechanics are known to contribute to the progression and endpoints of the disease. Despite much focus by the research community, there is no cure for atherosclerosis, and we cannot yet predict who will suffer an atherothrombotic event, nor when. Well-characterized animal models are necessary to study the disease, and consideration into different phenotypes of the disease are necessary. Plaque rupture and plaque erosion tend to affect different demographics, and their mechanisms likely differ. Future research to better identify, treat, and eventually prevent atherosclerosis in humans will require focus and collaboration from both the

biology and the mechanics communities.

# CHAPTER II

## HYPOTHESIS AND SPECIFIC AIMS

Atherosclerosis, the formation of fibrous- and lipid-rich plaque on the walls of arteries, affects nearly all adults in the Western world and is a significant cause of morbidity and mortality. While most plaques cause no symptoms, any disruption of the plaque could cause a thrombus to form within the lumen of the artery, potentially leading to a vascular event such as myocardial infarction or stroke if the thrombus occludes blood flow. Plaque rupture, the event traditionally thought to be the cause of atherosclerosis-related thrombosis, is known to occur as a result of the interplay between biological and mechanical factors. Proteolytic enzymes such as matrix metalloproteinases (MMPs) can weaken the cap of the plaque, and local mechanical stresses become so great at the surface that the fibrous cap ruptures, exposing the thrombogenic necrotic core of the plaque to the blood pool.

However, two noteworthy exceptions to the plaque rupture phenomenon have presented themselves: plaques do not rupture in mice, and in humans, particularly women, some plaques will erode and form a thrombus without rupturing. The objective of this proposed research is to investigate these exceptions to the plaque rupture phenomenon from both a quantitative histological and a mechanical standpoint in order to provide insight toward the long-term goal of identifying and treating plaques that are likely to cause thrombosis.

Clear biochemical and anatomical differences exist between mice and humans. Differences in structure and shape of murine and human plaques may result in entirely different mechanical environments that could explain the atherosclerosis-prone mouse model's resistance to plaque rupture. Similarly, differences in structure and shape of atherosclerotic lesions that become disrupted in humans may explain the phenomenon of plaque erosion and its noted prevalence in women. All plaque disruption is a mechanical event, whether it is rupture of the fibrous cap or denudation of endothelial cells on the surface of a plaque. Therefore, a comprehensive examination of plaque biomechanics is essential to understand why some plaques erode, others rupture, and still others remain undisrupted.

## *2.1 Central hypothesis*

Plaques that do not rupture experience different hemodynamic and mechanical environments than plaques that are prone to rupture.

## *2.2 Approach*

Using a computational fluid dynamics (CFD) model of blood flow, we simulated wall shear stress (WSS) distribution, and with an established finite element analysis (FEA) model, we computed solid mechanical stresses within human coronary artery and mouse arterial walls. Both the CFD and the FEA models simulated vascular biomechanical stresses on a lesion-specific basis. Our overall approach was to use these models to evaluate how differences in plaque shape and composition affect stress distribution and relate to plaque rupture and plaque erosion. We also proposed to use quantitative histological staining to investigate how stress distributions correspond with tissue markers related to plaque disruption. Therefore, we investigated the following specific aims:

## *2.3 Aim 1: Solid Mechanical Modeling of Plaque Rupture in Mice*

*Determine the distribution of stresses in the walls of murine atherosclerotic lesions under physiological conditions and relate this to likelihood of rupture.*

We proposed to answer the question: Is there a biomechanical explanation for the lack of observed plaque rupture in murine atherosclerotic lesions? Plaque rupture in mice is a controversial topic, with published claims of spontaneous plaque rupture in mice disputed by other researchers. Using FEA to reconstruct the solid mechanical environment of mouse plaques, we attempted to determine how the relative distribution of stresses compares to that in human plaques. We also examined how morphological features like plaque shape and composition differ between mice and humans.

The specific hypothesis was: The composition and shape of plaques in mice is characteristically different from that in humans, which leads to a unique distribution of mechanical stresses between species.

To study this, we computationally studied histological cross-sections of "vulnerable" plaques from humans and mice. We analyzed the relative composition of the lesions, as well as the size and

shape of morphological features like the extent of lipid and the relative thickness of fibrous caps. We also computed the relative distribution of mechanical stresses to examine the location of local maxima of Von Mises stresses.

## *2.4 Aim 2: Role of Inflammation and Solid Mechanics in Plaque Rupture and Plaque Erosion*

*Investigate the distribution of mechanical stresses within vessel walls and on the plaque cap in plaque erosion and plaque rupture specimens.*

We proposed to answer the question: Can the difference in phenotypes between vulnerable and disrupted human plaques be explained by solid biomechanics? Plaque rupture has been well established as a phenomenon with both biological and solid mechanical causes. Plaque erosion, which has only been described recently, is thought to have biological causes. Whether solid mechanics plays a role as well is uncertain, as very little consideration of the subject has been published to date. Using FEA to calculate the relative distribution of Von Mises stresses in eroded, ruptured, "vulnerable", and stable human plaques, we investigated characteristic differences in the mechanical environments between the phenotypes. We also investigated if markers of proteins and biological processes spatially correlate with mechanical stresses, suggesting a possible mechanism for induction of the different plaque disruption phenomena.

The specific hypothesis was: Solid mechanical stresses and strains in the vessel wall are associated with inflammatory markers in plaque rupture but not in plaque erosion.

To study this, we obtained consecutive serial cross-sections of human coronary atherosclerotic plaques identified to have experienced plaque rupture or plaque erosion, or stable plaques characterized as thin- or thick-cap fibroatheromas. We stained one section for gross morphology using Movat's pentachrome, which we used to identify the different tissue types as input for our lesion-specific FEA computer model. We then stained serial sections for a variety of markers thought related to inflammatory and remodeling processes to seek possible correlation between mechanical stresses and expression of these markers.

## *2.5 Aim 3: Computational Fluid Dynamics Simulations of Flow in Plaque Erosion*

*Examine the local hemodynamic environment around plaques that demonstrate pathological features of erosion.*

We proposed to answer the question: Can the occurrence of erosion in human plaques be explained by hemodynamics? WSS has been studied extensively and is known to play a major role in atherogenesis. Several case studies have suggested that WSS may also have consequences for plaque rupture, but no similar role of WSS in plaque erosion has been studied to date. Plaque erosion may result from endothelial denudation, although the mechanism of endothelial cell loss in these patients is not known. One possible pathway for endothelial damage is through very high magnitudes of WSS. Given that plaque erosion is more prevalent in women and young men, and that women on average have smaller diameters of coronary arteries than men, flow is one possible explanation for induction of plaque erosion.

Therefore, our hypothesis was: Patients with plaque erosion will experience locally elevated WSS magnitude in regions where erosion has occurred.

We reconstructed coronary arteries of human patients in the Emory University catheterization lab with plaque rupture, plaque erosion, and stable plaques in order to compute the flow environment within these vessels. 3D reconstructions were made from biplane angiogram images of human coronary arteries confirmed to exhibit plaque erosion by OCT. We used CFD to calculate flow metrics like WSS and OSI to investigate an association between flow features and thrombus location in plaque erosion.

## *2.6 Significance and innovation*

Although atherosclerotic mouse models are widely studied, debate continues about whether mice can experience spontaneous plaque rupture. The goal of this model system is typically to recapitulate human physiological processes, but without widely-accepted evidence that plaques can spontaneously rupture, the mouse model is limited in its utility for studying plaque endpoints. Researchers frequently speak about a "vulnerable" phenotype of plaques in mice, but without evidence of spontaneous plaque rupture, this term incorrectly implies that mouse plaques are more or less stable under certain conditions. In this research, we examined the relative distribution of mechanical stresses in

murine plaques to better understand their propensity for spontaneous plaque rupture. Other groups have previously published studies of murine plaque mechanics, but ours considers a wider spectrum of acute and chronic models of atherosclerosis than prior work. We also directly compare mouse plaques to human plaques in order to draw conclusions about characteristic differences in plaque mechanics between the organisms. This study will help researchers to better understand how mice and men differ and discern whether using terms like "vulnerable plaques" to describe lesions in mice is appropriate.

Plaque erosion is a more recently-discovered phenomenon whose cause is not well understood. The role of solid and fluid mechanics in plaque rupture has been studied widely, but to date, almost no mechanical analysis has been performed on plaque rupture specimens. Our existing knowledge on plaque rupture is almost entirely biological. This research presents some of the first fluid and solid mechanical analysis of human coronary arteries that experienced plaque erosion and compares them directly to tissues that experienced plaque rupture as well as thin- and thick-cap fibroatheromas that are not disrupted. The goal of this analysis is a better understanding of the mechanism of plaque rupture and plaque erosion, which could eventually lead to improved diagnosis and even possible treatment before these events have led to fatality.

# CHAPTER III

# SOLID MECHANICAL MODELING OF PLAQUE RUPTURE IN MICE

Adapted from "Biomechanical Modeling and Morphology Analysis Indicates Plaque Rupture Due to Mechanical Failure Unlikely in Atherosclerosis-Prone Mice" by Ian C. Campbell, Daiana Weiss, Jonathan D. Suever, Renu Virmani, Alessandro Veneziani, Raymond P. Vito, John N. Oshinski, W. Robert Taylor. *Am J Physiol Heart Circ* (in press, Epub November 30, 2012).

## *3.1 Introduction*

Plaque rupture is a major cause of atherosclerosis-related thrombosis in the modern world that, despite concerted research efforts, still is not fully understood. Most knowledge of plaque rupture in humans comes from histological evaluation of autopsy specimens or from *in vivo* imaging of high-risk patients after plaque rupture has already occurred; neither technique has led to direct observation of plaque rupture in progress. Therefore, scientists are forced to study the etiology of plaque rupture either retrospectively in patients who already had a lesion rupture or prospectively in patients who may or may not provide evidence of rupture at a later date. Extensive morphological studies of histology specimens and mathematical modeling of biomechanics have led to identification of the thin-cap fibroatheroma (TCFA) as the atherosclerotic plaque phenotype currently thought to be most "vulnerable" to rupture [17].

Despite identification of this phenotype, it is still not possible to accurately predict rupture. Because longitudinal studies to identify rupture are impractical in humans, scientists frequently study atherosclerosis-prone mice, which are known to rapidly and reliably form atherosclerotic plaques over a period of weeks to months instead of years to decades, as is the case in humans. Rodents are naturally resistant to atherosclerosis, but a wide variety of techniques for inducing atherosclerosis exist [66]. As the mechanism behind each of these techniques is unique, the severity and specific characteristics of the atherosclerotic burden varies among models [66]. Among the factors modulated by researchers are transgenic strain (with the ApoE$^{-/-}$ and LDLr$^{-/-}$ being the most popular), diet (especially lipid composition), age, gender, and pharmaceutical agents (e.g. angiotensin II).

Angiotensin II induces hypertension, which is a common comorbidity of atherosclerosis in humans. However, much of the effect of angiotensin II on the vessel wall is proinflammatory [118]. Anatomic location of the plaque is another variable, as the brachiocephalic artery has been reported to produce lesions with some similarities to human "vulnerable" plaques [119]. Regardless of which permutation of conditions any particular research group uses, the overall goal is the same: to recapitulate features of human atherosclerosis in a mouse model to better understand the pathophysiology of the disease and, eventually, to develop treatments for its prevention and management.

In addition to the need for a robust animal model of atherosclerotic plaque formation, researchers desire a relevant animal model for the study of thrombotic endpoints such as plaque rupture. However, spontaneous plaque rupture in mice is a controversial topic [5–7, 73, 120, 121]. Several published reports of murine plaque rupture exist [122, 123], but others question whether plaque rupture is really occurring in mice, suggesting that reports may actually be sectioning artifact, intraplaque hemorrhage, or a completely different form of lesion disruption not seen in human plaques [6]. Bond and Jackson, who developed a putative mouse model of plaque rupture, contest these claims and suggest that a mouse model need not be morphologically identical to human plaques in order to be useful [77]. Many publications discuss "ruptured" and "vulnerable" plaques in mice, although a unifying definition of the phenomenon does not exist. Schwartz and colleagues have argued that, because the topic is so controversial, researchers avoid using the terms "vulnerable" and "stable" to describe phenotypes of murine plaques until the community better understands plaque disruption in mice [6].

Within this context, it is prudent to evaluate the morphological and mechanical stress differences between mouse and human plaques. In the existing literature, several morphological risk factors for human plaque rupture exist. The most well-known of such parameters is the thickness of the fibrous cap overlying a necrotic core, but others such as the size and shape of the necrotic core and the presence of microcalcifications embedded in the fibrous cap are emerging as well [23]. The functional consequence of these features is that a concentration of mechanical stress occurs on the fibrous cap or shoulders of the plaque, and if the magnitude of the stress is sufficient, the lesion will rupture [105]. Biological factors such as inflammation are closely associated with plaque rupture as well, but the final failure is, by definition, a physical, mechanical event. However, little is known

about whether these geometric and mechanical risk factors translate to mice. Histological inspection of murine plaques reveals distinct morphological differences from human atherosclerotic lesions, the most obvious of which is size: a mouse aorta's diameter is only a fraction of the diameter of a human coronary artery.

In this study, we set out to quantify the morphological and mechanical phenotypes across a range of mouse models. In order to consider the extremes of atherosclerosis-prone mice, on one end of the spectrum, we investigated a chronic, more intrinsic model of atherogenesis, and on the other end we equipped two popular strains of mice with an aggressive set of provocative factors for acute atherosclerosis. Here, we provide a side-by-side quantification of the morphological and mechanical stress distribution differences between mouse and human plaques. We hypothesized that the plaque extent and composition would be significantly different between mouse and human plaques. We further hypothesized that the relative distribution of locations of peak mechanical stress characteristically found in mice is different from that found in human atherosclerotic lesions.

## *3.2 Methods*

### 3.2.1 Mouse models

We considered three models of advanced atherosclerosis in mice, two of which acutely form plaques, and the other was a chronic model. The first acute model included 15 male ApoE$^{-/-}$ mice aged 8 weeks fed a high-fat (HF) diet (D12336, Research Diets, Inc.) for 8 additional weeks with simultaneous subcutaneous infusion of Angiotensin II (AngII) via osmotic minipump (0.75 mg/kg/day, Sigma Aldrich). The second acute model included 12 male LDLr$^{-/-}$ mice aged 8 weeks fed a HF diet for 8 additional weeks with AngII via minipump [69, 70]. The chronic model of spontaneous lesion formation included 12 male ApoE$^{-/-}$ mice fed a regular chow diet (LabDiet 5001 Rodent Diet, PMI) for 1 year without AngII. All animal research was approved by the Emory University Institutional Animal Care and Use Committee (IACUC).

### 3.2.2 Tissue harvest

One day preceding harvest, each animal's systolic blood pressure was recorded via tail-cuff measurement (BP-2000, Visitech Systems). Animals were harvested using humane euthanasia techniques (slow inhalation of $CO_2$). Upon expiration, animals were perfused with saline followed by

10% buffered formalin for 5 minutes at 80 mmHg (approximate diastolic blood pressure) by direct cardiac injection. Then, to preserve the conformation of the lumen as closely as possible, mice were then perfused with Batson's #17 Vascular Casting Compound (Polysciences) at each mouse's diastolic blood pressure (assumed to be 40 mmHg below the mouse's measured systolic blood pressure) in order to preserve the in vivo conformation of the lumen. Pressure was maintained using an IV pressure infuser (Infu-Surg, Ethox) and measured with an inline manometer. Upon hardening of the vascular casting compound, the aortic tree between the heart and the descending thoracic aorta was excised, fixed 48 hours in formalin, and then transferred to 70% ethanol.

### 3.2.3 Human specimens

Human coronary artery plaques of thin-cap fibroatheroma (TCFA) phenotype were selected from an existing tissue bank by an expert in cardiovascular pathology (Renu Virmani, CVPath Institute). Specimens were obtained as part of a consultation service for the Office of the Chief Medical Examiner of the State of Maryland. Fresh hearts were perfused with 10% neutral-buffered formalin at 100 mmHg for 15 minutes, and then the coronary arteries were excised and further fixed in formalin before embedding.

### 3.2.4 Histology and microscopy

Murine aortic specimens were embedded in methyl methacrylate (MMA) resin then sectioned at 5 μm using an automated rotary microtome. Consecutive serial sections were obtained at the brachiocephalic artery immediately distal to bifurcation from the arch and at three sites in the descending thoracic aorta each separated by approximately 1 cm. Tissues were deplasticized and stained to identify plaque morphology using a hybrid Masson's trichrome and Von Kossa's calcium staining technique [56]. Human specimens were embedded in paraffin, sectioned at 5 μm, and then stained with Movat's pentachrome. To ensure that the difference in stains between humans and mice did not bias our evaluation of the morphology, we stained 9 mouse sections (3 per phenotype) with Movat's pentachrome. Images of all stained slides were obtained via brightfield microscopy. Sections with major sectioning artifact were discarded.

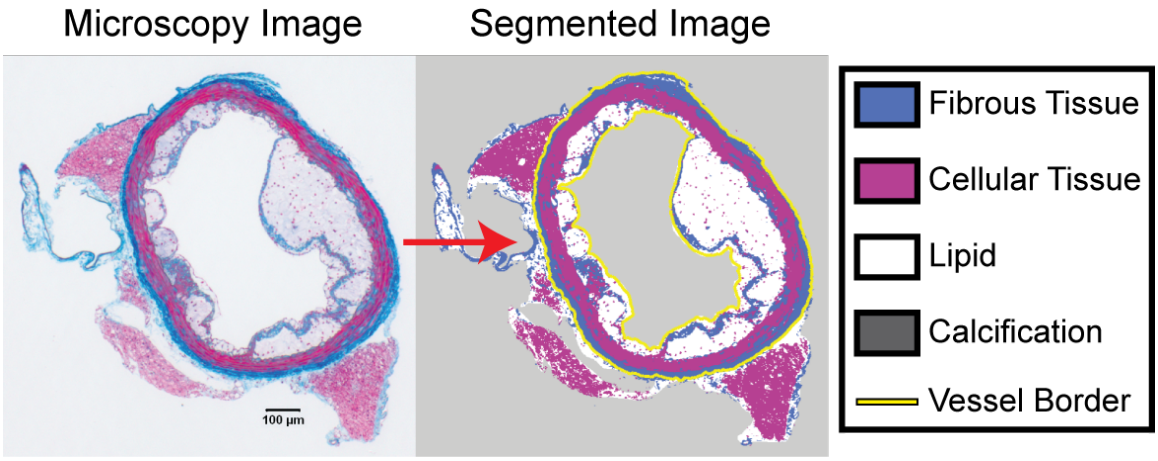


Figure 3.1: Semi-automated segmentation of atherosclerotic lesions: A sample cross-section of an atherosclerotic LDLr$^{-/-}$ mouse aorta stained with a combination of Masson's trichrome and Von Kossa's calcium stain. The microscopy image (left) was loaded into custom Matlab software and segmented (right) using a semi-automated algorithm. In brief, tissue types were automatically identified using a k-means clustering algorithm and then touched up (for example, to distinguish lipid from background) using an implementation of the Live Wire algorithm [125]. Perimeter of the lumen and adventitia were also identified with Live Wire (red line).

### 3.2.5 Image segmentation

We classified the tissue of atherosclerotic blood vessels into four primary components [56]: cellular tissue (primarily media), fibrous tissue, lipid, and calcification (Figure 3.1). Images were imported into custom image analysis software implemented in Matlab (R2011b) and segmented using *k*-means clustering based on staining color [124]. Manual revision, when necessary, was performed using an implementation of the Live Wire edge-detection algorithm [125].

### 3.2.6 Morphological analysis

We measured four morphological parameters and one histological parameter in our microscopy images using Matlab, shown in Figure 3.2. In brief, we traced the internal elastic lamina (IEL), external elastic lamina (EEL), and lumen border in all images. A method for accurately measuring tissue thickness developed by Yezzi et al. was used to compute the distance between any two contours [126], and the radius of each vessel was defined as the radius of the minimum bounding circle around the EEL. We calculated:

1. lesion coverage of the wall (defined as the fractional portion of the circumference of the vessel where the thickness between the IEL and lumen was non-zero)

2. plaque burden (the percent of the area inside the IEL containing lesion)

3. normalized mean lesion thickness, a measure of how far plaques protrude into the lumen (defined as the distance between the IEL and the lumen only where non-zero, normalized to media thickness, defined as the distance between the IEL and EEL)

4. normalized lesion eccentricity (the distance between the centroid of the lumen border contour and the EEL contour, normalized to vessel radius)

5. relative composition of the lesion based upon the segmented image (the lesion was defined as any tissue between the IEL and the lumen contour).

The statistical differences between models were computed by one-way ANOVA followed by Tukey's honestly significant difference test, with $\alpha$=0.05. Results are shown in Figures 3.6 and 3.7, and statistics are tabulated in Table 3.1.

### 3.2.7 Computational solid mechanics

We computed the relative distribution of stresses in each segmented vessel using an established lesion-specific computational mechanical modeling technique in Ansys 13.0 APDL software [56]. We used a 2D plane strain large deformation finite element model. The cross-sectional shape of each lesion was imported into Ansys and finely meshed with tens of thousands of elements. Based upon image segmentation, linear elastic isotropic material properties were calculated for each element using a constrained rule-of-mixtures approach [100,101]. We then simulated a pressure of 40 mmHg (representing the incremental pressure of the pulse from diastole to systole) normal to the lumen surface and calculated the relative distribution of Von Mises stress (Figure 3.3).

Our computational model is based upon an existing technique that we selected because of its ability to use high-resolution histology imagery to generate lesion-specific relative stress distributions [56]. Because model geometry is based upon tissue data pressure-fixed in its diastolic conformation, we are able to recreate the mechanical environment of the vessel resulting from the incremental pressure of each cardiac pulse. The downside to this technique is that, because the tissue is embedded for histology, we cannot derive residual stresses and therefore cannot compute exact stress magnitudes. As the deformations considered in our model are small compared to those

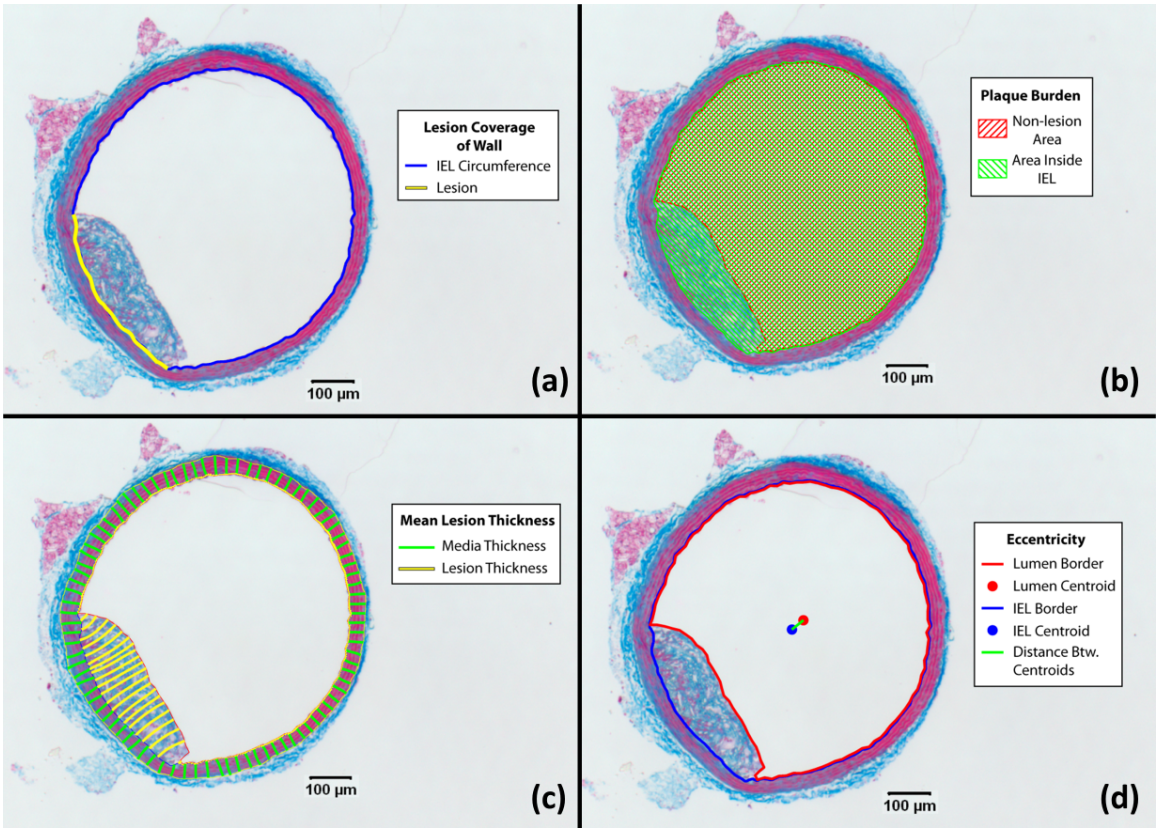


Figure 3.2: Measurement of morphological parameters from histology: Lesion coverage of wall (a) was defined as the percent of the vessel circumference with nonzero thickness between the internal elastic lamina (IEL) and the lumen border. Plaque burden (b) was defined as the percent of the area inside the IEL occupied by the lesion. Mean lesion thickness (c) was defined as the mean thickness of the lesion normalized to the mean thickness of the media [126]. Eccentricity (d) was defined as the distance between the centroid of the lumen border and the centroid of the IEL border, normalized to vessel radius.

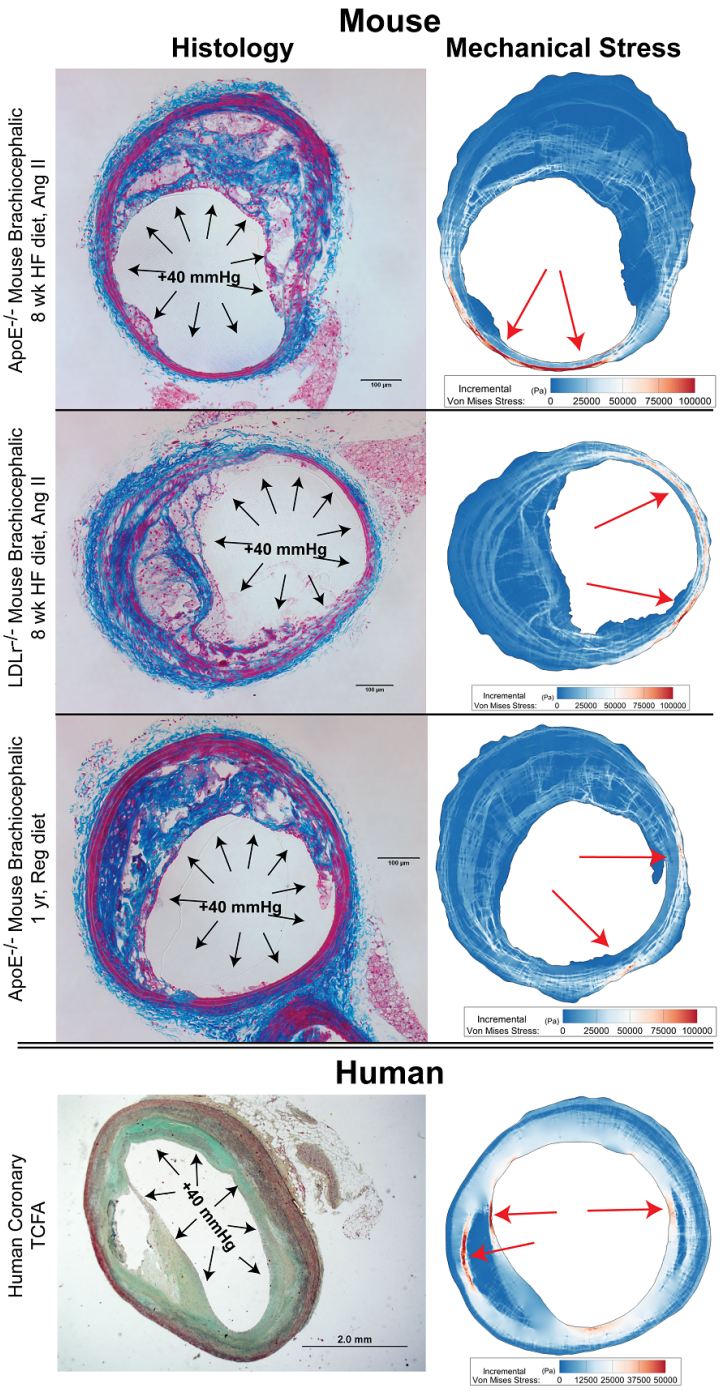


Figure 3.3: Computer model of stress distributions in plaques: We harvested atherosclerotic plaques from three different mouse models (top three rows) and obtained thin-cap fibroatheroma (TCFA) specimens from human coronary arteries (bottom row). Using finite element analysis techniques, we computed the distribution of solid mechanical stresses in each vessel cross-section. Local maxima of stress (red arrows) indicate that in mice, highest stresses are on the media and adventitia, particularly on plaque-free walls, whereas in humans, local maxima tend to be on the thin fibrous cap or shoulders of plaques. Tukey's honestly significant difference test results are noted for comparisons of brachiocephalic aorta vs. human coronary and all descending aortae pooled together vs. human coronary.

resulting from initial pressurization of the vessel, the relative distribution of stresses should be minimally affected by this missing pre-stress data. The relative distribution of stresses provides insight into the lack of plaque rupture in mice, and no published data on the stress magnitudes necessary to cause plaque rupture in mice exists, anyway.

Our model took advantage of several theoretical simplifications to exploit the properties of the system. Biological tissues are nonlinear, viscoelastic materials which are complex to represent theoretically [12]. However, because material properties are known to be approximately bilinear and because we only simulated the pressure range between diastolic and systolic blood pressure, material properties for each tissue component could be represented with a linear elastic modulus [100]. Higher order hyperelastic models, commonly used in simulations computing exact stress magnitudes, are inappropriate for our scenario because data on the unloaded vessel is unavailable to us.

For each element of the mesh, we applied linear elastic material properties based upon a constrained rule-of-mixtures approach [100, 101]. Mechanical properties for each of the four primary tissue components were derived by Beattie et al. [22]: lipid: $3.88 \times 10^5$ dynes/cm$^2$, cellular: $2.45 \times 10^6$ dynes/cm$^2$, fibrous: $1.82 \times 10^7$ dynes/cm$^2$, calcified: $1.07 \times 10^8$ dynes/cm$^2$. Based upon our segmented histology, we overlaid a fine-resolution mesh generated by Ansys software based upon the contours of the lumen and outer edge of the adventitia. For each element of the mesh, the rule-of-mixtures approach dictates that the effective elastic modulus is equal to the weighted average of the elastic moduli of tissue components present in that element. As the mesh was extremely fine, the majority of elements represented only a single tissue type.

Additionally, biological tissues have been shown to exhibit anisotropy, particularly along fiber directions [101]. Unfortunately, the atherosclerotic lesions that we are simulating are extraordinarily complex and protrude non-uniformly into the lumen. Without information on the specific fiber directions within the lesion, anisotropy is nearly impossible to model correctly, particularly in the traditional cylindrical coordinate system by which most anisotropic material properties in the literature are described. The cross-sections of the blood vessels in our study are only approximately circular, and therefore a polar coordinate system cannot be easily adopted.

### 3.2.8 Computational mechanical loading conditions

In our model, we simulated an incremental pressure of 40 mmHg normal to the lumen, equal to the difference in pressure between tissue fixed at 80 mmHg and a typical systolic blood pressure of 120 mmHg. Because the nonlinear material properties of arterial tissue are roughly bilinear, large deformations occur below 80 mmHg that yield very little stress [100]. Above the breakpoint in these bilinear material properties, minimal deformation occurs but large stresses accumulate. Thus, by fixing our tissue at 80 mmHg, we underestimate the overall magnitude of stress but input optimal starting geometry. Since the stress-strain relation is approximately linear in this region, simulating higher magnitudes of stress (for example, simulating an incremental pressure of 120 mmHg) will primarily affect the local stress magnitudes rather than distribution. Because we only considered stress distribution and not exact magnitudes in this study, we have minimized the limitation of missing patient-specific incremental stresses. Calculation of exact magnitudes of stress requires knowledge of residual stress as well as wall stresses from pressures below diastolic blood pressure. Estimation of residual stress requires destructive measurements of tissue, impossible for our banked dataset. Estimation of wall stresses from pressures below diastole is possible with inverse method techniques, but the relative contribution of these stresses is expected to be small based upon the approximately bilinear stress-strain relationship for these tissues. We can approximate the distribution of stresses in the wall from pulsatile blood pressure but not the exact magnitudes, which is why we only consider the relative distribution of stresses in the present study.

To overcome morphological distortion in the human specimens, cross-sections were digitally pre-inflated. This technique resulted in more circular lumens as would be found in vivo and eliminated stress and strain concentrations at sites of steep bending not associated with features of the plaque, presumed to be tissue processing artifacts. After 10 iterations of this pre-inflation technique, stress and strain concentrations at sites of presumed histology artifacts disappeared, but stress and strain concentrations located at sites associated with plaque morphology (on the thin fibrous cap, plaque shoulders near the lipid core, etc.) remained. Sensitivity analysis revealed that results were unaffected after about 10 pre-inflation iterations.

### 3.2.9 Postprocessing analysis

We examined the relative distribution of stresses by mapping sites of highest stress by plotting each Von Mises stress distribution in Tecplot 360 software. We displayed stresses greater than a threshold value, defined as the vessel's mean stress + 4 standard deviations. The locations of stresses greater than this threshold were tallied based upon their location (Figure 3.4): fibrous cap over lipid core, shoulder of plaque, elsewhere on or in plaque other than fibrous cap over lipid core, or on media/adventitia. Media was defined as a circular ring staining positively for cellular tissue (red in Masson's trichrome), and adventitia was defined as all contiguous tissue outside the EEL. Contiguous tissue between the IEL and the lumen was considered plaque, with fibrous cap over lipid core specifically defined as fibrous tissue (blue in Masson's Trichrome) forming a thin strip separating lumen from lipid. Plaque shoulder was defined as the zone where fibrous or cellular tissue of a plaque meets the media at the periphery of the plaque. For each section, we quantified the location of stress peaks, recording a binary tally for the presence of a local maximum of stress in each region of each section. Some sections had multiple local maxima but were only counted once per location per section: for example, a plaque with one local maximum on the shoulder of the plaque and two distinct peaks in the media would receive one tally for the shoulder and one for the media. The threshold of 4 standard deviations was determined empirically as the highest integer multiple of the standard deviation that identified at least one local maximum per section. To ensure that our choice of stains (Masson's trichrome and Von Kossa's calcium in mice and Movat's pentachrome in humans) did not affect our stress analysis, we performed identical analysis on consecutive serial section pairs stained with both protocols and confirmed that the tallies of local maxima of stress were exactly identical (Figure 3.5).

### 3.2.10 Plaque cap thickness analysis

In only the subset of lesions exhibiting a local maximum of stress located on a fibrous cap over lipid-rich core, we computed the thickness of the fibrous cap at the site of peak stress relative to the mean thickness of the media around the entire vessel [126]. Differences between groups were assessed using an unpaired, two-tailed $t$-test with $\alpha$=0.05 and Bonferroni correction for multiple comparisons.

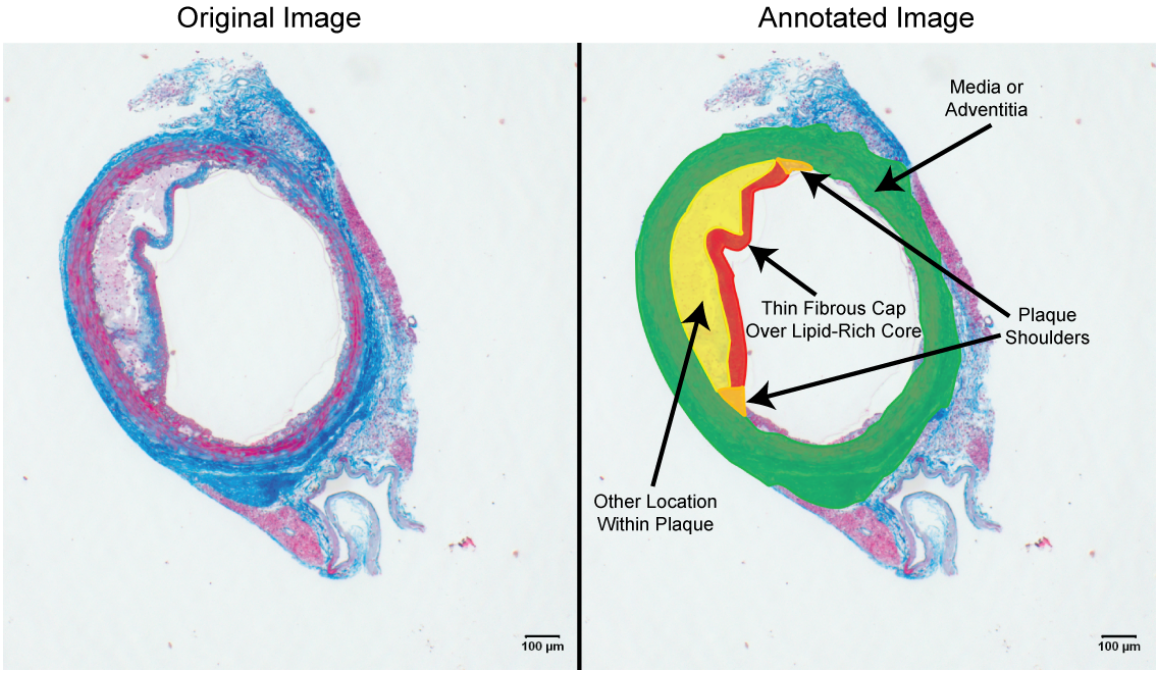


Figure 3.4: Annotation of locations: We identified the location of local maxima of Von Mises stresses (Figure 3.3) according to several anatomic criteria, denoted here. Peak stresses were either identified as being located on a thin fibrous cap over a lipid-rich core or plaque shoulders, the two locations where plaque rupture are known to occur in human lesions, or on the media or adventitia or elsewhere in the plaque. Tukey's honestly significant difference test results are noted for comparisons of brachiocephalic aorta vs. human coronary and all descending aortae pooled together vs. human coronary.

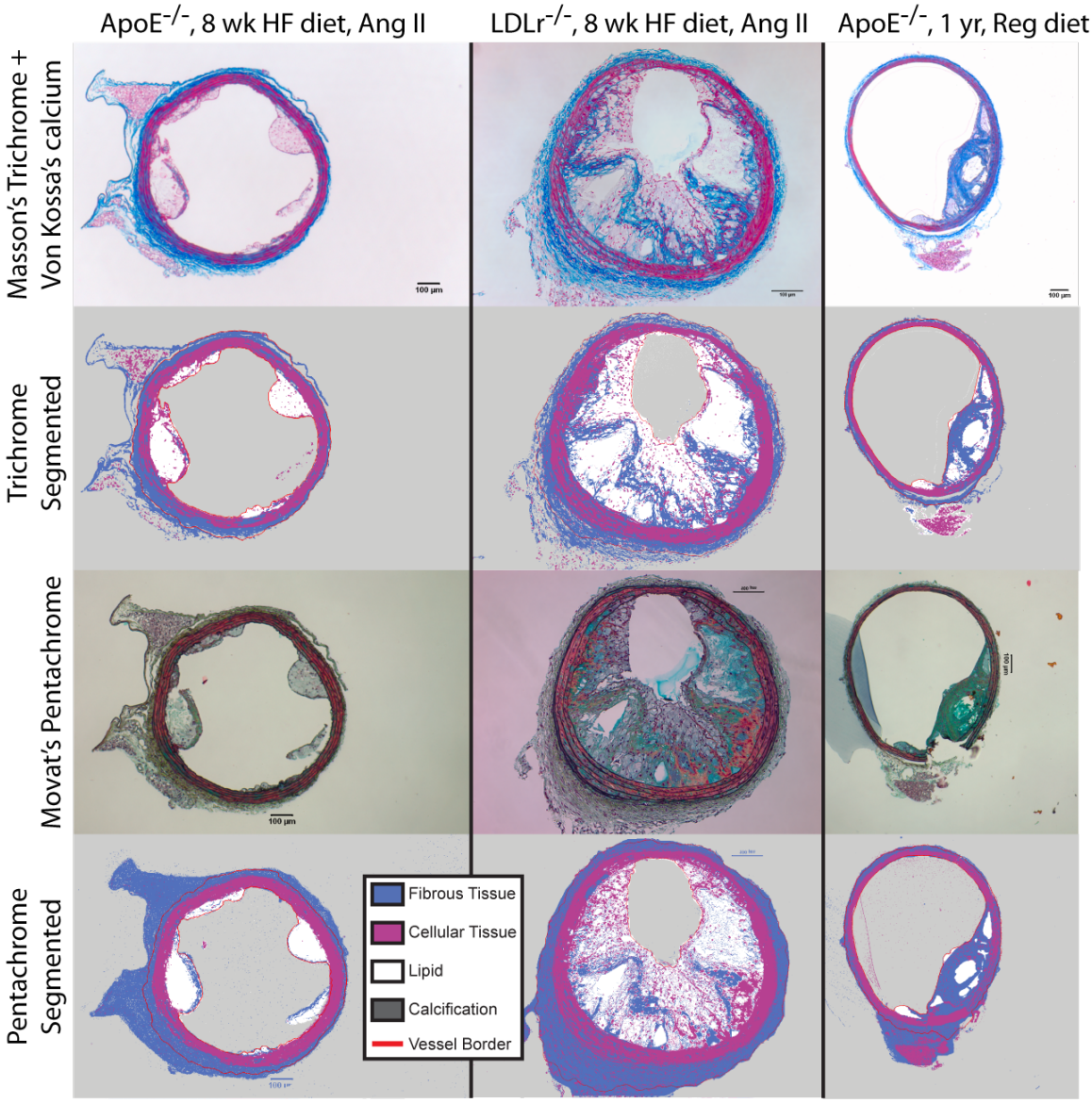


Figure 3.5: Validation of staining protocols: We stained consecutive serial sections of mouse tissue with Masson's Trichrome and Von Kossa's calcium protocols (top) and with Movat's Pentachrome protocol (bottom). Here, representative images paired with their segmentation demonstrate qualitative agreement. The location of local maxima of stress (not shown) did not differ between specimens. Only tissue inside the lines marked "vessel border" was included in our study, so periadventitial segmentation differences will not affect results. A representative problem with the Movat's pentachrome stain in our tissues is visible in the LDLr$^{-/-}$ and older ApoE$^{-/-}$ specimens: the vascular casting compound absorbed dye, partially obscuring nearby tissue.

### 3.2.11 Calcification analysis

To assess of the presence of microcalcifications, we scanned the brachiocephalic arteries and descending aortas of a subset of our mice (3 LDLr$^{-/-}$ fed HF diet for 8 weeks with AngII and 3 ApoE$^{-/-}$ fed regular diet for 1 year) using microCT (μCT 50, Scanco Medical, Brttisellen, Switzerland). Tissues were scanned in 70% ethanol. A positive control scan of hydroxyapatite powder (Fisher Scientific) was analyzed with scanning electron microscopy (DS-130F, Topcon Positioning Systems, Livermore, CA) to determine its particle size. This powder was then scanned with microCT to confirm the equipment's ability to resolve microcalcifications. Additionally, adjacent sections of the ascending aorta were stained with alizarin red to further confirm the presence of calcium.

## *3.3 Results*

We computed morphological metrics and relative stress distributions in plaques without significant sectioning artifacts from mice without premature mortality. In total, we evaluated plaques from 10 young ApoE$^{-/-}$ mice, 11 young LDLr$^{-/-}$ mice, and 11 old ApoE$^{-/-}$ mice. Mortality was highest for the group of young ApoE$^{-/-}$ mice, with 10 mice expiring within 10 weeks. This animal model has previously been reported to experience aortic aneurysms and dissection at approximately this rate [70, 127]. One LDLr$^{-/-}$ mouse expired prematurely, and one older ApoE$^{-/-}$ developed dermatitis and was sacrificed. We evaluated brachiocephalic, proximal descending thoracic aorta, mid descending thoracic aorta, and distal descending thoracic aorta plaques totaling 34 sections in young ApoE$^{-/-}$ mice, 42 sections in young LDLr$^{-/-}$ mice, and 49 sections in old ApoE$^{-/-}$ mice. In humans, we evaluated 11 coronary plaque sections.

### 3.3.1 Morphology Analysis

In all four morphological metrics we examined, atherosclerotic plaques from each of the three mouse models were significantly smaller than human lesions. Murine lesions covered less of the wall, plaque burden was lower, the normalized mean lesion thickness was lower, and the normalized eccentricity of plaques was lower. Results are shown in Figure 3.6, and statistics are tabulated in Table 3.1. In all mouse models, the brachiocephalic artery had greater plaque burden, normalized mean lesion thickness, and normalized eccentricity from any of the descending aorta plaques we

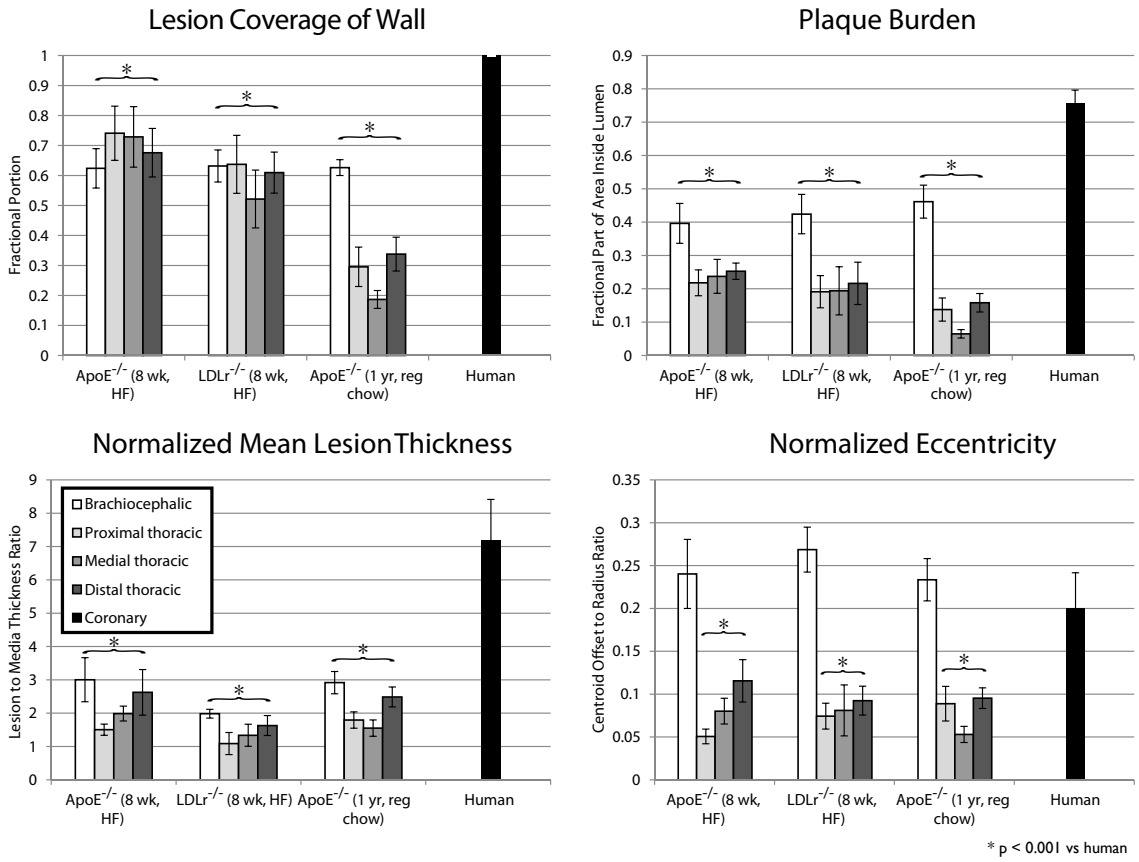


Figure 3.6: Morphological measures of murine and human plaques: Geometric features of atherosclerotic plaques were measured from histology specimens of lesions from humans and mice. Error bars represent standard error.

considered, and the difference sites in the descending aorta were mostly not different from one another. In the chronic model of plaque formation, the brachiocephalic artery lesions covered a greater fraction of the wall than the descending aorta plaques, but this trend was not observed in either of the acute models.

The relative composition of human plaques was different from murine plaques, as well. Human plaques were, on average, significantly more fibrotic and calcified and contained less cellular tissue than mouse plaques. The foam cell/necrotic core content was significantly higher in young mice than in humans, but our chronic ApoE$^{-/-}$ mouse model was not significantly different in lipid content than human coronary plaques. Differences are shown in Figure 3.7, and statistics are tabulated in Table 3.1.

Table 3.1: Statistical results from Tukey's honestly significant difference post hoc test for morphological metrics. P-values are shown for comparisons among the following groups: yA: young ApoE$^{-/-}$, yL: young LDLr$^{-/-}$, oA: old ApoE$^{-/-}$, H: human

| **Metric** | **yA v yL** | **yA v oA** | **yL v oA** | **yA v H** | **yL v H** | **oA v H** |
|---|---|---|---|---|---|---|
| Percent of wall covered with lesion | 0.29219 | < 0.00001 | 0.00010 | 0.00198 | 0.00001 | < 0.00001 |
| Plaque burden | 0.97702 | 0.14574 | 0.27482 | < 0.00001 | < 0.00001 | < 0.00001 |
| Lesion thickness | 0.19357 | 0.99999 | 0.14242 | < 0.00001 | < 0.00001 | < 0.00001 |
| Eccentricity | 0.95805 | 0.98027 | 0.77581 | 0.09288 | 0.17335 | 0.04070 |
| % Fibrous | 0.11130 | 0.00146 | < 0.00001 | < 0.00001 | < 0.00001 | 0.00445 |
| % Lipid | 0.00036 | 0.00138 | < 0.00001 | 0.08164 | < 0.00001 | 0.99999 |
| % Cellular | 0.30812 | 0.99999 | 0.25562 | 0.00044 | 0.01725 | 0.00029 |
| % Calcium | 1.00000 | 0.84934 | 0.83289 | < 0.00001 | < 0.00001 | 0.00001 |

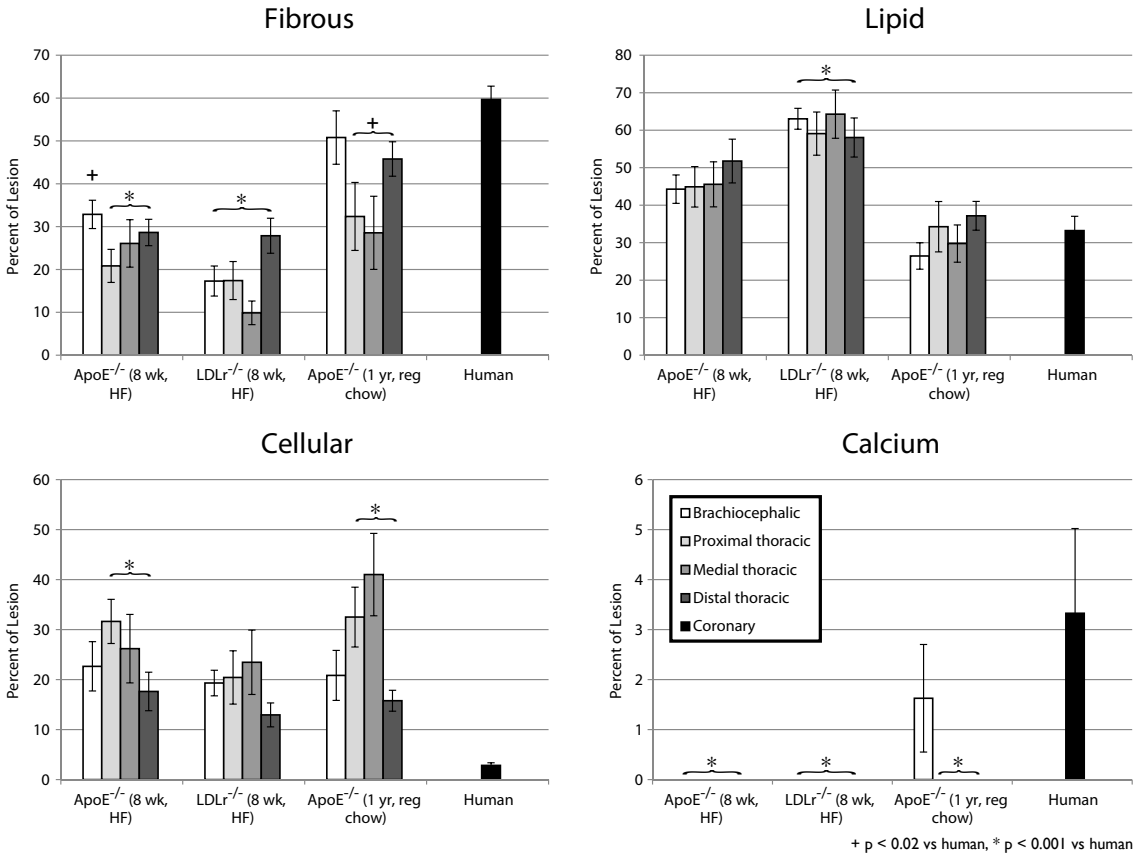


Figure 3.7: Relative composition of atherosclerotic plaques in mice and humans: Based upon segmented atherosclerotic plaques (Figure 3.1), we calculated the relative composition of lesions for humans and mice. Error bars represent standard error.

Table 3.2: Tally of stress concentration locations

| | Total Sections | Fib. Cap Over Lipid Core | Shoulder of Plaque | Inside Plaque | Media or Adv. |
|---|---|---|---|---|---|
| **ApoE$^{-/-}$ (8 wk HF, AngII)** | 34 | 4 | 2 | 7 | 34 |
| Brachiocephalic | 9 | 0 | 2 | 3 | 9 |
| Proximal Descending | 9 | 1 | 0 | 2 | 9 |
| Medial Descending | 10 | 2 | 0 | 1 | 10 |
| Distal Descending | 6 | 1 | 0 | 1 | 6 |
| **LDLr$^{-/-}$ (8 wk HF, AngII)** | 42 | 4 | 0 | 5 | 42 |
| Brachiocephalic | 11 | 0 | 0 | 2 | 11 |
| Proximal Descending | 10 | 0 | 0 | 3 | 10 |
| Medial Descending | 10 | 0 | 0 | 0 | 10 |
| Distal Descending | 11 | 4 | 0 | 0 | 11 |
| **ApoE$^{-/-}$ (1 yr reg chow)** | 49 | 0 | 2 | 7 | 49 |
| Brachiocephalic | 8 | 0 | 1 | 3 | 8 |
| Proximal Descending | 11 | 0 | 0 | 1 | 11 |
| Medial Descending | 10 | 0 | 0 | 0 | 10 |
| Distal Descending | 20 | 0 | 1 | 3 | 20 |
| **Total Mice** | 125 | 8 | 4 | 19 | 125 |
| Brachiocephalic | 28 | 0 | 3 | 8 | 28 |
| Proximal Descending | 30 | 1 | 0 | 6 | 30 |
| Medial Descending | 30 | 2 | 0 | 1 | 30 |
| Distal Descending | 37 | 5 | 1 | 4 | 37 |
| **Human TCFA** | 11 | 10 | 1 | 2 | 4 |

### 3.3.2 Mechanical Analysis

In mice, only 8 of 125 (6.4%) sections had high stress regions on a thin fibrous cap over a lipid core, while all 125 of 125 (100%) plaques examined had regions of peak stresses located in the media and adventitia. All lesions with local maxima of stress on the fibrous cap were located in the descending aorta, not the brachiocephalic artery. Four of 125 (3.2%) lesions had stress peaks on the plaque shoulder, most of which were in the brachiocephalic artery, and 19 of 125 (15.2%) had stress peaks inside the plaque. By contrast, in humans, 10 of 11 (90.9%) of plaques had regions of peak stress on the thin fibrous cap over a lipid core, and the 1 section without a peak stress region on the fibrous cap exhibited a concentration of stress on the plaque shoulder (9.1% of 11 lesions). 4 of 11 (36.4%) of regions of stress peaks were on the media or adventitia, and 2 of 11 (18.2%) had a local maximum of stress inside the plaque itself. Results are tabulated in Figure 3.8 and Table 3.2.

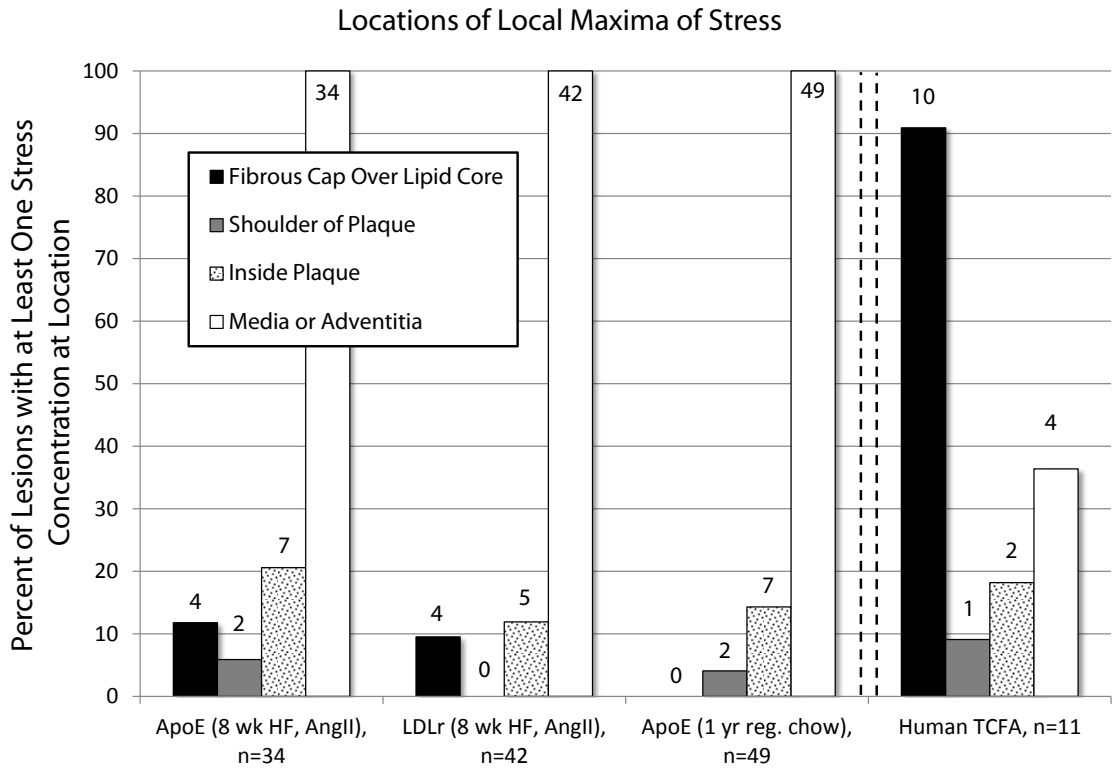


Figure 3.8: Locations of local maxima of stress: After computational solid mechanical modeling of Von Mises stress distributions in atherosclerotic plaques, we quantified the percentage of vessels exhibiting local maxima of stress in specific locations. A local maximum was defined as stresses greater than 4 standard deviations above the vessel's mean stress. Very few mouse vessels exhibited peak stresses in a fibrous cap over lipid-rich core, whereas nearly all human thin-cap fibroatheromas (TCFA) did. By contrast, every single mouse vessel had peak stress in the adventitia or media, whereas less than half of human plaques did. Mice were fed high-fat (HF) or regular chow (reg. chow) diets, and some mice received Angiotensin II (AngII). Above each bar is the raw number of vessels with a local maximum at the specified location.

### 3.3.3 Fibrous Caps

The relative thickness of murine lesions experiencing a stress peak on the fibrous cap was higher or indistinguishable from that in humans. In young ApoE$^{-/-}$ mice, the mean relative thickness (ratio of fibrous cap thickness at site of peak stress to mean media thickness) was 0.842 ± 0.105 (n=4 mice with local maximum stress on fibrous cap, mean ± SEM cap thickness: 29.8 ± 4.0 μm, media thickness: 35.3 ± 1.0 μm), in young LDLr$^{-/-}$ mice, the mean ratio was 0.322 ± 0.056 (n=4, mean ± SEM cap thickness: 11.8 ± 1.9 μm, media thickness: 37.2 ± 1.4 μm), and in human coronary arteries the mean ratio was similar at 0.349 ± 0.025 (n=11, mean ± SEM cap thickness: 43.8 ± 2.4 μm, media thickness: 156.3 ± 7.3 μm). The difference in relative thicknesses between humans and young ApoE$^{-/-}$ mice was significant (p=0.019), but between humans and young LDLr$^{-/-}$ mice was not (p=0.867).

### 3.3.4 Micro and macrocalcifications

We observed histologically the presence of macrocalcifications in the brachiocephalic artery in our chronic model of plaque formation, the ApoE$^{-/-}$ mouse aged one year on a regular chow diet (Figure 3.9). We did not observe similar macrocalcifications in either of our 8-week mouse models. Putative microcalcifications, by contrast, were observed in all three mouse models with both Von Kossa and alizarin red stains (Figure 3.10). In our histological examination of the ascending aortas in our mice, we observed punctate positive staining for calcium on the aortic valve leaflets.

In microCT analysis of our older ApoE$^{-/-}$ mice (chronic model), regions of radiodensity similar to the hydroxyapatite powder (positive control) were present, including isolated voxels of positive signal that would appear to be "microcalcifications" (Figure 3.11). Whether these were located within the thin fibrous cap as proposed by Vengrenyuk et al. [113] cannot be discerned due to low contrast between tissue and surrounding ethanol. Similar positive speckling was not observed in any samples of the acute model we scanned.

## *3.4 Discussion*

The major findings of this study are that the shape, size, and composition of atherosclerotic plaques are different between mice and humans, and as a result, the relative distribution of solid mechanical

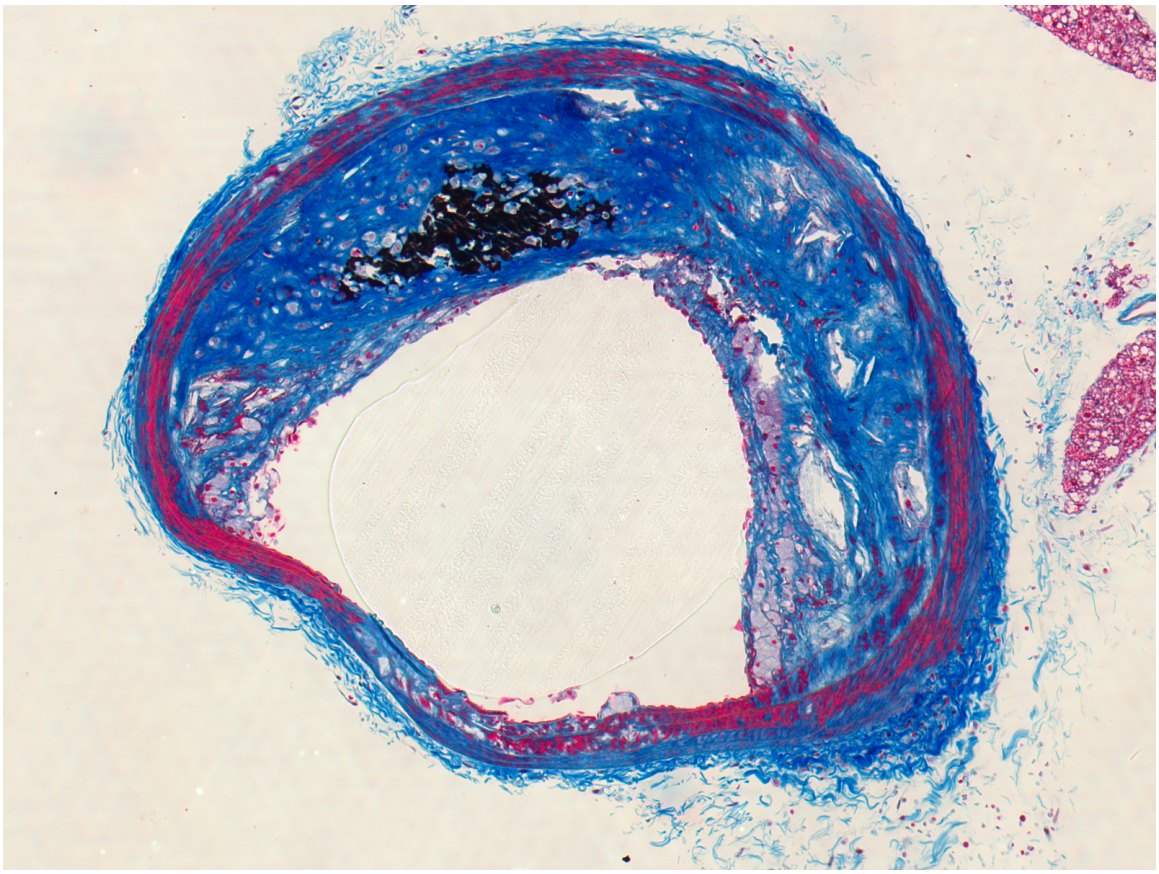

Figure 3.9: Macrocalcification in the brachiocephalic artery of ApoE$^{-/-}$ mouse: Von Kossa's calcium stain was performed in conjunction with a modified protocol for Masson's Trichrome, so black stain is positive for calcification.

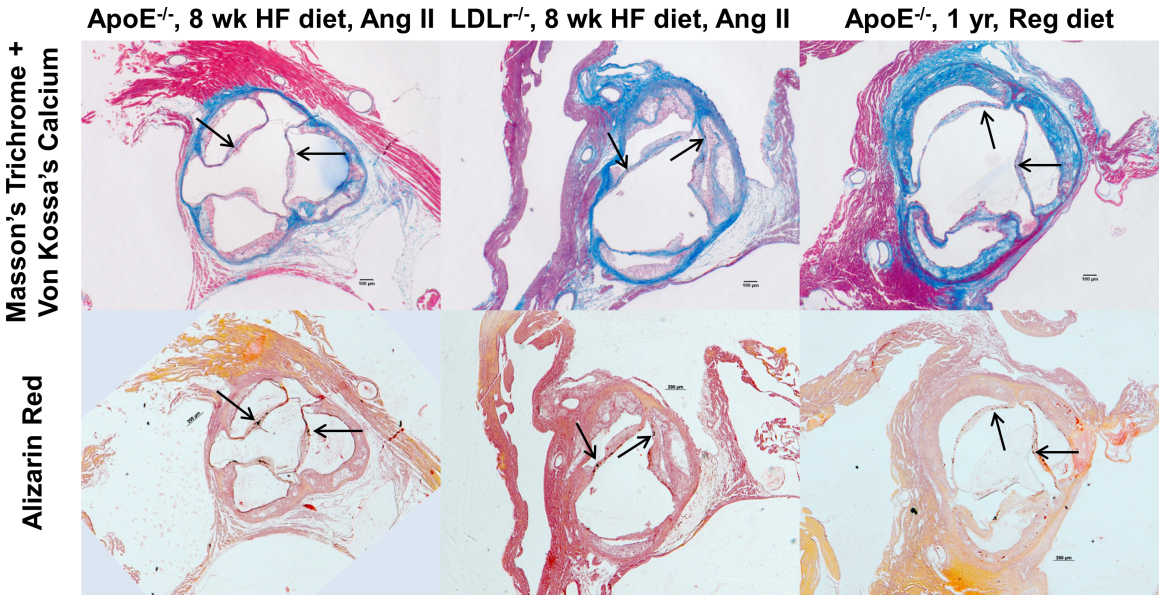


Figure 3.10: Microcalcifications in the ascending aorta of mouse models: Microcalcifications are visible in (left) ApoE$^{-/-}$ (8 wk HF diet, AngII), (middle) LDLr$^{-/-}$ (8 wk HF diet, AngII), and (right) ApoE$^{-/-}$ (1 yr, regular chow diet) mouse models as confirmed by Von Kossa's calcium stain (top row) and alizarin red stain (bottom row).

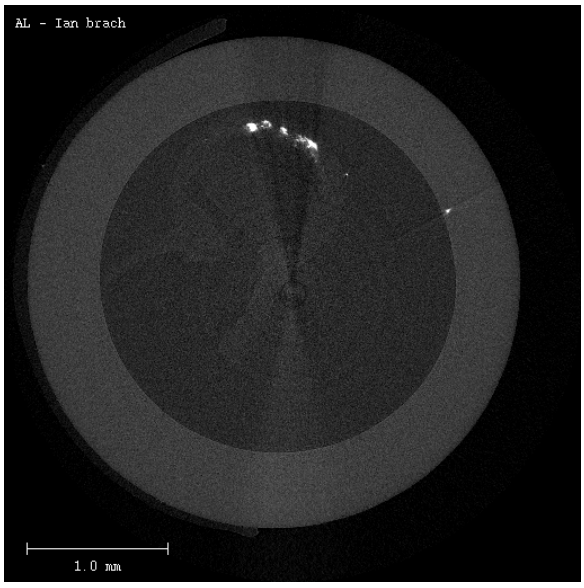


Figure 3.11: MicroCT reveals calcifications in mouse artery: Small white speckles in this older ApoE$^{-/-}$ mouse at the brachiocephalic bifurcation indicate the presence of calcium. The vessel wall is very faint, so precisely identifying where inside the lesion these calcifications lie is difficult.

stresses in mice does not result in local maxima on a thin fibrous cap over a lipid-rich necrotic core, as is the case in humans. Therefore, our results demonstrate that atherosclerotic lesions in mice and men have significant morphological and mechanical differences. Given the differences in genes, vessel diameter, posture (which implicitly may affect the blood flow patterns that modulate lesion progression), time course, and location of lesions, a distinction between mice and humans is not unreasonable to expect. However, the consequences of these dissimilarities suggest that other characteristics of lesions, such as propensity for plaque rupture, may be different as well. As a link between lesion morphology and mechanical environment has been established, we felt that a direct comparison of the mechanical differences between human and murine plaques was prudent [23].

Our mechanical analysis is based on an established technique for calculating the relative distribution of stresses from histology specimens [56]. We selected Von Mises stress as our metric because it approximates the magnitude of the local stress tensor at any given point and because it has been associated with inflammatory processes that may underlie the biological basis of plaque rupture [56]. Here, we showed that the relative distribution of solid mechanical stresses in mice is such that the highest stresses are on the media and adventitia rather than on the thin fibrous cap of atherosclerotic lesions. By contrast, our results demonstrate that human plaques experience these highest stresses on the fibrous cap or shoulders of the lesion, in line with current understanding of the mechanics of plaque rupture [62]. The nature of our model is a relative analysis of the wall stress distribution, so we have no way of knowing if these localized concentrations of high stresses are of sufficient magnitude to disrupt the tissue. What the relative distribution of stresses can tell us, however, is that because stresses are highest on media and adventitia, these mice would be susceptible to whole-vessel aortic or carotid rupture before any intra-plaque rupture resulting from lumenal blood pressure might occur. Such catastrophic vessel bursting has not, to our knowledge, been reported in these mouse models. Therefore, spontaneous plaque rupture, if it is possible in mice, seems unlikely to be driven solely by the overall mechanical environment.

From a purely mechanical perspective, the fact that stresses are locally the highest on the thin, plaque-free portions of the wall in mice is not unexpected. The punctate distribution of plaques in mice, which in our models tended to be primarily focal, almost like lipid-rich growths adhered to the surface of otherwise healthy media and adventitia, is a key difference between mouse and

human lesions. The highly focal distribution of plaques in mice was especially noticeable at the brachiocephalic bifurcation from the aortic arch, a site where many investigators have searched for evidence of murine plaque rupture. Lesions in the brachiocephalic artery were always located on the upstream side of the bifurcation (where low and oscillatory shear stress occur), while the downstream wall never formed neointima [128]. Maximum stresses were distributed on the healthy, thin wall and were of much lower magnitude within the lesion itself. Whereas in humans, some amount of fibrotic neointimal hyperplasia is frequently observed on all portions of the wall (100% of the human coronary lesions in this study had complete circumferential hyperplasia), our mouse models did not recapitulate this feature of the lesions, which likely influences the distribution of mechanical stresses.

The time scale of plaque formation may be a plausible explanation for this phenomenon. In humans, plaques, particularly those of the TCFA phenotype, develop over a period of 40-70 years, orders of magnitude longer than the lifespan of even our chronic mouse model of atherosclerosis. In humans, this gradual plaque formation results in "Glagov remodeling" wherein lesions remodel outward and preserve lumen diameter until the plaque burden has reached a certain threshold, at which point the plaque begins to encroach upon the lumen [44]. In many of our mouse plaque specimens, which were pressure-perfused with a vascular casting compound in an attempt to histologically preserve the relative in vivo conformation of the vessel, we could closely circumscribe a circle around the EEL (Figure 3.12). The circular media with lesions protruding into the lumen suggests that Glagov remodeling may not be recapitulated in our mouse models, which is further evidence that mouse plaques are morphologically and mechanically different from human plaques.

Another noteworthy morphological difference with mechanical implications between mice and men is that of the fibrous cap. A current criterion for a TCFA in human arteries is a fibrous cap thinner than 65 microns. In mice, whose vessels and plaques are much smaller than in humans, almost every fibrous cap is below this threshold, and yet plaque rupture is certainly not as prevalent as in humans. Although peak stresses occasionally occurred on the surface of murine lesions (6.4%), these almost never coincided with the presence of a thin fibrous cap over a lipid-rich region of the plaque. In humans, current understanding of the mechanics of plaque rupture is that peak stresses on the thin fibrous cap or its shoulders lead to tissue disruption [62]. Our mechanical model

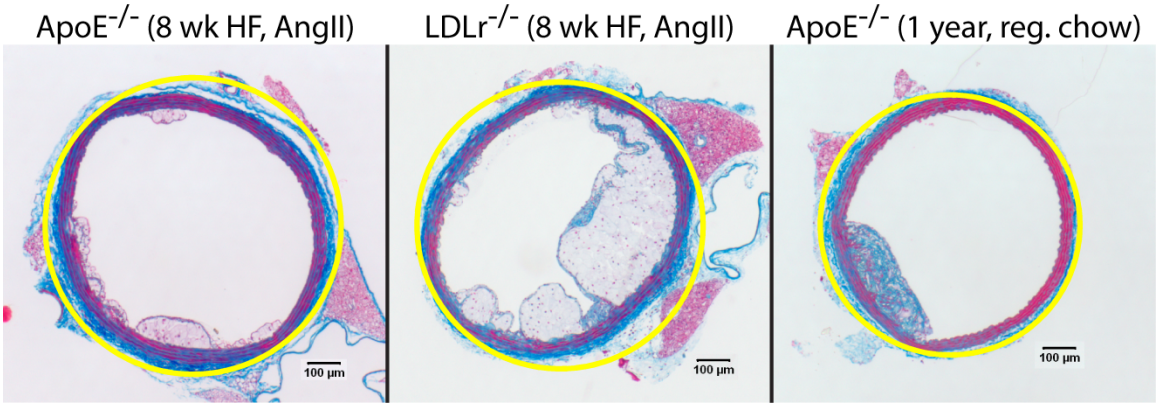


Figure 3.12: Glagov remodeling does not occur in some mouse plaques: The minimum bounding circle circumscribed around the external elastic lamina (yellow line) in pressure-fixed mouse aortas very closely approximates the geometry of the media. Atherosclerotic lesions in these vessels protrude inward from the media into the lumen rather than remodeling outward to preserve the shape and diameter of the lumen, in contrast with the Glagov theory of remodeling in humans [44].

recapitulated this finding, with 100% of human TCFA specimens demonstrating a local maximum of stress on the fibrous cap or its shoulders. In mice, however, local stress concentrations did not appear to be associated with the presence of a thin fibrous cap. We observed numerous thin fibrous caps in mice without a local maximum of stress on that site, and the few stress concentrations we observed that were adjacent to the lumen occurred on relatively "thick" caps. Additionally, none of the murine plaques with superficial stress concentrations were brachiocephalic plaques, suggesting that if spontaneous plaque rupture can occur in mice, this may not be the best candidate site. Buried fibrous caps, which some have proposed are evidence of prior rupture that has healed, were present in many of our murine specimens (for example, see Figure 3.3, upper left) [129]. Because histology is simply a snapshot in time, we cannot comment on the history of these plaques beyond observing that some buried fibrous caps are indeed present and that they did not seem to be host for local maxima of stress, either.

In addition to differences between mice and humans, we observed differences in morphology and composition among our mouse models. Fibrous caps experiencing a local maximum of stress were different between our two young mouse models, with both the absolute and relative thickness lower in LDLr$^{-/-}$ mice, perhaps due to a different rate of fibrotic processes. Plaques from LDLr$^{-/-}$ mice contained more lipid and less fibrous tissue than either of their ApoE$^{-/-}$ counterparts, suggesting that fibrotic processes may differ between these genetically distinct mice.

Although we considered both acute and chronic models of plaque formation in mice, lesions shared quantitative morphological similarities among all three models. For all four morphological metrics we considered, brachiocephalic plaques were similar to other models' brachiocephalic plaques, and other than the amount of the wall covered by lesion, descending aortic plaques were morpholologically similar to other models' descending aortic plaques. In the descending aorta, plaques in older ApoE$^{-/-}$ mice cover less of the wall than their younger counterparts. Considering that some rupture studies investigate murine brachiocephalic plaques because of purported similarity to human coronary plaques, the difference in magnitude of morphological metrics between mice and humans is striking.

Calcification is another morphological feature potentially tied to plaque rupture [114]. That we saw extensive calcification (Figure 3.9) only in our older mice and not in either of our 8-week mouse models suggests that formation of macrocalcification only occurs on longer timescales (such as that of humans, where plaques form over decades). We did not include the ascending aortas of mice in our mechanical analysis because of the extra complication of modeling the valve leaflets and because there is little evidence of purported plaque rupture in mice at this site, but there we observed tiny, punctate calcifications (we avoid definitively calling them microcalcifications because no established definition of the phenomenon exists that can be applied to mice) with both histology and microCT. In humans, valve calcification is regarded as a different pathophysiology as atherosclerosis, so it is unclear if the presence of these tiny calcifications in both the valve leaflet and around the lipid-laden cells on the leaflet are relevant for our understanding of plaque rupture. We did include the effects of calcifications in our modeling technique, but we saw only evidence of macrocalcifications in our particular sections. A recent study by Maldonado et al. observed microcalcifications in 9 of 92 specimens, so given our sample size of 11 human coronary arteries, the absence of microcalcificiations is not unexpected [114].f

Our findings agree with and build upon previous studies investigating the solid mechanics of murine blood vessels from Broisat et al. [130] and Vengrenyuk et al. [131]. Vengrenyuk et al. investigated how fibrous cap thickness affected stress magnitude in ApoE$^{-/-}$ mouse plaques, although the threshold magnitude for rupture to occur is not known [131]. More recently, Broisat et al. studied the solid mechanics of brachiocephalic plaques in female ApoE$^{-/-}$ mice of varying ages

and found that the distribution of solid mechanical stresses was not favorable for plaque rupture to occur [130]. These prior studies provided initial evidence that spontaneous plaque rupture is mechanically unlikely in mice and established a need for expanded evaluation of the solid mechanics of commonly-studied atherosclerotic mouse models with direct comparisons to human plaques.

However, these prior studies did not use identical mechanical modeling or histological embedding techniques, and thus it is difficult to compare results from the acute model of atherosclerosis studied by Broisat et al. with the chronic model studied by Vengrenyuk et al. Because many assumptions go into mechanical modeling, it is important to validate the findings against existing knowledge, which is why we included human TCFA specimens in the present study. These other studies calculated specific magnitudes of mechanical stresses, but we only focused on the relative distribution of stresses because of the known limitations of our technique for calculating such quantities.

Our study investigated both ends of the spectrum of atherosclerotic mouse models, both chronic and acute, in a manner such that a range of murine plaque morphology and mechanics could be compared to human coronary plaques. Although this is not a comprehensive investigation of all possible permutations of atherosclerotic mouse models, it represents a telling cross-section of the spectrum of mouse models. Our rationale for selecting such extreme models of lesion formation was that if mice with the largest plaques don't appear to experience spontaneous plaque rupture, rupture seems even less likely in more moderate models. We considered a different set of animal models than either previous study on mechanical modeling of murine plaques. We focused exclusively on male mice since gender is known to affect plaque phenotype in mice as well as humans, and we included hypertension, a common comorbidity of atherosclerosis [65, 69]. We included the LDLr$^{-/-}$ strain, often studied but not previously considered in mechanical studies, and we considered plaques from the descending thoracic aorta in addition to the brachiocephalic artery, a site not included in previous analyses [66]. In this study, we considered all of these features in order to analyze a different subset of mice and compare them directly to humans, and our results in both mice and in humans are consistent with the findings of prior studies.

A recent study by Ohayon et al. investigated the role of species-specific material properties in computational solid mechanical simulations [132]. They found that using human material properties

in simulations of murine plaques led to an overestimation of stresses inside the plaque. Although their mechanical modeling approach and geometry generation technique differed from ours, this finding suggests that we may be overestimating the frequency of local maxima outside the media and adventitia in mice shown in Figure 3.8. This strengthens our conclusion that the relative distribution of stresses is fundamentally different between mice and humans.

It is interesting to note that lesion morphology was variable both between and within each of our experimental groups. Even though we employed inbred mouse strains given identical treatments to induce atherosclerosis, the exact extent, shape, and location of lesions varied from mouse to mouse. In humans, the etiology of lesions was even more variable, since so many physiological and lifestyle factors influence plaque formation. Therefore, we expect lesion-to-lesion variability to be even higher in humans than in mice. Because we only harvested mice at 8 weeks and at 1 year, we do not have any data on intermediate phases of lesion development in these animals. Given that we observed differences in fibrous tissue content between our three mouse models, it would be interesting to harvest additional timepoints in future studies to track the progression of plaques from immature to advanced phenotypes. Gross examination of murine cross-sections suggests that advanced lesions contain more complex morphology such as more internal fibrous bands sequestering small, individual necrotic cores than in lesions from acute models. However, because lesion-to-lesion variability is high and because lesion harvest requires euthanizing the animal, quantitative assessment of these trends is complex.

One limitation to our current study is that our human and mouse tissues were histologically prepared differently. Both our embedding and staining protocols differed because the tissues came from different sources. Human coronary arteries were obtained from an existing tissue bank: already formalin fixed, paraffin-embedded, and stained with Movat's pentachrome. This technique provides high-quality preservation of vessel composition, but some morphological distortion occurs during tissue processing and sectioning. To overcome such processing artifacts in our murine dataset, we embedded tissue in MMA and perfused the lumen with a vascular casting compound. A consequence of this technique is that Movat's pentachrome staining is impossible: the vascular casting compound, transparent in Masson's trichrome staining, swells during Movat's staining and absorbs the black elastic/nuclear stain (visible in Figure 3.5). In many sections, it obscures the surrounding

tissue, making analysis impossible. Rather than discard the majority of our murine dataset where this occurred, we opted to stain with Masson's trichrome after demonstrating that the stain did not affect our mechanical analysis.

In order to ensure that our lesion-specific model was based upon accurate histology data, we developed a novel vessel harvesting technique that employs vascular casting and plastic resin embedding to maximize the accuracy by which we capture lesion morphology in its in vivo conformation. Even when a mouse aorta is formalin fixed under pressure, the vessel remains compliant and collapses as soon as pressure is released, presenting a significant problem for investigators attempting to preserve the lumen geometry. Failure to preserve the lumen in its circular in vivo conformation will lead to calculation of high strains at sites where the vessel collapses, making it impossible to distinguish the mechanics of the vessel from the mechanics of the histology artifact. By perfusing our mice with vascular casting compound, we were able to minimize such artifact by preserving the lumen in its pressurized, circular conformation.

A second consideration sometimes overlooked in histology-based models is the choice of embedding medium. Although frozen and paraffin sections both offer high compatibility with commercial antibodies for immunohistochemistry, both suffer from morphological distortion of the tissue during sectioning, as the vessel stretches axially in the cutting direction. By embedding our tissues in methyl methacrylate resin and then cutting with a motorized diamond blade microtome, we could evenly apply pressure across the surface of the block to minimize sectioning artifacts. Additionally, because of the stiffness of methyl methacrylate, we were able to cut calcified mouse plaques in many cases with minimal shattering or shredding of neighboring tissue. Unfortunately, unlike frozen sections, the methyl methacrylate embedding process requires tissue dehydration through graded alcohols, so lipid (which shows as negative space in our sections) cannot be detected through stains like Oil Red O.

In this study, we derived our material properties from published values of elastic moduli for human coronary arteries. Recently, Tracqui et al. measured tissue-specific mechanical properties for several components of atherosclerotic lesions in ApoE$^{-/-}$ mice, and these properties were used in the publication of Broisat et al. [130, 133]. However, Tracqui did not publish values for the media or for calcifications, which are essential components of our computational model, and Broisat used

a hyperelastic model of the unloaded media that cannot be applied to our pressure-fixed tissue data. Similarly, Hayenga et al. also measured material properties of murine atherosclerotic plaques but also did not differentiate between the different components of plaque that we identified in our model with histology [134]. Rather than arbitrarily selecting material properties for the missing components from the literature, we decided to use an internally consistent dataset of material properties all measured from identical atherosclerotic lesions. Although one might extrapolate that the material properties of mouse plaques are different from humans' based upon our results showing unique mechanical environments between organisms, we prioritized self-consistency of modeling parameters over use of animal-specific properties in only a portion of the model. The relative stress distribution is insensitive to small differences in elastic moduli as well as to large differences as long as the relative order of magnitude of the tissue components remains constant, and the order of magnitude between tissue components in our model is comparable to those measured by Tracqui [112]. Additionally, Ohayon et al. recently found that the use of human material properties to calculate murine solid mechanics overestimates stresses inside of plaques [132]. Therefore, because we used human material properties, our methods likely lead to overestimation of the frequency of local maxima of stress in mice.

Preliminary modeling revealed that human tissues suffered from tissue processing artifacts, likely related to paraffin embedding and sectioning. Von Mises stress and strain maps revealed stress and strain concentrations at sites of morphological distortion in the original histology, such as steeply-curved edges of the lumen. These concentrations were not located at sites related to the composition of the plaque, such as at the edge of necrotic core or fibrous cap, and were instead at seemingly random locations. Because these probably resulted from tissue distortion during embedding and sectioning rather than from the innate biomechanics of human plaques, we "pre-inflated" these plaques in our computer model by applying a pressure of 40 mmHg normal to the lumen, allowing the tissue to deform, then remeshing and repeating the process for a total of 10 iterations. All modeling protocols during the pre-inflation steps were identical to those used for the final inflation step for human tissues as well as for mouse tissues (which were not pre-inflated because they did not suffer from similar histology artifacts). Von Mises stress data from the 10th iteration was used for our final analysis for human specimens. To ensure that pre-inflation was not affecting our final

results, sensitivity analysis was performed. This demonstrated that stress and strain concentration sites did not change after the 10th iteration and that the only sites that changed between the first and 10th iteration were those at sites of presumed tissue distortion.

Although our modeling technique determines only relative levels of stress, results are still useful for understanding the mechanical environment in murine plaques. Additional steps, such as estimation of initial stress or a full 3D reconstruction of the lesions, while elegant, would add considerable complexity and carry their own set of assumptions and limitations. In this study, we isolated the role of Von Mises stress in plaque rupture, although additional factors such as fluid shear stress and hydrostatic pressure likely play a role. Here, we specifically wanted to investigate the role of solid mechanics in plaque rupture. Our lesion-specific, histology-based analysis of the morphology and mechanics of human and murine atherosclerotic plaques indicates that solid mechanics may not predispose mice to plaque rupture in mice in the same way as they do in humans. Additional morphological metrics could have been considered in addition to those included in this study, but those we measured provide clear evidence that the relative shape and composition of murine lesions are unique from human lesions.

In the literature, researchers not infrequently interpret plaque morphology in mice as a transformation to a "more vulnerable phenotype". Our results suggest that such terminology may be inappropriate. Geometric risk factors for plaque rupture in humans such as thin fibrous caps and large necrotic cores do not appear to be associated with a distribution of mechanical stresses likely to cause rupture in the mouse models we examined. Certainly, spontaneous plaque rupture in mice is controversial. This study suggests that, if spontaneous plaque rupture does occur in mice, then unlike humans, it does so through a different mechanism than mechanics.

# CHAPTER IV

# ROLE OF INFLAMMATION AND SOLID MECHANICS IN PLAQUE RUPTURE AND PLAQUE EROSION

## *4.1 Introduction*

Thrombotic occlusion of the coronary arteries, a leading cause of morbidity and mortality worldwide, may be caused by a number of events. The most extensively studied phenomenon is plaque rupture, in which an advanced fibroatheroma develops through inflammation-mediated mechanisms and eventually fissures, exposing the blood to pro-thrombogenic necrotic core and resulting in thrombus formation. More recently identified is a second major cause of sudden coronary death, termed plaque erosion, where a thrombus forms that does not communicate with the necrotic core of an atherosclerotic plaque. Plaque erosion occurs frequently: two studies found that 40% of fatal coronary thrombi resulted from erosion [30, 34]. However, demographics with highest incidence of plaque erosion differ from traditional candidates for rupture: plaque erosion tends to occur in younger individuals, particularly women [17].

Despite identification of the plaque erosion phenomenon, its mechanism is not well understood. The leading hypothesis for erosion (and its namesake) suggests that endothelial denudation over an atherosclerotic plaque presents a thrombogenic substrate to the blood. The cause of this focal denudation is not known, but possibilities including vasospasm and highly shearing flow have been suggested [34]. Endothelial apoptosis leads to denudation in animal models [37, 135], but histological studies have shown that inflammatory cells like macrophages and lymphocytes prevalent in ruptured plaques that may induce apoptosis are not as widespread in eroded plaques [36]. Therefore, there is a need to better understand the factors leading to plaque erosion.

In addition to the biological mechanisms of inflammation and tissue remodeling, other factors affecting the stability of plaques include mechanical stress and strain. The role of biomechanics in plaque rupture is well established: a thin fibrous cap over a necrotic core usually has local maxima of stress on the cap or the plaque shoulders, sites where rupture is known to occur [105]. Additionally,

mechanosensitive tissue markers related to inflammation and the development of atherosclerosis have been identified [56,57]. To date, no analysis has focused on the role of biomechanics in plaque erosion specimens. In this study, we investigated the roles of biomechanics and inflammation in plaque disruption. We hypothesized that solid mechanical stresses and strains in the vessel wall are associated with inflammatory markers in plaque rupture but not in plaque erosion.

## *4.2 Methods*

### 4.2.1 Overall Approach

We used a histology-based, lesion-specific computational modeling technique to calculate the distribution of stresses and strains in the walls of atherosclerotic plaques. We investigated lesions from four classifications: plaque erosion, plaque rupture, thin-cap fibroatheroma (TCFA, sometimes called "vulnerable" plaques), and thick-cap fibroatheroma (ThCFA, sometimes called "stable" plaques). We then studied the relationship between solid mechanics and markers of the pathogenesis of atherosclerosis and inflammation that have been associated with plaque rupture.

### 4.2.2 Human Tissue Histology

We obtained de-identified human coronary artery specimens from an existing tissue bank of hearts at CVPath Institute, Inc., obtained as a consultation service for the Maryland Office of the Chief Medical Examiner. Tissue harvest was described previously [30, 136]. We studied 32 plaque erosion, 14 plaque rupture, 14 TCFA, and 14 ThCFA specimens. Consecutive serial cross-sections for each subject were stained with Movat's pentachrome for lesion morphology and immunohistochemically with antibodies for CD68 for macrophages (Dako M0814), Factor VIII for endothelium (Strategic BioSolutions S40036NDI-D0), MMP1 for this collagenase (Enzo Life Sciences ADI-905-472), MMP9 for this elastase (Spring Bioscience E3660), a combination of CD31 and CD34 for *vasa vasorum* (Dako M0823 and Cell Sciences MON1164), smooth muscle actin for smooth muscle cells (Dako M0851), and TUNEL for apoptosis (Roche 12 156 792 910). Brightfield images of Movat's pentachrome and immunohistochemistry were acquired with a 4x objective and automatically stitched together using Microsoft Image Composite Editor (Microsoft Research, Redmond, WA). Confocal microscopy images of TUNEL staining were obtained with a 20x objective and automatically stitched together using Leica LAS AF (Leica Microsystems, Buffalo Grove, IL).

### 4.2.3 Image Segmentation

Movat's pentachrome images were automatically segmented to identify the composition and spatial distribution of tissue components using custom Matlab software (Figure 4.1). We used *k*-means clustering and Euclidean distance algorithms to identify the presence of fibrous, cellular, lipid/necrotic core, and calcified tissue based on staining color [124]. An expert observer modified this segmentation as necessary where, for example, calcium had shattered or necrotic core had shredded during sectioning. Then, the lumen and periadventitial borders were traced using an implementation of the Live Wire algorithm [125].

### 4.2.4 Computational modeling approach

Based on this segmented map of tissue composition, we developed a lesion-specific computer model of the distribution of stresses in a cross-section of each of the 74 vessels. We used an established finite element analysis modeling technique implemented in Ansys 14.0 software [56]. We calculated maps of the relative distribution of Von Mises Stress and Strain in each vessel using this technique. This technique does not compute the exact magnitude of stress and strain because it does not incorporate residual stress. Therefore, to compare values between lesions, we computed the stress and strain excursion, defined as the percent difference of stress or strain from the lesion's median value.

### 4.2.5 Computational Solid Mechanics Assumptions

We used an established 2D, lesion-specific modeling approach to simulate mechanical stresses and strains within cross-sections of coronary atherosclerotic plaques [56]. Implemented in Ansys 14.0 software (Ansys, Inc., Canonsburg, PA), this model was based on pressure-fixed histology sections stained with Movat's pentachrome for morphology and then segmented. Because this tissue is pressure-fixed, we do not have data on the stress-free conformation of each vessel and therefore cannot easily compute the residual stress values. Consequently, this model is useful for generating the relative distribution of stresses but not exact magnitudes.

Linear, elastic, isotropic material properties were used for all tissue components [100]. Although biological tissues are known to be nonlinear, viscoelastic, and anisotropic [12, 101, 102],

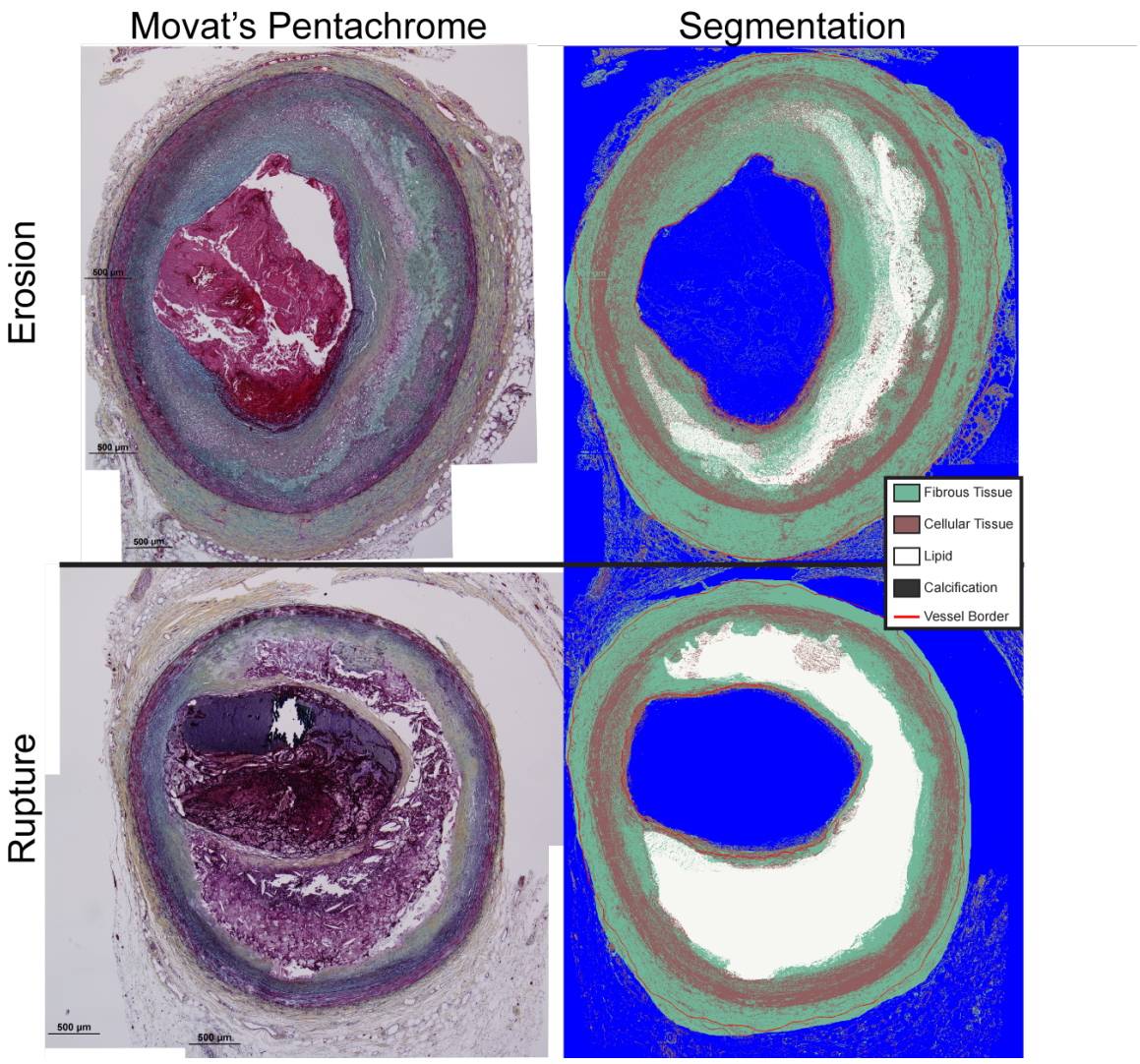


Figure 4.1: Histology segmentation: We segmented histologic cross-sections of human coronary arteries stained with Movat's pentachrome (left) in order to determine their composition (right) on a lesion-specific basis. Based on staining color, we identified whether tissues were fibrous, cellular, lipid/necrotic core, or calcified. We also traced the lumen and external border using an implementation of the Live Wire algorithm [125].

assignment of such material properties to pressure-fixed tissue is mathematically complex and requires a battery of simplifying assumptions. For example, properly applying anisotropic material properties in a subject-specific model of a complex lesion requires knowledge of fiber directions that we do not have, and therefore we assume isotropic material properties.

Material properties of vascular tissues can be approximated with a bilinear stress-strain curve, with a break point between the two realms occurring slightly below our fixation pressure. Below this threshold, very little stress is generated as the vessel inflates. Therefore, although we are unable to calculate the stresses in the wall from blood pressures below diastole, we assume these stresses are relatively low. The relative contribution from stresses above diastolic pressure is much greater (and is the basis for our model), which is why we can use our technique to determine the relative distribution of high and low stress and strain but not the exact magnitude.

To model each vessel, we generated a fine-resolution finite element mesh of several hundred thousand elements between the lumen and periadventital boundary. For each element, we used a rule-of-mixtures approach [100, 101] to estimate the elastic modulus for that element, based on our segmented pentachrome image. We then simulated an incremental pressure of +40 mm Hg (approximately equal to the difference between diastole, the pressure at which the vessel was fixed, and systole) normal to the lumen. The resulting Von Mises stress and strain distributions for each vessel were generated, representing the distribution of stresses in the lesion at peak systole.

### 4.2.6 Computational "pre-inflation" of histology specimens

Some vessels suffered from histology artifacts such as compression along one axis. These artifacts were apparent because the lumen was not approximately circular, as would be the case in vivo in a pressurized vessel (Figure 4.2, left). The consequence of this artifact in our mechanical model was an artificially-high region of both stress and strain at sites of highest deformation (Figure 4.2, middle). These obscured the physiological stress and strain distribution, and therefore, we "pre-inflated" each vessel to allow it to distend into a more natural starting conformation. For 10 iterations, we applied a +40 mm Hg incremental pressure normal to the lumen, computed the new conformation of the vessel, and then remeshed the vessel to overcome highly-skewed elements. The final iteration was used for our analysis (Figure 4.2, right) and did not exhibit local stress concentrations at sites

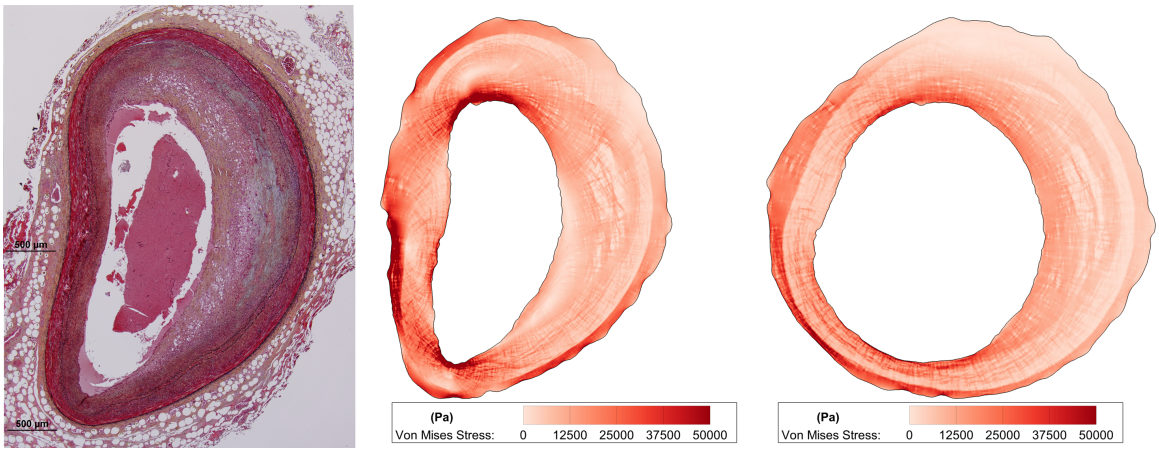


Figure 4.2: Preinflation technique for mechanical modeling: Many histology specimens suffered from fixation and embedding artifacts, such as the vessel at left, which is horizontally compressed relative to its in vivo conformation where the lumen would be mostly circular. Consequently, the computed stress and strain distributions were skewed in regions of high deformation during computational analysis (middle). Therefore, we "pre-inflated" vessels by simulating pressure normal to the lumen, allowing the vessel to deform, and remeshing the vessel for 10 iterations. This extra processing step minimized the effect of tissue artifacts and presented us with more physiologically-relevant anatomy for our analysis (right).

of histology artifacts. Sensitivity analysis on the number of iterations revealed that after 10 steps, results were not significantly affected.

### 4.2.7 Morphology and Composition

We calculated the relative composition of each lesion phenotype from image segmentation results. We also evaluated several geometric parameters to evaluate whether the shape of lesions differed by phenotype. We computed plaque burden (percent of area inside internal elastic lamina [IEL] containing lesion), lesion cross-sectional area (area of tissue inside the IEL), vessel radius (computing the smallest possible circle to contain each vessel), vessel eccentricity (distance between lumen centroid and IEL centroid, normalized to vessel radius), and the average thickness of the media (computing the distance between the inner and outer boundaries of the media, where present) [126].

### 4.2.8 Mechanics and Tissue Marker Analysis

To evaluate if mechanical stress and strain was associated with positive staining for each of the 7 tissue markers, we registered each stained image against the pentachrome image that was the basis for mechanical modeling. We traced the lumen in each image and performed rigid registration

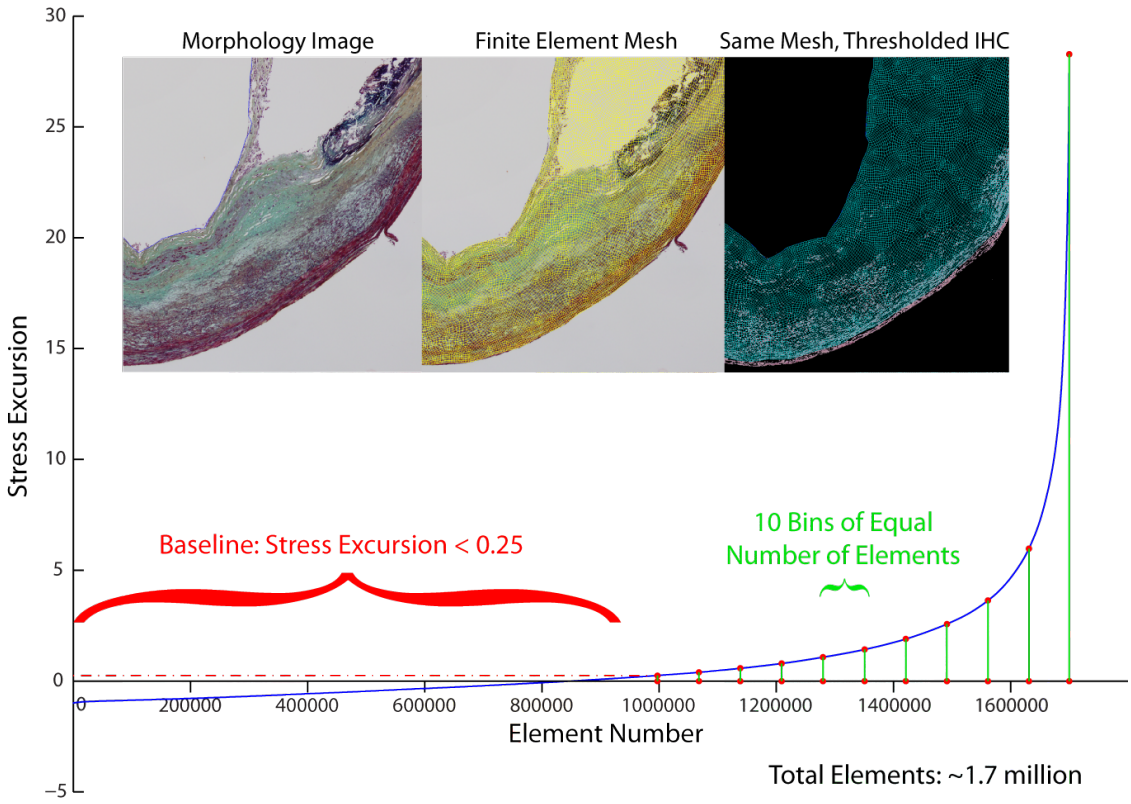


Figure 4.3: Stress and strain excursion association with positive staining: Von Mises stress and strain excursion were computed for each lesion by breaking down each vessel into a fine-resolution mesh. After sorting the elements in order of increasing stress (or strain) excursion, we pooled results into a baseline group (excursion $< 0.25$) and tertiles or deciles containing an equal number of elements. Thus, higher-numbered groups (Figures 4.7, 4.8, 4.9, 4.10, 4.14, and 4.15) represent regions of higher stress or strain excursion. Negative stress excursion represents stress below the median value, not a negative magnitude of stress or strain.

using cross-correlation of the distance of the lumen border from its centroid to determine the necessary degree of rotation [126, 137]. Regions exhibiting histology artifacts such as folding or ripping were locally excluded from analysis. Images were thresholded to identify positive staining using empirically-determined color levels. For each element of the fine-resolution mesh used for computational mechanics, we determined the stress and strain excursion, and whether there was positive staining.

To determine if there was an association between stress/strain excursion and each stain, we pooled results within each of the four lesion phenotypes and sorted them in order of ascending stress or strain excursion (Figure 4.3). We then divided each phenotype into a baseline group with excursion $< 0.25$, and then tertiles and deciles of equal-number elements.

### 4.2.9 Total Staining

To evaluate the total expression of each marker per vessel, we thresholded each stained image and calculated the percent of each vessel with positive staining. Results were tallied for each phenotype.

### 4.2.10 Endothelial Denudation and Apoptosis

To determine the extent of endothelial apoptosis and denudation, we quantified the amount of positive staining for Factor VIII and TUNEL within 10 μm of the lumen border. We manually traced the lumen of each image then dilated the contour using a signed distance function. We tallied the percent of positive pixels within this region for each phenotype. Sections with significant thrombus adhered to the wall were excluded because we could not differentiate between positive staining from endothelium or from thrombus.

### 4.2.11 Statistical Analysis

To evaluate differences between tertiles and deciles in our mechanics and histology analysis, we performed a chi-squared analysis to determine if an association existed. If so, we subsequently performed a two-proportion post hoc test to compare each tertile or decile to its baseline. After Bonferroni correction for multiple comparisons with $\alpha$=0.05, any post hoc test with $p < 0.0045$ was considered significant.

For total staining, endothelial denudation and apoptosis, and morphology and composition analyses above, statistical differences between phenotypes were assessed with one-way ANOVA followed by Tukey's honestly significant difference post hoc test. After Bonferroni correction for multiple comparisons with $\alpha$=0.05, any post hoc test with $p < 0.008$ was considered significant.

## *4.3 Results*

### 4.3.1 Mechanics

We successfully segmented 32 eroded plaques, 14 ruptured plaques, 14 TCFA, and 14 ThCFA plaques (Figure 4.1) and calculated the lesion-specific distribution of Von Mises stress and strain (Figure 4.4) for each.

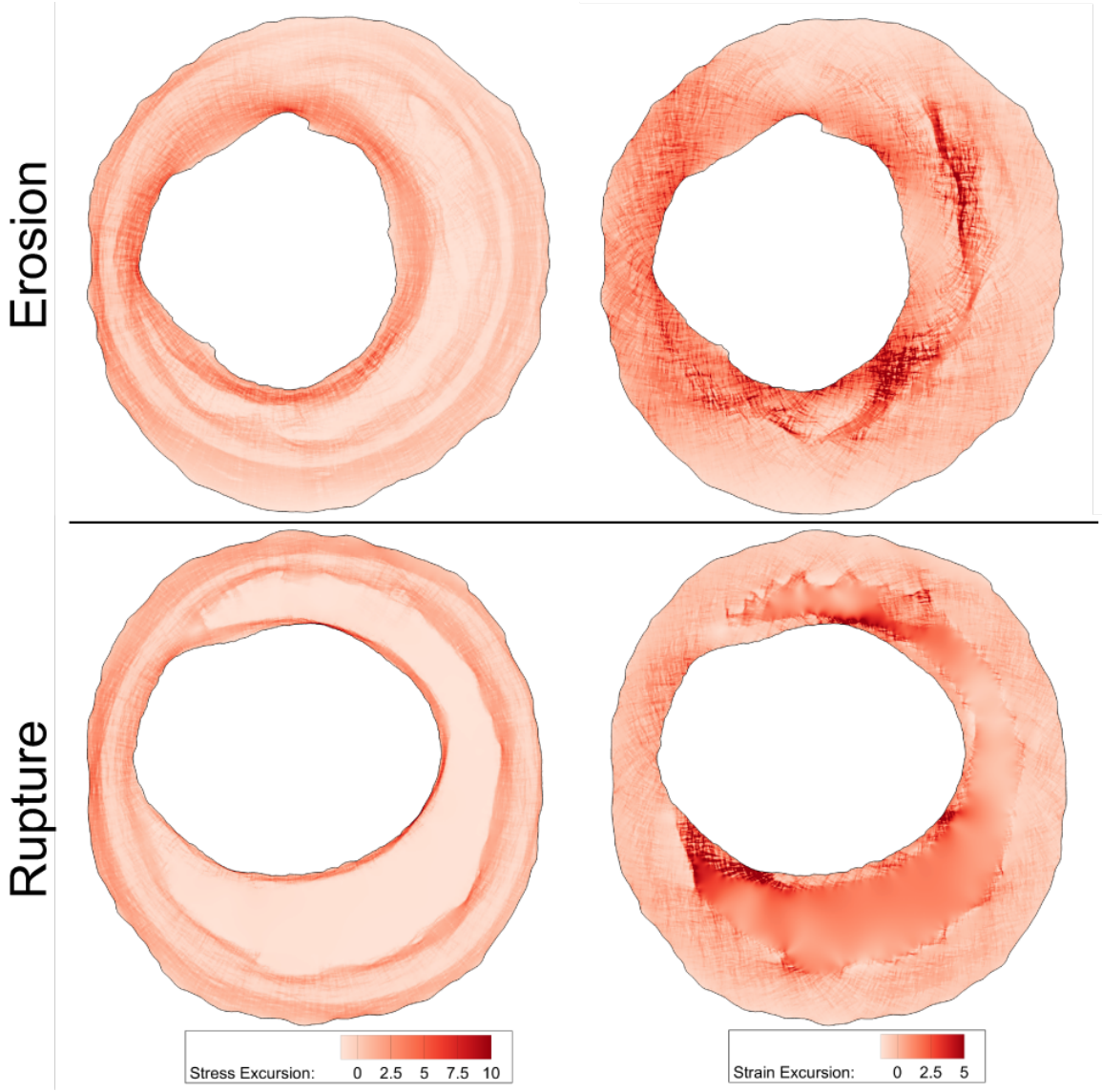


Figure 4.4: Stress and strain modeling: We computed the relative distribution of Von Mises stress and strain for each lesion. Shown here are stress and strain maps for the two vessels segmented in Figure 4.1, displayed as excursion (normalized difference from the median).

### 4.3.2 Morphology and Composition

There was no difference in the proportion of lesion made of fibrous tissue or lipid/necrotic core between any of the phenotypes (Figure 4.5). Eroded plaques contained significantly more cellular tissue than ruptured or TCFA plaques but were not different from ThCFA plaques. Eroded and ThCFA plaques also had significantly less calcium than ruptured plaques. Eroded plaques had less calcium than TCFAs ($p < 0.05$). Eroded plaques had significantly smaller radii than TCFA plaques ($p < 0.008$) but were not different from ruptured or ThCFA plaques (Figure 4.6). There was no difference in plaque burden or eccentricity between lesions, but the cross-sectional area of eroded plaques was less than ruptured or TCFA plaques ($p < 0.05$).

### 4.3.3 Inflammatory Markers

CD68, MMP1, MMP9, and Apoptosis staining varied positively with increasing mechanical strain excursion for ruptured and TCFA plaques (Figure 4.8, Figure 4.7). No such association was observed for eroded and ThCFA plaques for these same markers. Characteristic associations between these markers and mechanical stress excursion were not observed (Figure 4.10, Figure 4.9). Without regard to mechanics, ruptured and TCFA plaques exhibited significantly higher mean staining across the entire section for MMP9 (Figure 4.11) and apoptosis ($p < 0.008$) (Figure 4.13) as compared to eroded and ThCFA plaques.

### 4.3.4 Media

Smooth muscle actin (SMA) varied positively with increasing mechanical strain excursion for eroded and ThCFA plaques. It varied negatively for TCFA plaques, and had no dominant association for ruptured plaques. Similarly, the total staining for SMA exhibited the opposite trend than for inflammatory markers: across the entire vessels, eroded plaques had significantly more smooth muscle than did ruptured plaques (p ¡ 0.008) (Figure 4.12). Mean thickness of the media was significantly higher ($p < 0.008$) in eroded and ThCFA plaques than ruptured plaques (Figure 4.12).

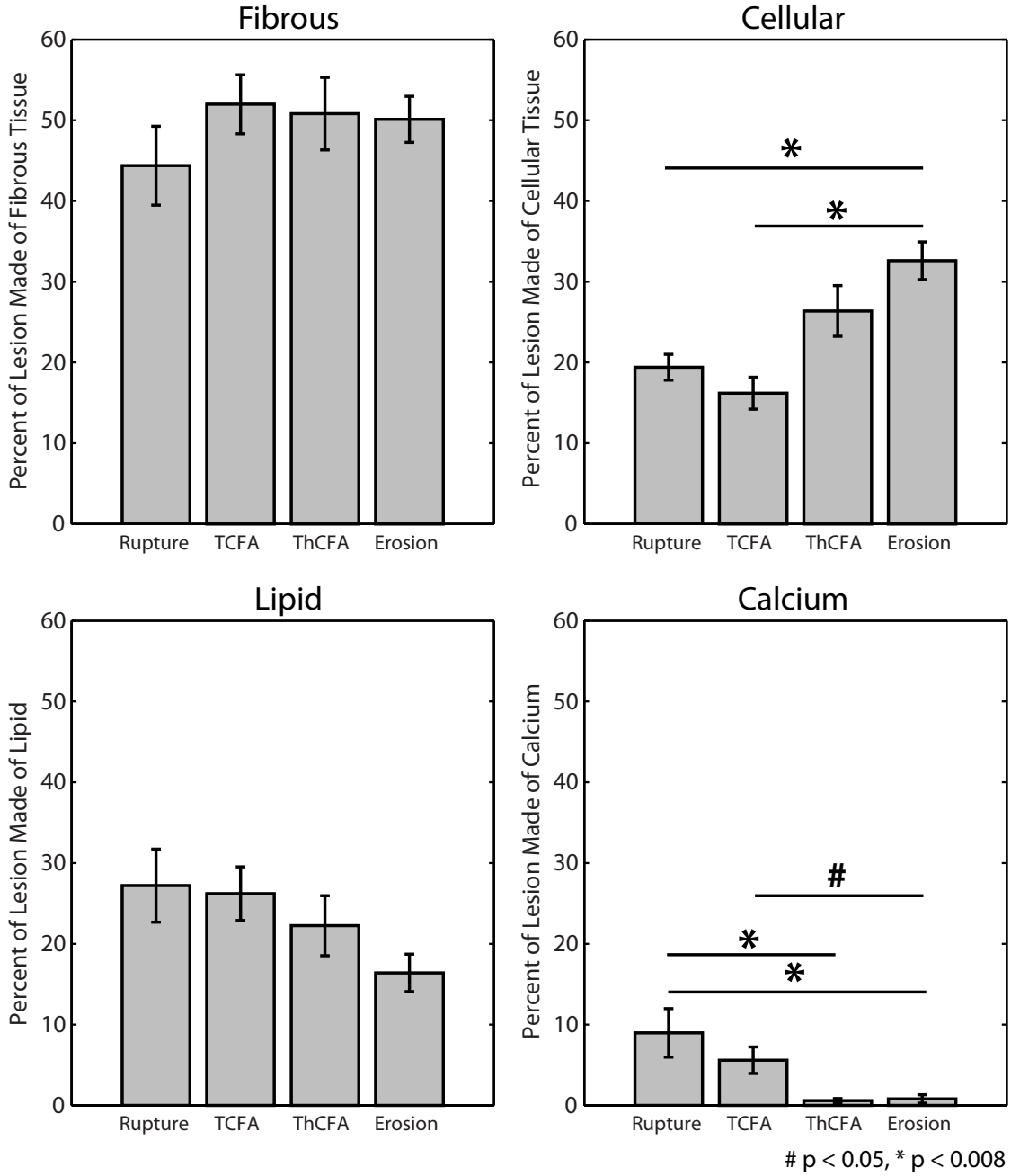


Figure 4.5: Relative composition: Based on image segmentation (Figure 4.1), we calculated the relative composition of lesions for each of the four phenotypes. Plaque erosion specimens were significantly more cellular and less calcified than ruptured plaques.

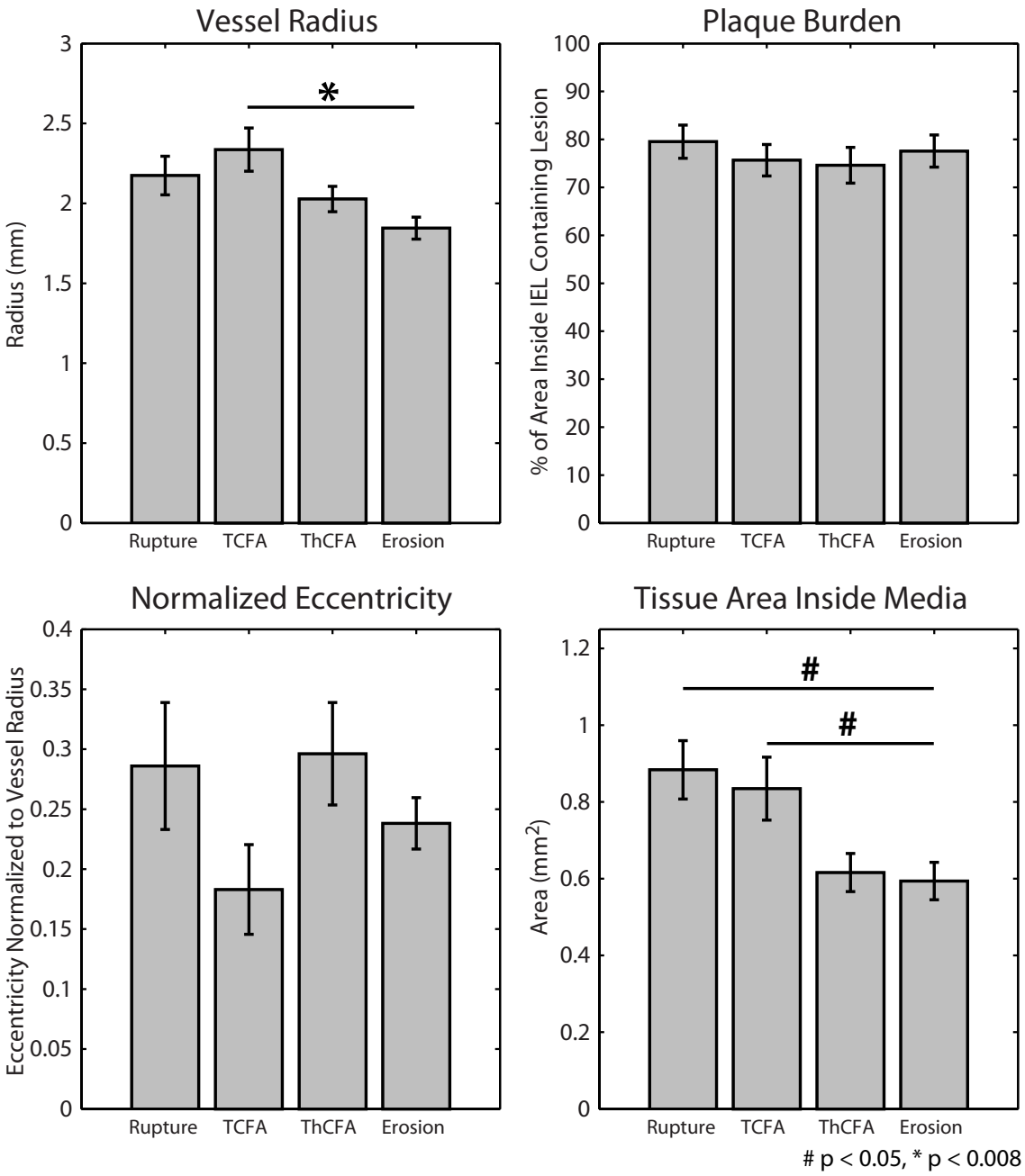


Figure 4.6: Morphological metrics: We calculated vessel radius (by circumscribing a circle around each vessel, upper left), the plaque burden (the percent of the area inside the IEL containing lesion, upper right), the eccentricity (distance between lumen centroid and IEL centroid, normalized to vessel radius, lower left) and area containing tissue inside the IEL (lower right). Differences between phenotypes were not significant, except for radius between erosion and TCFA.

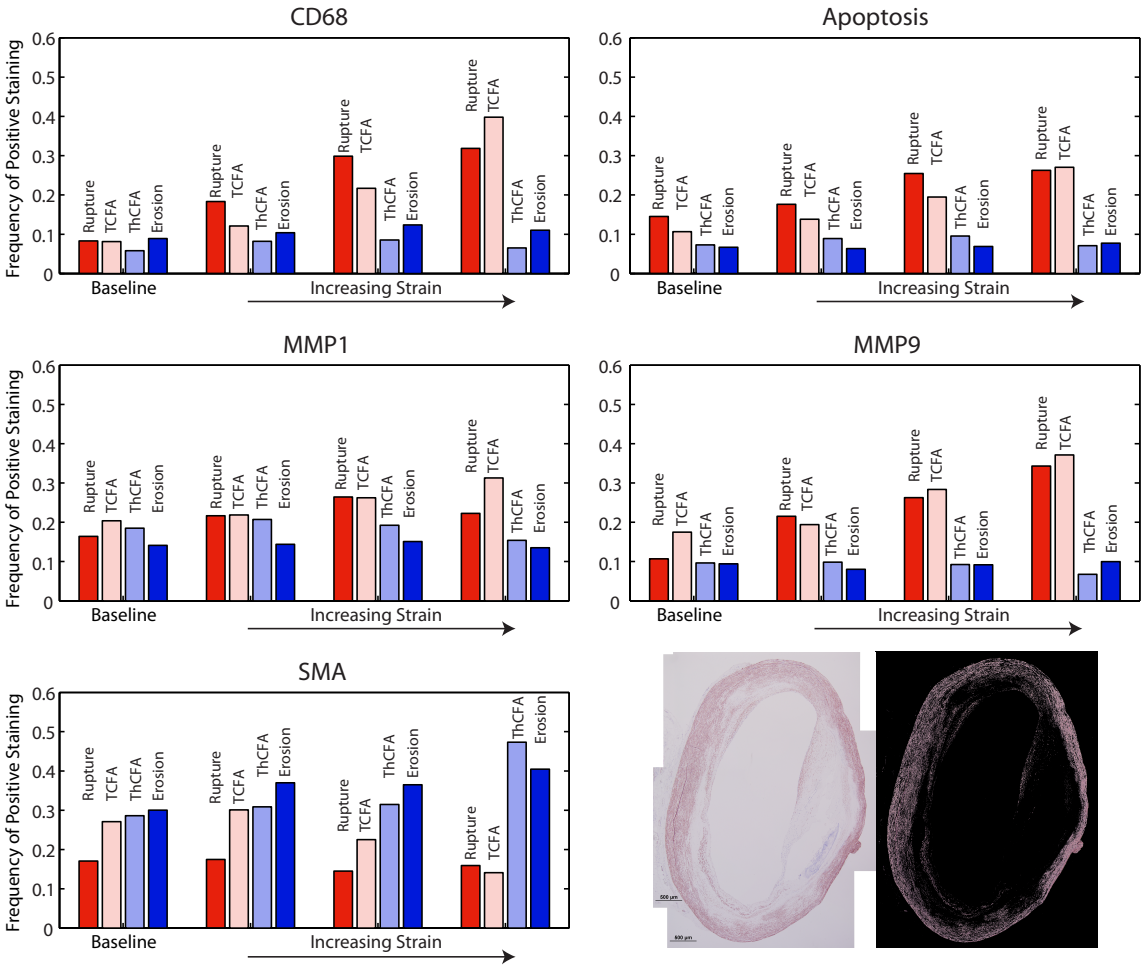


Figure 4.7: Positive staining and mechanical strain: We examined positive staining for inflammatory markers in images registered against Von Mises strain maps (Figure 4.4). We divided strain excursion into a baseline group (excursion $< 0.25$) and tertiles of equal number of elements (see Figure 4.3) then examined the frequency of positive staining associated with each level of mechanical strain. Inflammatory markers in ruptured plaques and TCFAs varied positively with increasing strain, whereas eroded plaques and ThCFAs did not vary as dramatically. Thresholding for positive staining for SMA in an example TCFA is shown at lower right.

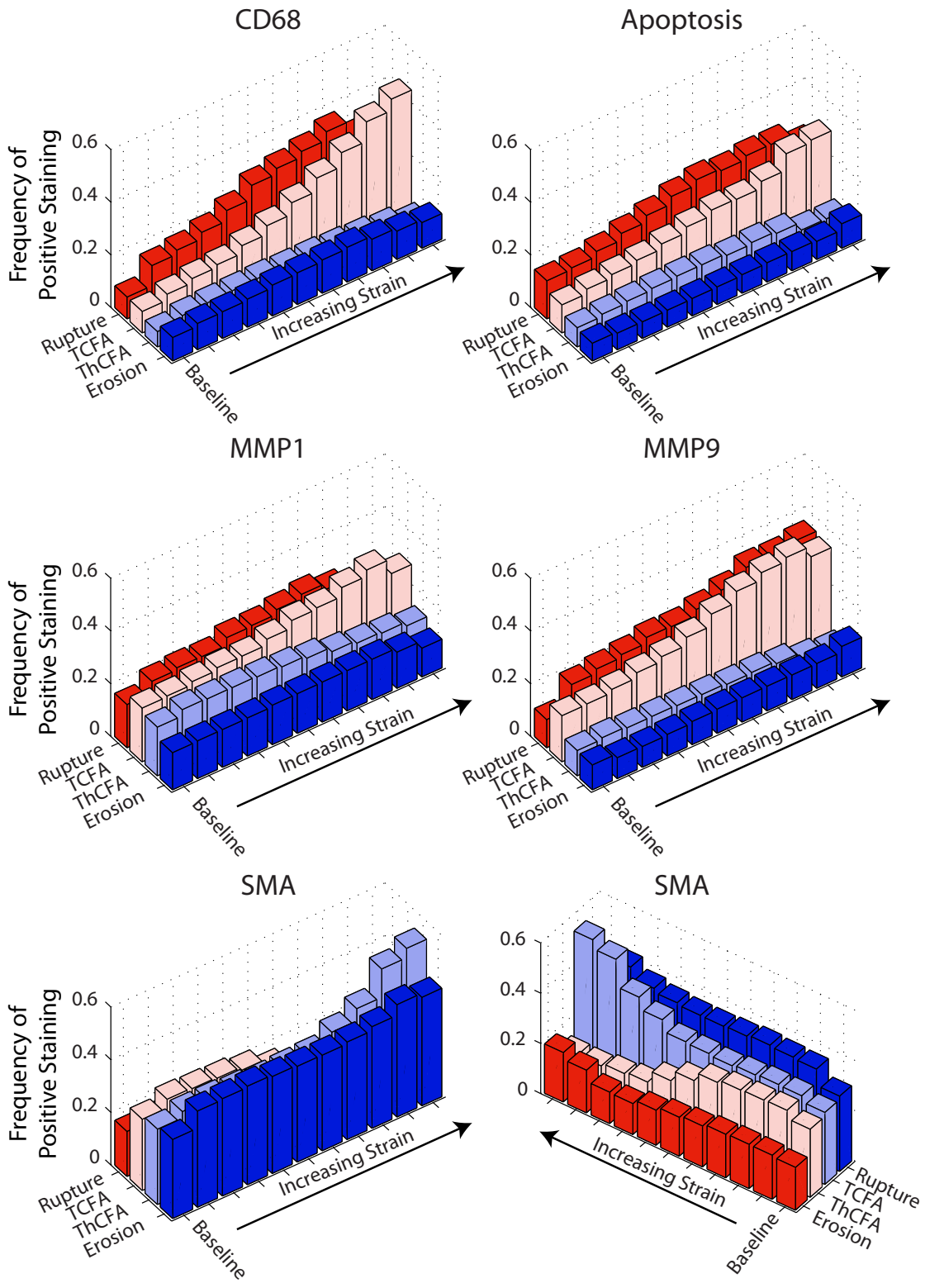


Figure 4.8: Positive staining and mechanical strain: We examined positive staining for inflammatory markers in images registered against Von Mises strain maps (Figure 4.4). We divided strain excursion into a baseline group (excursion $< 0.25$) and deciles of equal number of elements (see Figure 4.3) then examined the frequency of positive staining associated with each level of mechanical strain. Inflammatory markers in ruptured plaques and TCFAs varied positively with increasing strain, whereas eroded plaques and ThCFAs did not vary as dramatically.

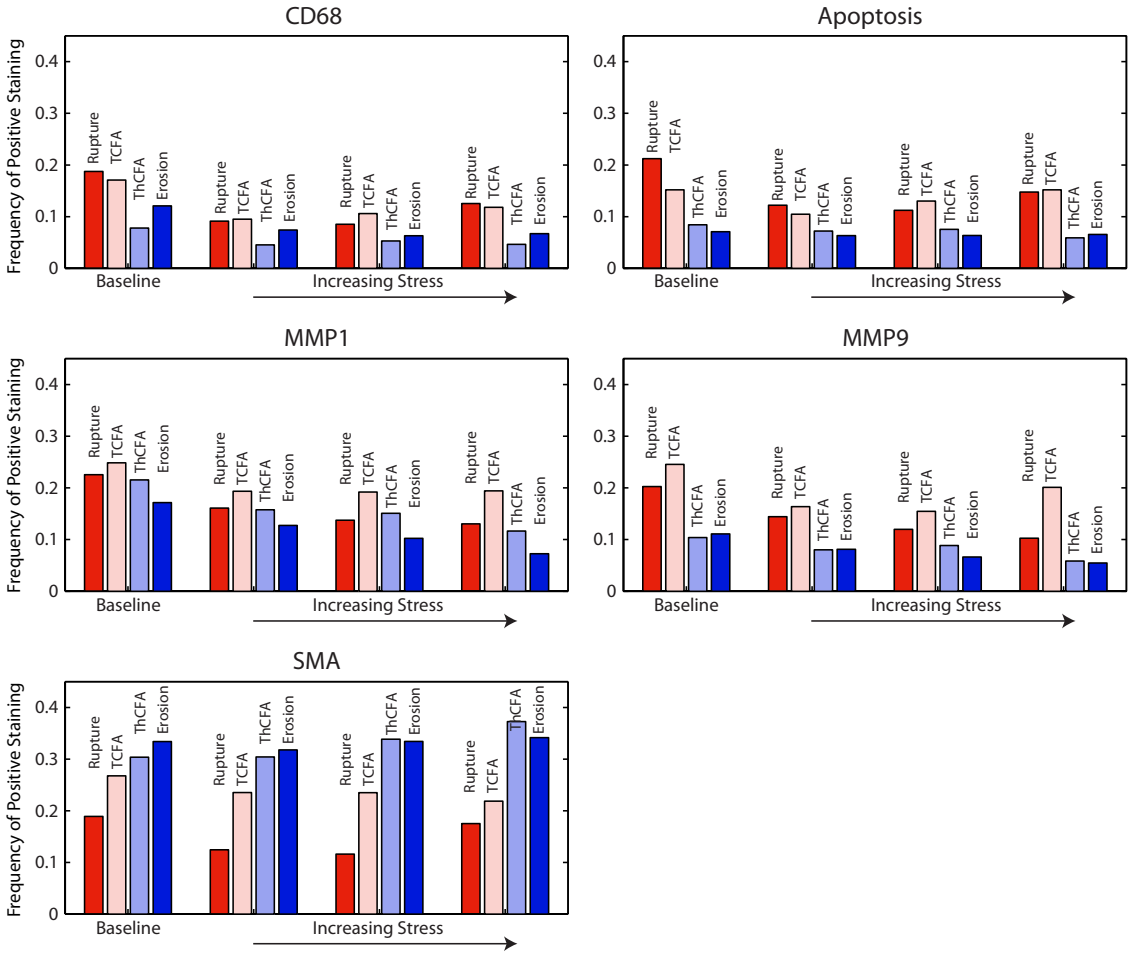


Figure 4.9: Positive staining and mechanical stress: We examined positive staining for inflammatory markers in images registered against Von Mises stress maps (Figure 4.4). We divided stress excursion into a baseline group (excursion $< 0.25$) and tertiles of equal number of elements (see Figure 4.3) then examined the frequency of positive staining associated with each level of mechanical strain.

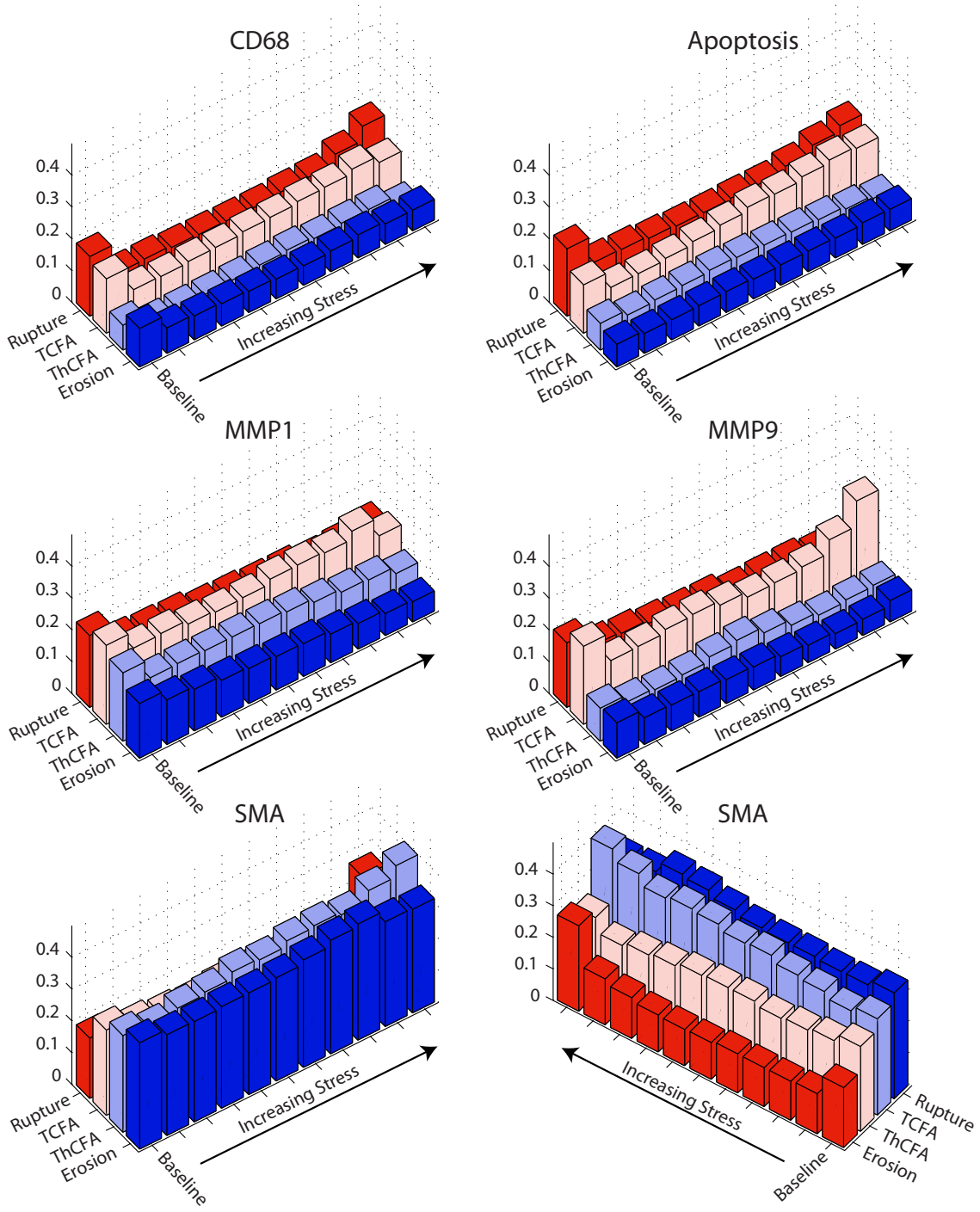


Figure 4.10: Positive staining and mechanical stress: We examined positive staining for inflammatory markers in images registered against Von Mises stress maps (Figure 4.4). We divided stress excursion into a baseline group (excursion $< 0.25$) and deciles of equal number of elements (see Figure 4.3) then examined the frequency of positive staining associated with each level of mechanical strain.

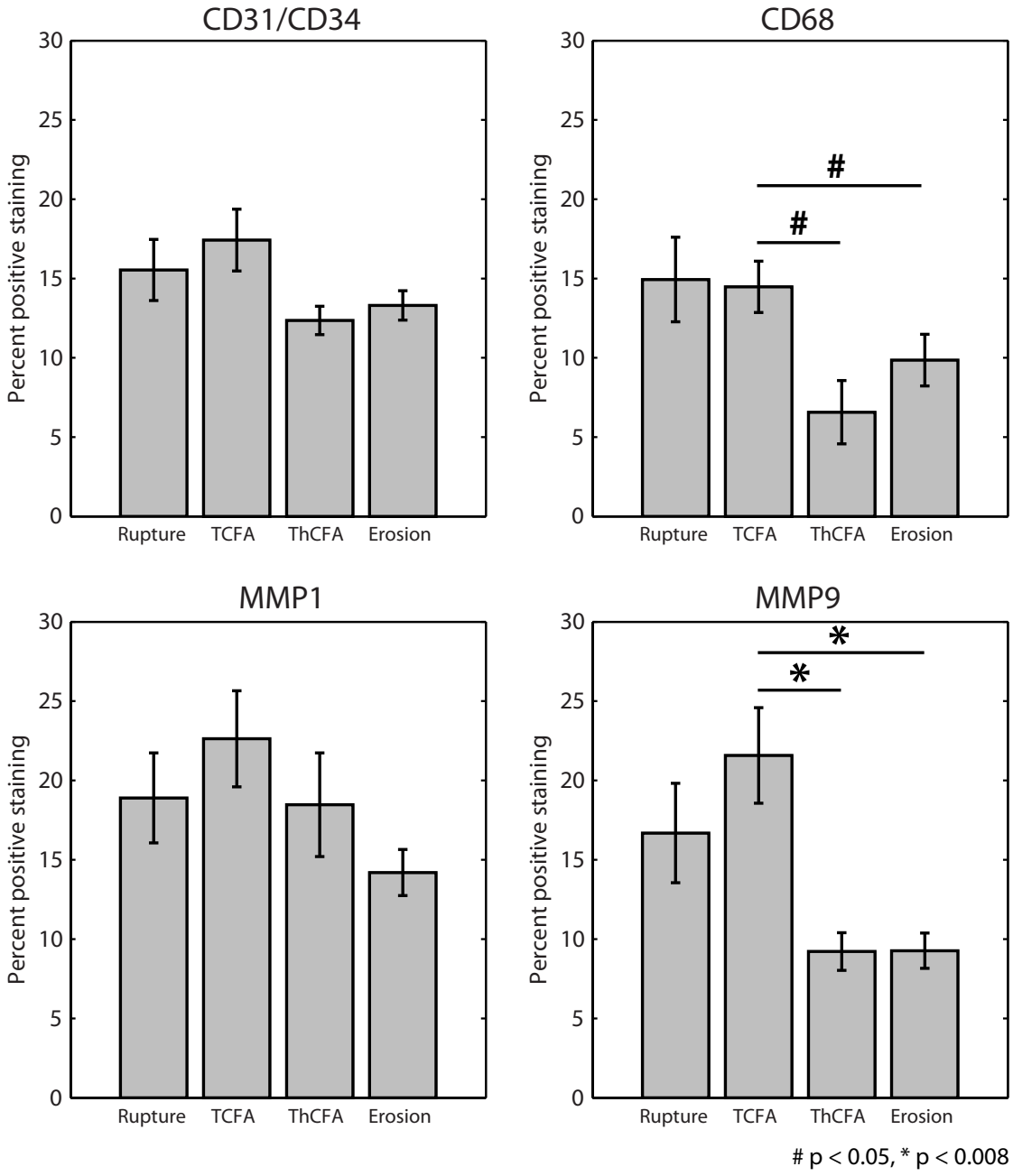


Figure 4.11: Eroded and stable plaques have the least total positive staining for inflammatory markers: Four stains, CD31/CD34 (an endothelial marker for angiogenesis and microvessels, upper left), CD68 (a macrophage marker, upper right), MMP1 (a collagenase, lower left), and MMP9 (a gelatinase, lower right) all exhibit the same relative levels of staining. Ruptured plaques and TCFAs exhibited the highest levels of positive staining, and eroded plaques and ThCFAs exhibited the lowest.

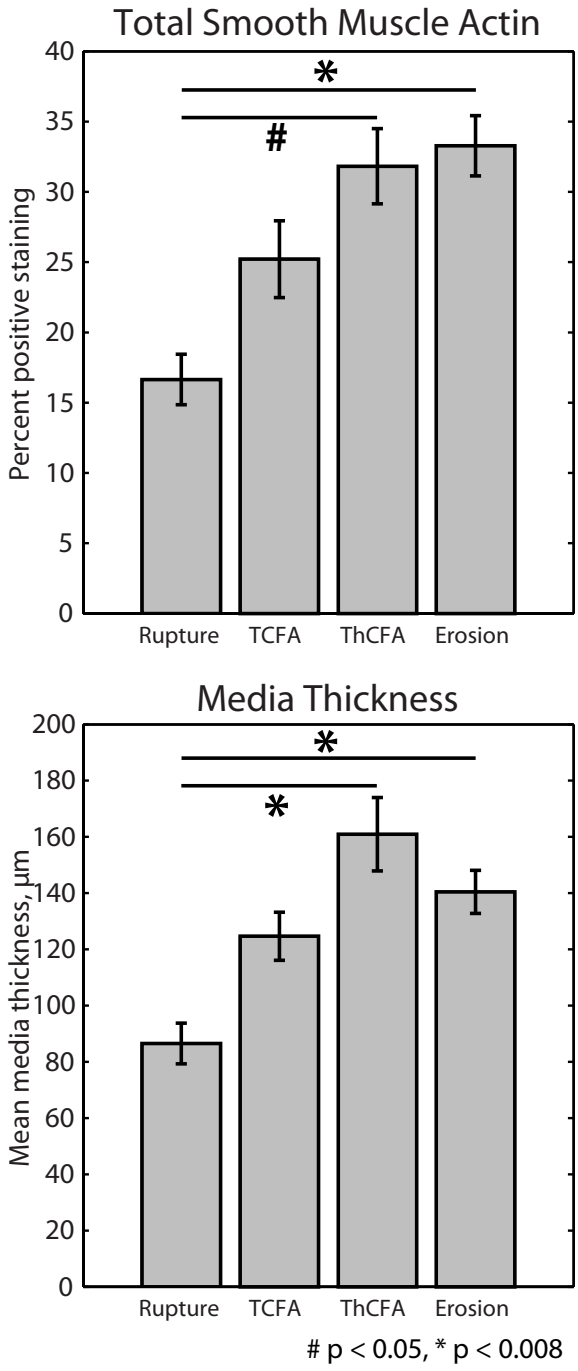


Figure 4.12: Media is lost in ruptured plaques relative to eroded plaques: Immunohistochemistry for smooth muscle actin (top) revealed that eroded plaques have significantly more smooth muscle than do ruptured plaques. Additionally, the media is significantly thicker (bottom) in erosion than rupture.

### 4.3.5 Endothelium

Focusing specifically on the lumenal endothelium, there was no significant difference in endothelial apoptosis between the four phenotypes of plaques. There were significantly more ($p < 0.008$) Factor VIII-positive cells in eroded plaques than in ruptured or TCFA plaques (Figure 4.13). Eroded plaques were not significantly different from ThCFA plaques. Across the entire vessel, there was no outstanding association for either of the endothelial markers CD31/CD34 or Factor VIII with either stress or strain for any of the phenotypes (Figure 4.14, Figure 4.15).

## *4.4 Discussion*

In this study, we demonstrated differences in composition, mechanics, and inflammation between plaque rupture and plaque erosion, suggesting that considerably different etiologies are at play in each phenotype. With increasing mechanical strain, there is no corresponding increase in inflammation in plaque erosion, whereas these two properties are closely associated in plaque rupture. We also noted numerous similar characteristics between plaque rupture and its vulnerable phenotype the TCFA, as well as similarities between eroded and stable plaques. Both eroded and ThCFA phenotypes express relatively higher levels of smooth muscle cells and have thick, intact media, while the opposite is true for both ruptured plaques and TCFA. These findings are consistent with present understanding that inflammatory processes are necessary for progression to plaque rupture and suggest that alternative mechanisms must be considered to understand and prevent plaque erosion. These also suggest that at least a subset of ThCFA plaques may be a "vulnerable" phenotype for erosion.

The divide in etiologies is most apparent in the relationship between mechanical strain and inflammatory markers. With increasing strain, CD68, MMP1, MMP9, and apoptosis all increased in TCFAs and ruptured plaques. In ThCFAs and eroded plaques, however, we observed no such association between inflammation and strain. Macrophages and MMP1 have been shown previously to be stress and strain sensitive in atherosclerotic lesions [56]. Therefore, their lack of response in this subset of lesions, not to mention their lower overall staining in these same lesions, suggests that plaque erosion is not a consequence of the inflammatory processes leading to plaque rupture.

This difference between plaque rupture and plaque erosion may have significant implications

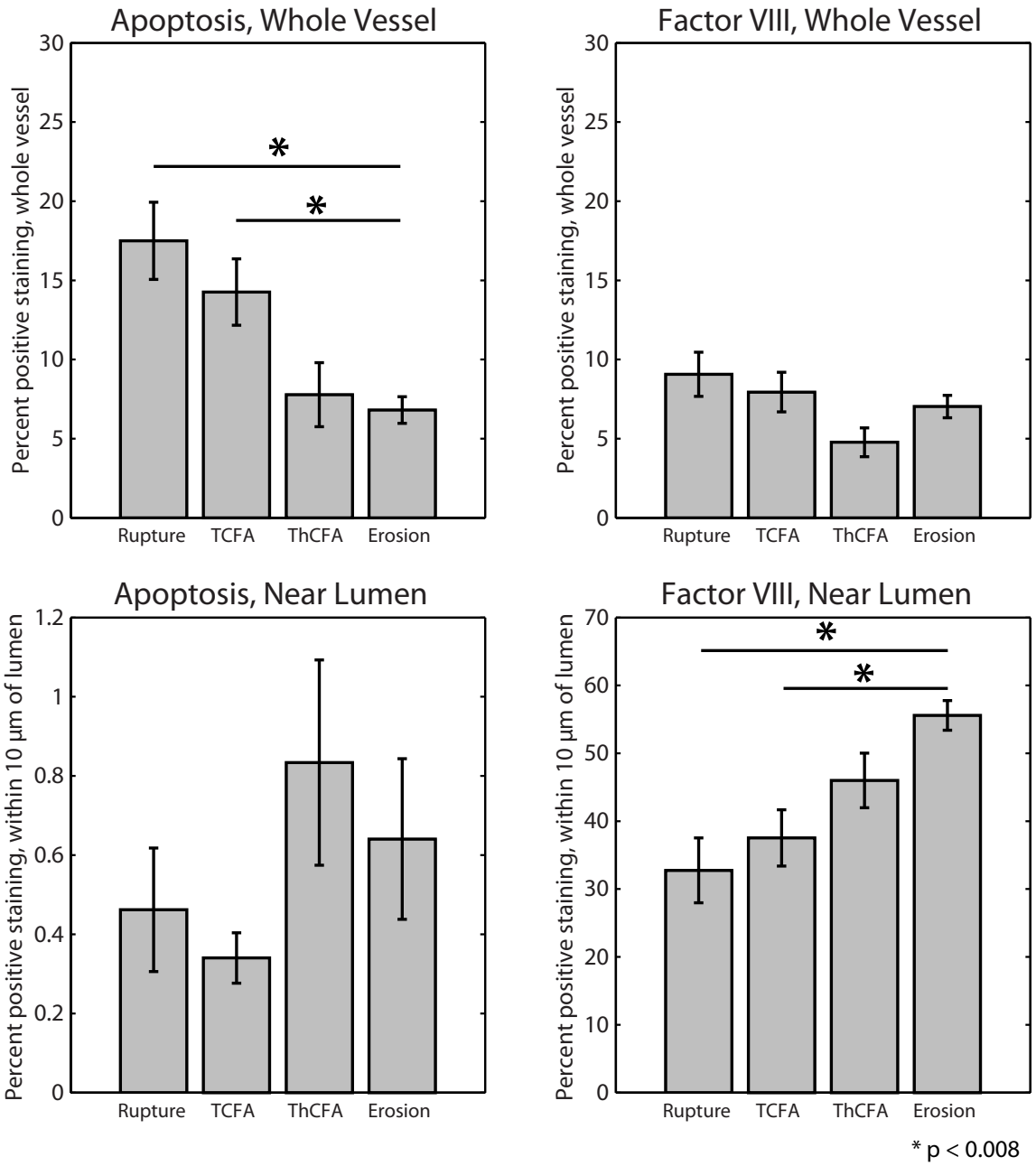


Figure 4.13: Apoptosis and Factor VIII for whole vessel and near lumen: Plaque erosion has been hypothesized to result from endothelial denudation, possibly resulting from apoptosis. When examining the whole vessel, eroded plaques are significantly less apoptotic then ruptured plaques or TCFAs and have slightly less Factor VIII. When isolating the endothelium (by examining a region within 10 μm of the lumen) eroded plaques did not have a significantly greater number of apoptotic cells and had significantly more Factor VIII positive cells than ruptured plaques or TCFAs.

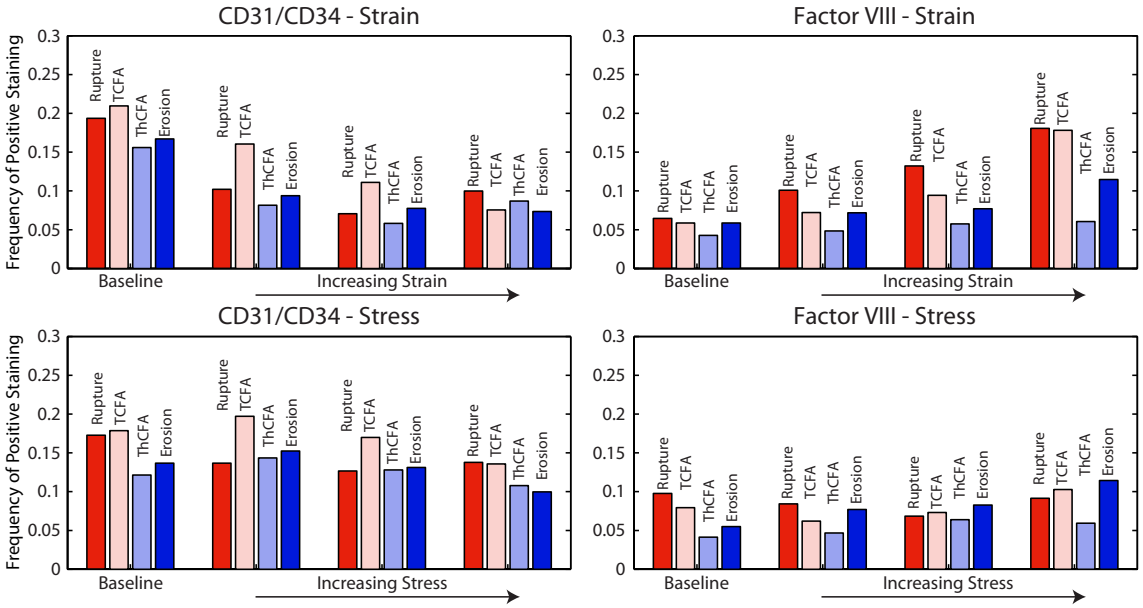


Figure 4.14: Positive staining for endothelial markers and mechanical stress and strain: We examined positive staining for endothelial markers in images registered against Von Mises stress and strain maps (Figure 4.4). We divided stress excursion into a baseline group (excursion $< 0.25$) and tertiles of equal number of elements (see Figure 4.3) then examined the frequency of positive staining associated with each level of mechanical strain.

for patient care. Whereas plaque rupture is largely an inflammatory disease, plaque erosion appears to be less so. Anti-inflammatory therapeutic techniques used to treat atherosclerotic plaques may not be appropriate to prevent plaque erosion.

This is not an idle comment. Two major clinical trials (CIRT and CANTOS) have recently been launched investigating whether anti-inflammatory strategies will reduce cardiac event rates [138, 139]. These trials are motivated by prior studies indicating positive associations between C-reactive protein (CRP) levels and incidence of cardiac events [140–142]. While CRP screening may identify patients with inflammation at risk of plaque rupture, these trials are not likely to target patients at risk of plaque erosion. While much is still unknown about the exact mechanism of erosion, our data suggests that its etiology differs from that of the current prototypical "vulnerable plaque" and as such may require a different approach for prevention and treatment.

One hypothesis warranting further investigation is the role of endothelial apoptosis and denudation in erosion. Previous studies have established this as a likely mechanism [37, 135], but the impetus for this apoptosis, especially if not inflammatory as suggested by the present study, remains

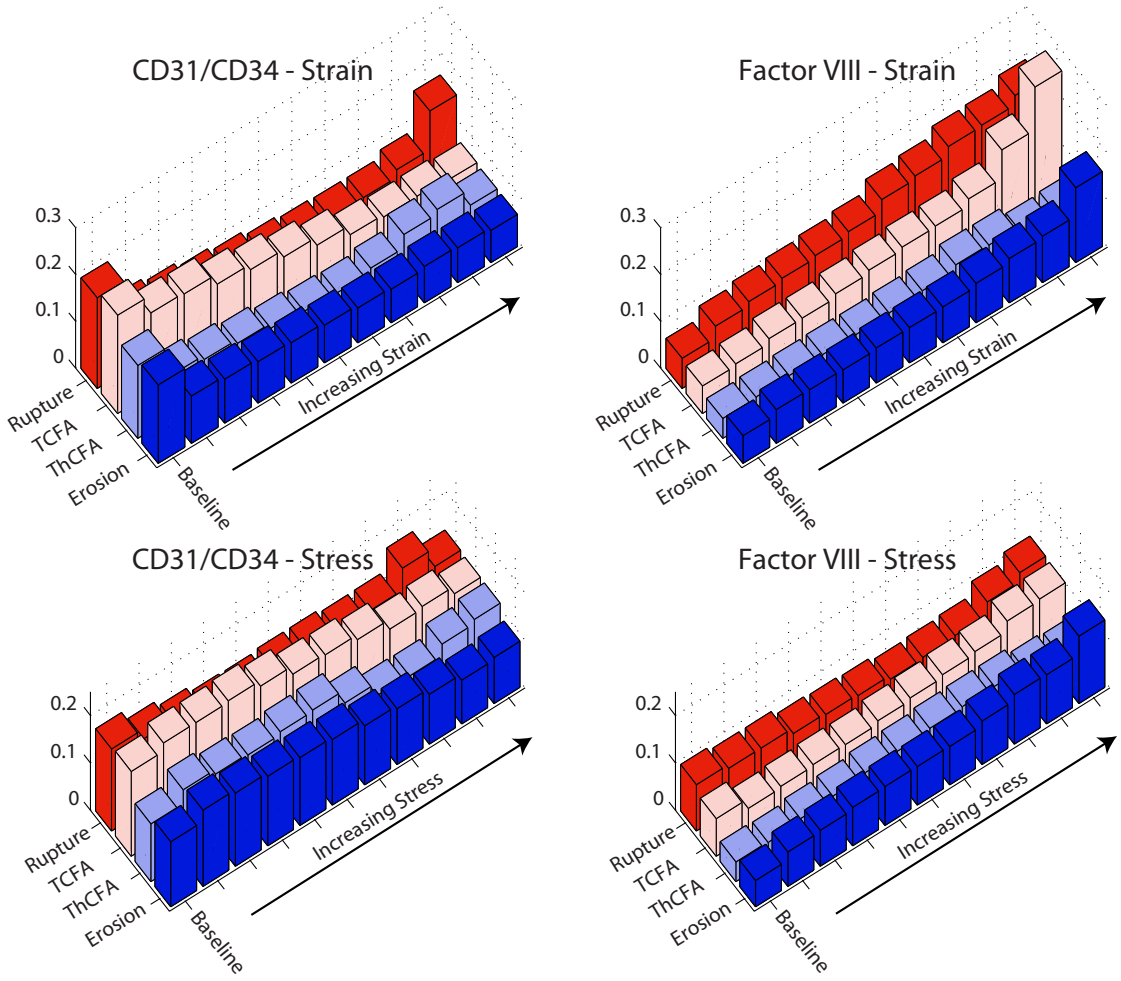


Figure 4.15: Positive staining for endothelial markers and mechanical stress and strain: We examined positive staining for endothelial markers in images registered against Von Mises stress and strain maps (Figure 4.4). We divided stress excursion into a baseline group (excursion $< 0.25$) and deciles of equal number of elements (see Figure 4.3) then examined the frequency of positive staining associated with each level of mechanical strain.

elusive. We see significantly less apoptosis in plaque erosion than in rupture or TCFAs when considering the whole vessel, and when focusing specifically on the endothelium we see no significant difference in apoptosis between any of the lesion phenotypes.

No difference in endothelial apoptosis in erosion specimens could be explained by denudation: if the endothelium was absent, then the TUNEL stain could not detect endothelial apoptosis. However, we saw significantly more Factor VIII, a marker of endothelium, in erosion specimens. This may be biased by our study methodology: we excluded regions where thrombus adhered to the wall because of the impossibility of distinguishing whether its source was endothelium or thrombus [143]. But, regions where thrombus has adhered to the wall are precisely the sites where denudation is expected. Despite this limitation, these findings are perplexing. If denudation occurs because of a "sick", apoptotic endothelium, we would still expect more apoptosis and much less Factor VIII near the lumen in erosion. If widespread apoptosis leading to denudation is not the explanation, further refinement of this etiological hypothesis is warranted.

Another noteworthy difference between eroded and ruptured plaques is the proliferation of smooth muscle cells and the media. We observed that the media was significantly thicker in erosions and ThCFAs than in ruptures. Loss of media in advanced atherosclerotic plaques is an established phenomenon [10,27], but does not seem to be at play in either eroded or ThCFA plaque phenotypes. Smooth muscle cells are essential for pathological intimal thickening to occur [17, 39] and so their loss in vulnerable and ruptured plaques likely sets up a different biomechanical environment than in erosive-phenotype plaques. This may also have fluid dynamics consequences, as the degree of stenosis may modulate shear stress magnitudes.

We did not observe as strong a relationship between stress and expression of inflammatory markers as we did with strain. Although high magnitudes of stress are necessary for tissue fissuring to occur, cells do not directly sense stress. Instead, they sense strain, which is deformation of the tissues. As the vessel wall distends under pulsatile blood pressure, cells deform and, via mechanotransduction such as cytoskeletal interaction with membrane-bound proteins or deformation of surface receptors, modulate biological processes. Therefore, that inflammatory processes are more strongly associated with strain is not unexpected. However, it is interesting to note that eroded and ThCFA plaques, which were more cellular and therefore should experience greater magnitudes

of strain for given pressures, did not demonstrate an association between strain and inflammation. Ruptured and TCFA plaques, which were less cellular and more calcified and should be stiffer, showed a much stronger association between strain and inflammation.

Our histology-based mechanical modeling and data analysis techniques are based on the methods of Hallow et al. [56]. Whereas we compared plaque rupture, erosion, TCFA, and ThCFA, Hallow et al. compared plaques at four stages of progression based upon the AHA classification system (see section 1.3.1) without respect to endpoints or vulnerability. Our plaques were classified based upon the scheme of Virmani et al. [15] (see section 1.3.2), which stratifies plaques based upon different criteria. The lesions in our study could have been classified as intermediate, advanced, or mature in the prior study's classification system. Therefore, although we both investigated the assocation between macrophages and MMP1 with stress and strain, we cannot directly compare any groups of plaques between the two studies. In the study of Hallow et al., the association between MMP1 and macrophages with stress and strain varied considerably among the four stages of lesion progression, and thus we are not surprised to see that our results do not match, given the non-overlapping classification schemes.

An established family of characteristics of plaque rupture is composition and morphology of lesions [15, 22, 23, 111]. Factors like the size and shape of necrotic core and fibrous cap thickness affect the distribution of mechanical stresses, which leads to plaque vulnerability and potentially then rupture. In the present study, plaque burden and eccentricity, as well as proportion of fibrous and lipid/necrotic tissue, were not different. Radius, lesion area, and percent cellularity and calcification were different between erosion and rupture or TCFA, but other than calcification, which may play a role in lesion stability [109, 144], these are not established characteristics of plaque vulnerability. That the morphology and composition were not, on the whole, different between plaque phenotypes strengthens our conclusion that inflammatory response to biomechanics is a key differentiator between plaques that rupture and plaques that erode.

Because we used pressure-fixed tissue as the basis for our mechanical modeling, we were only able to compute the relative distribution of stress and strain, not the absolute magnitude of either value [57]. Other studies modeling plaque rupture have attempted to discern a threshold for which a fibrous cap breaks [85, 105, 114]; no similar analysis is possible with our technique. For plaque

erosion, no gross tissue damage is expected. Unfortunately, because we do not have the ability to calculate absolute magnitudes, we cannot evaluate how the level of stress directly compares between rupture and erosion.

Additionally, erosion is not thought to be an acute event [33]. In many cases, a mural thrombus accumulates over a period of approximately a week [33], in contrast to rupture, where thrombosis is typically much more acute. As this thrombus organizes and heals in subjects with erosion, the vessel remodels and the lumen reshapes. Consequently, a histological cross-section of a vessel at the onset of plaque erosion may reveal different information than a cross-section from the time of death. With no present way to detect the initiation of plaque erosion in humans, we are limited to studying autopsy specimens until our understanding of the phenomenon improves.

There is great need for means to detect and treat plaque erosion. In this study, we have shown that the inflammatory response to the mechanical environment in atherosclerotic plaques is characteristically different between plaque rupture and plaque erosion. Ruptured plaques have a similar inflammatory response to mechanics as TCFAs, and eroded plaques respond similarly to ThCFAs. It is likely that management and treatment for patients experiencing plaque erosion will require an entirely different approach than current protocols used for those with plaque rupture.

# CHAPTER V

# COMPUTATIONAL FLUID DYNAMICS SIMULATIONS OF FLOW IN PLAQUE EROSION

## *5.1 Introduction*

The role of biomechanics in plaque disruption is widely studied: solid mechanics helps explain how a pressurized vessel wall experiencing a local maximum of stress can fissure and lead to plaque rupture. Pressurized blood isn't static, however, and fluid flow may play a role in plaque disruption as well. Although a direct link between rupture and flow mechanics like wall shear stress has not been clearly demonstrated, the role of shear stress in atherogenesis is well established [9, 81] and plaque rupture is known to occur preferentially downstream of bifurcations [145]. Low magnitude and oscillatory wall shear stress patterns tend to dominate in regions where plaques form, whereas higher magnitudes of wall shear stress are typically atheroprotective. Very high magnitudes of wall shear stress have been reported to cause endothelial damage (typically $> 70$ dynes/cm$^2$) or acute denudation (around 400 dynes/cm$^2$) [41, 55, 146].

In addition to modulating the progression of atherosclerosis, flow also affects thrombosis: high shear activates von Willebrand factor and results in platelet adhesion [47]. Given these relationships and the fact that solid mechanics alone has not yet explained why certain vulnerable plaques suddenly rupture, a role for fluid mechanics in both plaque rupture and plaque erosion deserves consideration. Initial case reports have shown a correlation between shear and site of plaque rupture [98, 99], but to date no study has considered the role of shear in localization of plaque erosion.

A leading hypothesis regarding the mechanism of plaque erosion is the loss of endothelial cells: a thrombogenic surface is presented to the blood pool when endothelium is denuded. This desquamation has been replicated in animal models by inducing apoptosis [37, 135], and both apoptosis and endothelial dysfunction may be induced by flow patterns [28]. Disturbed flow patterns have been shown to induce an erosion-like phenotype of apoptotic and detached endothelial cells in rabbits [135], although no animal model of spontaneous erosion exists.

Another possible mechanism by which flow might result in erosion is through extremely high magnitudes of shearing flow. This could forcefully detach endothelium, especially if it's already apoptotic. Mural thrombus formation would also be aided in this high-shear environment. Given that plaque erosion frequently occurs in women [17] and that women, on average, have narrower coronary arteries than men [147, 148], elevation of shear stress in patients with plaque erosion is possible. In this study, we used patient-specific computational fluid dynamics modeling to simulate blood flow through coronary arteries in patients with plaque erosion. We hypothesized that patients with plaque erosion will experience locally elevated WSS magnitude in regions where erosion has occurred. We also examined the local curvature and branching of human coronary arteries with eroded plaques in hearts obtained at autopsy. We hypothesized that curvature and branching would be associated with erosion location.

## *5.2 Methods*

We obtained coronary biplane angiograms from three patients who presented to the Emory University catheterization lab (Figure 5.1) and received a diagnosis of plaque erosion using optical coherence tomography (OCT, Figure 5.2). All patient research was performed under the approval of the Emory University Institutional Review Board.

### 5.2.1 3D Vessel Reconstruction

We reconstructed the anatomy of culprit arteries using Paieon CardioOp-B software (Paieon, Inc., New York City, sold as CV-3D by Toshiba Medical Systems, Inc., Tustin, CA). This commercial software allowed us to segment the borders of angiograms at diastole. We selected angiograms performed immediately after thrombectomy for two patients and at 12-day follow up catheterization after thrombectomy for the other patient in order to reconstruct anatomy without influence of the erosion's thrombus (Figure 5.3). Paieon produced coordinates of centerlines and corresponding radii for the culprit vessel and any nearby branches. Centerlines and radii were imported into custom Matlab software (R2011b, Natick, MA) to generate a 3D point cloud representing vessel borders, which was then imported into Geomagic Studio 2012 (Morrisville, NC) in order to generate a smooth 3D surface.

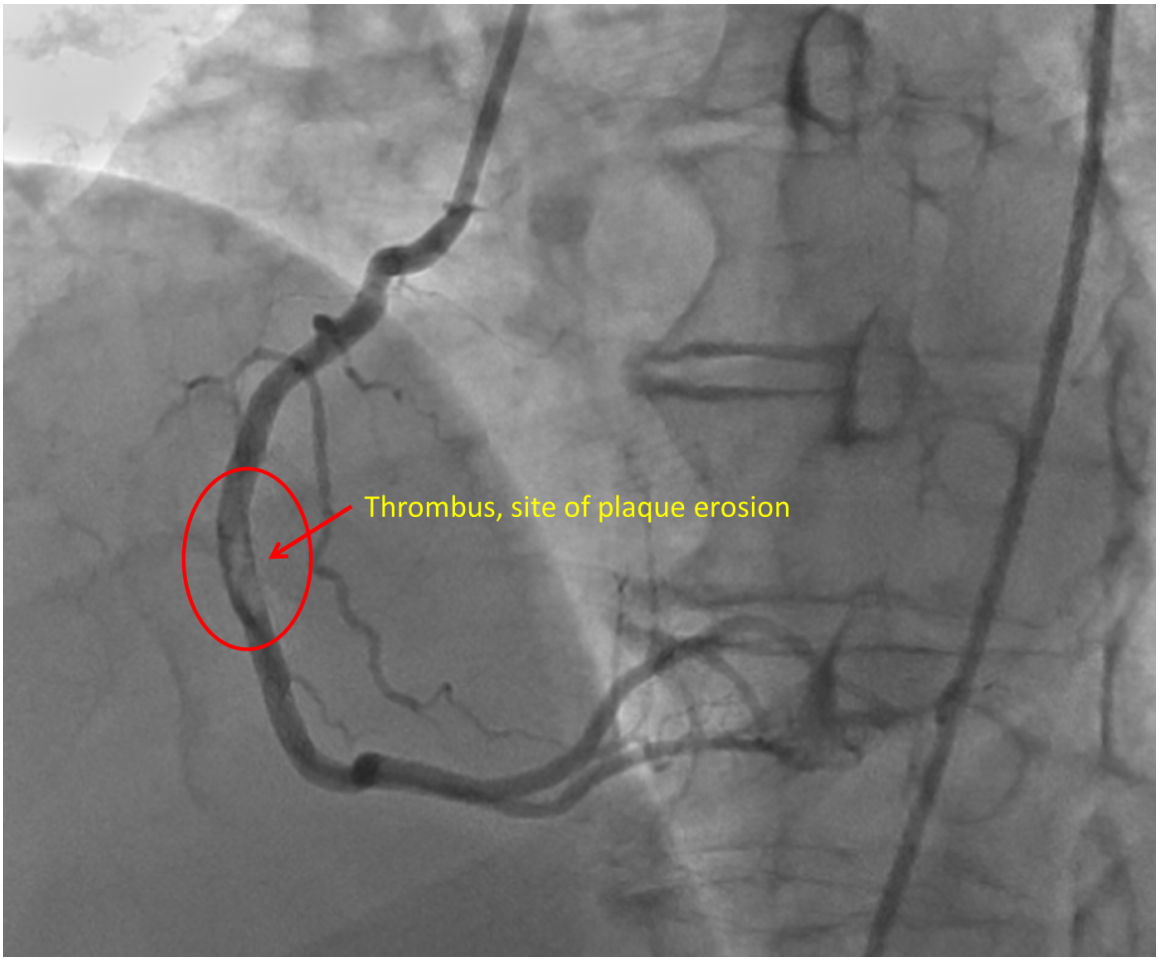


Figure 5.1: Plaque erosion in right coronary artery: This patient presented to Emory University Hospital and underwent cardiac catheterization. A large thrombus was identified in the right coronary artery, circled above in red. OCT identified the source of the thrombus as an eroded plaque.

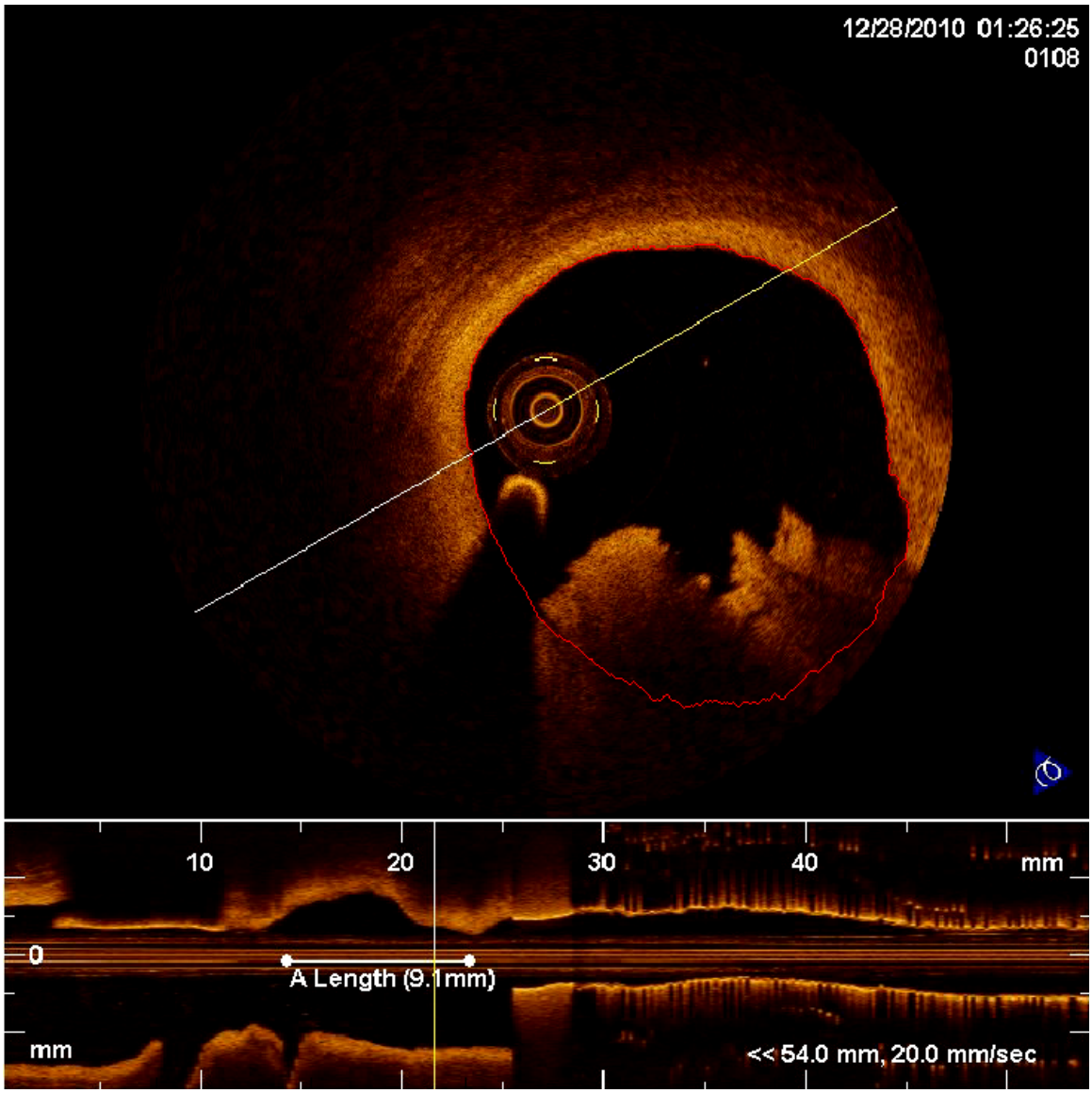


Figure 5.2: Optical coherence tomography identification of plaque erosion: Intravascular OCT reveals cross-sectional anatomy of a coronary artery. Thrombus appears at the bottom of the image as positive signal with jagged edges. We approximated the vessel boundary (red line) although behind thrombus, exact segmentation is impossible.

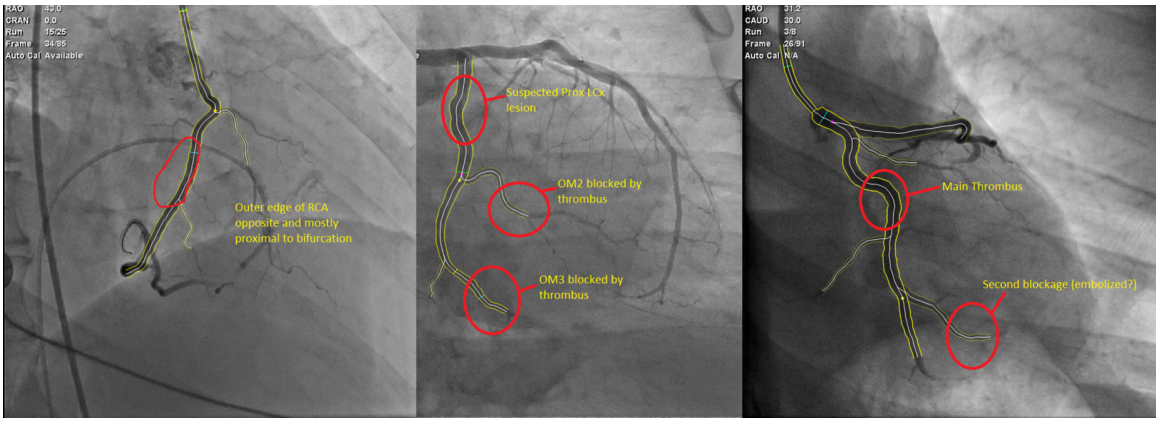


Figure 5.3: Segmentation of culprit vessels in Paieon software: We semi-automatically identified the silhouette of vessels in biplane angiograms for each of three patients using Paieon software.

### 5.2.2 Meshing and Flow Extensions

We then imported geometry into Ansys ICEM meshing software (Canonsburg, PA) to generate a 3D finite element mesh for computational fluid dynamics. Models were generated with between 1.2 and 1.9 million tetrahedral elements), as well as a prism boundary layer (8 layers deep, with a linear element size growth factor of 1.1 sized such that the innermost element was the same volume as the adjacent tetrahedral element). We added flow extensions to all inlets and outlets by projecting the contour of the inlet or outlet straight outward. Inlet flow extensions were one diameter long, and outlet flow extensions were 7 diameters long.

### 5.2.3 Computational Fluid Dynamics

Patient-specific computational fluid dynamics simulations were performed using Fluent 14.0 software (Ansys, Inc., Canonsburg, PA). We simulated pulsatile blood flow through rigid walls by prescribing a generic coronary flow waveform (Figure 5.4) as a blunt velocity inlet into our flow extension. This yielded a plug-shaped velocity distribution entering our model geometry. We simulated three continuous cardiac cycles and discarded the first two in order to remove transient artifacts from our model. We simulated 300 timesteps per cardiac cycle (for a total of 900 timesteps) for a heart rate of 75 beats per minute (0.0026667 seconds per timestep). Outlets were traction-free pressure outlets. Blood was modeled as a Newtonian fluid with density 1060 kg/m$^3$ [35] and dynamic viscosity 0.0035 Pa·s. We used the SIMPLE algorithm for pressure-velocity coupling and second-order

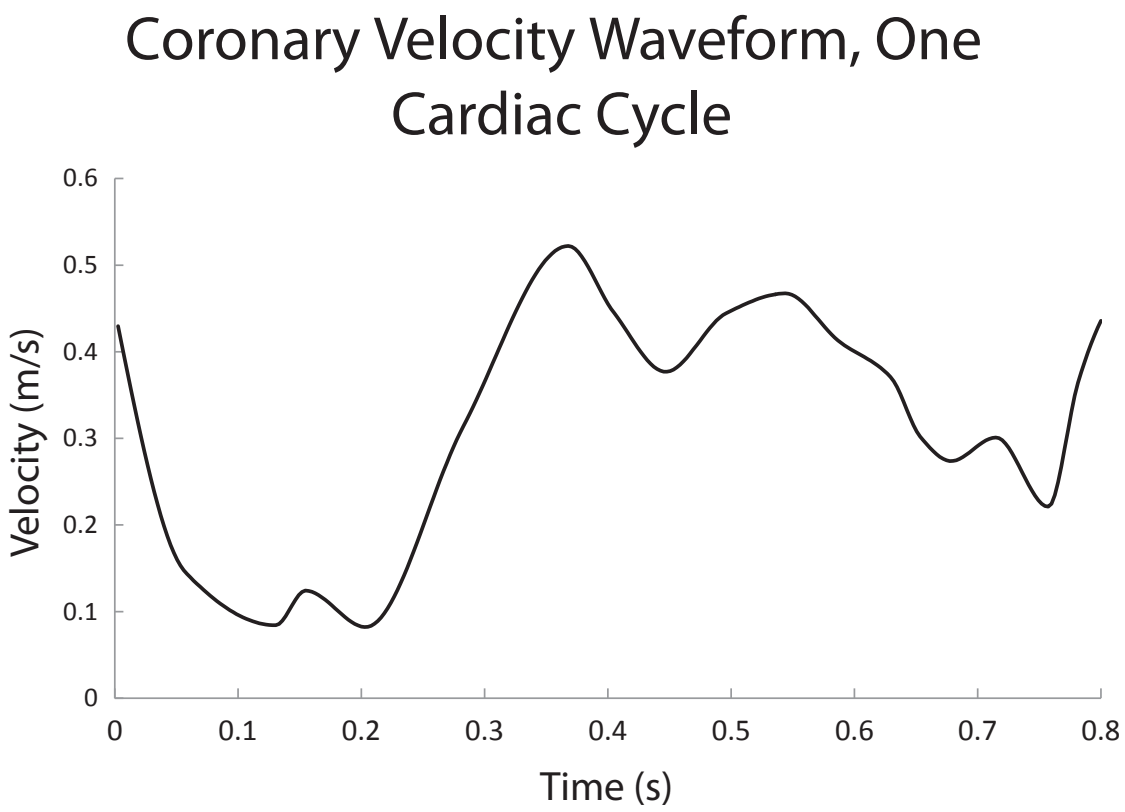


Figure 5.4: Coronary velocity waveform: We prescribed a blunt velocity profile through an inlet flow extension into each CFD model. This waveform was derived from a typical patient, as patient-specific velocity data were not available. (Waveform courtesy of Drs. Luke Timmins and Habib Samady).

Green-Gauss node based spatial discretization of pressure, momentum, and time. Convergence was prescribed as velocity and continuity residual $< 10^{-6}$.

### 5.2.4 Rendering and Postprocessing

Results were exported from Fluent in Ensight Gold format. Using custom Matlab code, we calculated temporal mean WSS and oscillatory shear index (using the algorithm of Moore et al. and a threshold of $\frac{\pi}{6}$). All data were rendered in Paraview (Kitware, Inc., Clifton Park, NY). We generated images of WSS and OSI, as well as animations of instantaneous WSS, streamlines, and particle paths. To assess that we had achieved mesh convergence, we re-meshed the same geometries at half resolution and confirmed that neither mean WSS nor OSI changed in distribution.

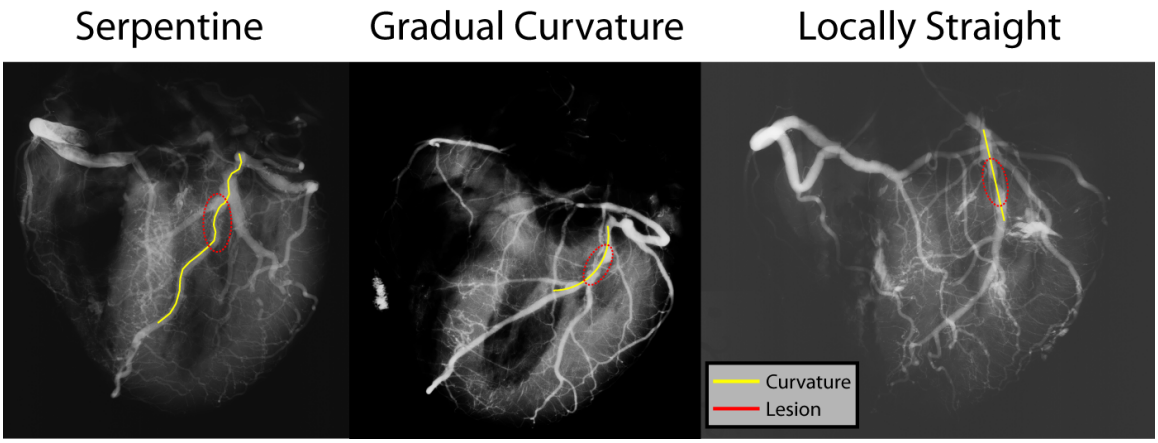


Figure 5.5: Identification of local curvature: For each lesion identified in x-ray angiograms, we tallied whether the local region was serpentine (left), gradually curving (middle), or locally straight (right).

### 5.2.5 Anatomical Location of Plaque Erosion and Rupture

We identified the site of plaque erosion and rupture in paired single-plane x-ray angiograms from explanted autopsy hearts [30]. These were a different set of individuals than those used for CFD. Hearts from the Maryland Medical Examiner's Office were perfused with barium gelatin and then x-rayed onto film, which was subsequently digitized with a flatbed scanner. Histological analysis of the hearts resulted in identification of plaque erosion in 13 hearts and plaque rupture in 6. Based on the site of greatest stenosis and histological description of the site of thrombosis, we identified geometric features of the coronary anatomy for each patient. We tallied whether each was in a section of vessel that was nearly straight, gradually curved, or highly serpentine (Figure 5.5). We also tallied whether bifurcations or trifurcations existed within 2.5 diameters length upstream, downstream, or immediately across from the site of thrombosis.

## *5.3 Results*

### 5.3.1 Computational Fluid Dynamics

We simulated blood flow in all culprit vessels, one each of the left anterior descending (LAD), left circumflex (LCx), and right coronary artery (RCA). In all three, thrombus location coincided with relatively low magnitudes ($< 2$ Pa) of mean WSS, but these regions were neither the lowest WSS in the vessel nor the only region with mean WSS $< 2$ Pa (Figure 5.6). The spatial distribution of peak WSS was nearly identical to that for mean WSS. Again, maximum WSS magnitude at sites of

Table 5.1: Tallies of local curvature at sites of plaque erosion and plaque rupture

| **Lesion Type** | **Serpentine** | **Gradually Curving** | **Straight** | **Total** |
|---|---|---|---|---|
| Erosion (autopsy heart) | 4 (30.8%) | 4 (30.8%) | 5 (38.4%) | 13 |
| Erosion (cath lab) | 1 (33.3%) | 1 (33.3%) | 1 (33.3%) | 3 |
| Rupture (autopsy heart) | 1 (16.7%) | 4 (66.7%) | 1 (16.7%) | 6 |

Table 5.2: Tallies of nearby branching (within 2.5 diameters) at sites of plaque erosion and plaque rupture

| **Lesion Type** | **Upstream Branch** | **Branch at Site** | **Downstream Branch** | **Total** |
|---|---|---|---|---|
| Erosion (autopsy heart) | 8 (61.5%) | 0 (0%) | 3 (23.1%) | 13 |
| Erosion (cath lab) | 0 (0%) | 0 (0%) | 1 (33.3%) | 3 |
| Rupture (autopsy heart) | 1 (16.7%) | 2 (33.3%) | 1 (33.3%) | 6 |

erosion was neither the highest for the vessel nor was it unique. Maximum WSS magnitudes at sites of erosion was < 12 Pa.

We found no association between thrombus location and OSI (Figure 5.7). Streamline analysis revealed some helical flow patterns within the region for part of the cardiac cycle, but this too was not unique to the region of thrombus formation (Figure 5.8). We visually observed essentially no reversal of flow in the region of the thrombus, although one lesion (LCx) was distal to a bifurcation and some reversal was observed upstream at the site of bifurcation.

### 5.3.2 Anatomical Location of Thrombi

Local curvature and downstream bifurcation were not associated with site of plaque erosion in explanted hearts, but an upstream bifurcation or trifurcation existed in 8/13 erosions. Among biplane angiograms from living patients (n=3), sites of erosion were again split evenly among local curvature. One patient had nearby upstream bifurcation, and one had adjacent downstream bifurcation. Of rupture specimens, two-thirds were in gradually curving regions, one-third had a bifurcation at the site of rupture, and one specimen had a nearby downstream trifurcation. Data are tallied in Tables 5.1 and 5.2.

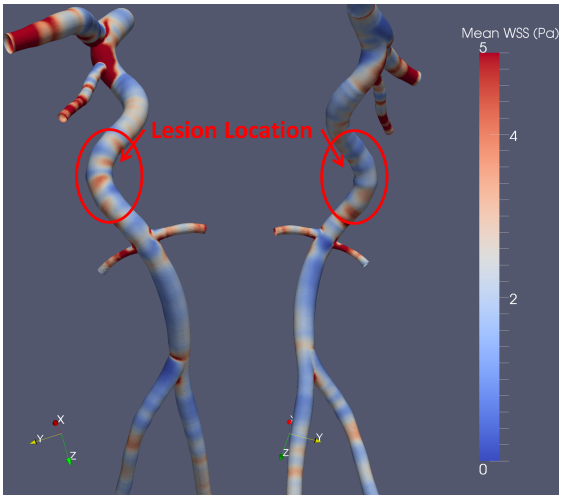


(a) Patient 1

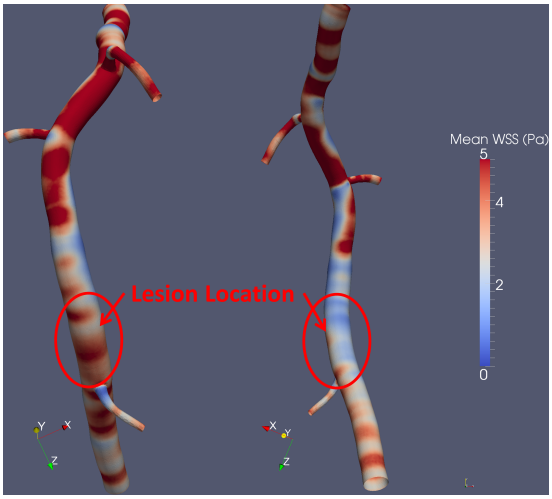


(b) Patient 2

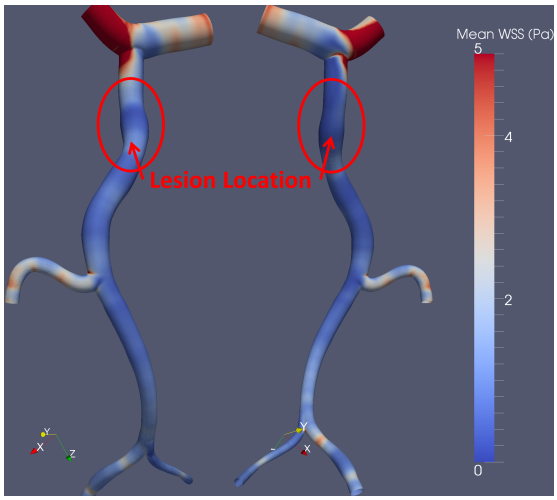


(c) Patient 3

Figure 5.6: Mean Wall Shear Stress: We computed the temporal mean WSS for all three patients. All patients' erosions were at sites containing low magnitudes of WSS, but these this is not a unique feature to the erosion sites.

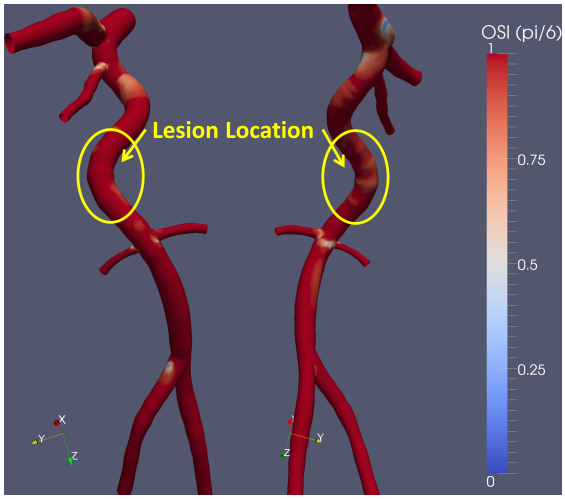


(a) Patient 1

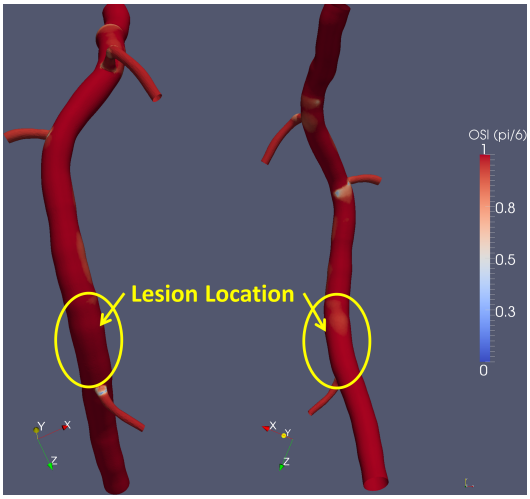


(b) Patient 2

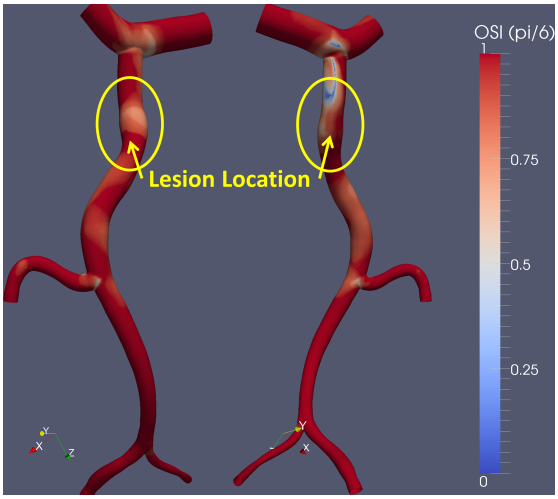


(c) Patient 3

Figure 5.7: Oscillatory shear index: We calculated oscillatory shear index, a measure of the duration of the cardiac cycle when flow deviates from its mean direction by more than $\frac{\pi}{6}$ radians. No remarkable patterns in OSI related to plaque erosion location were identified.

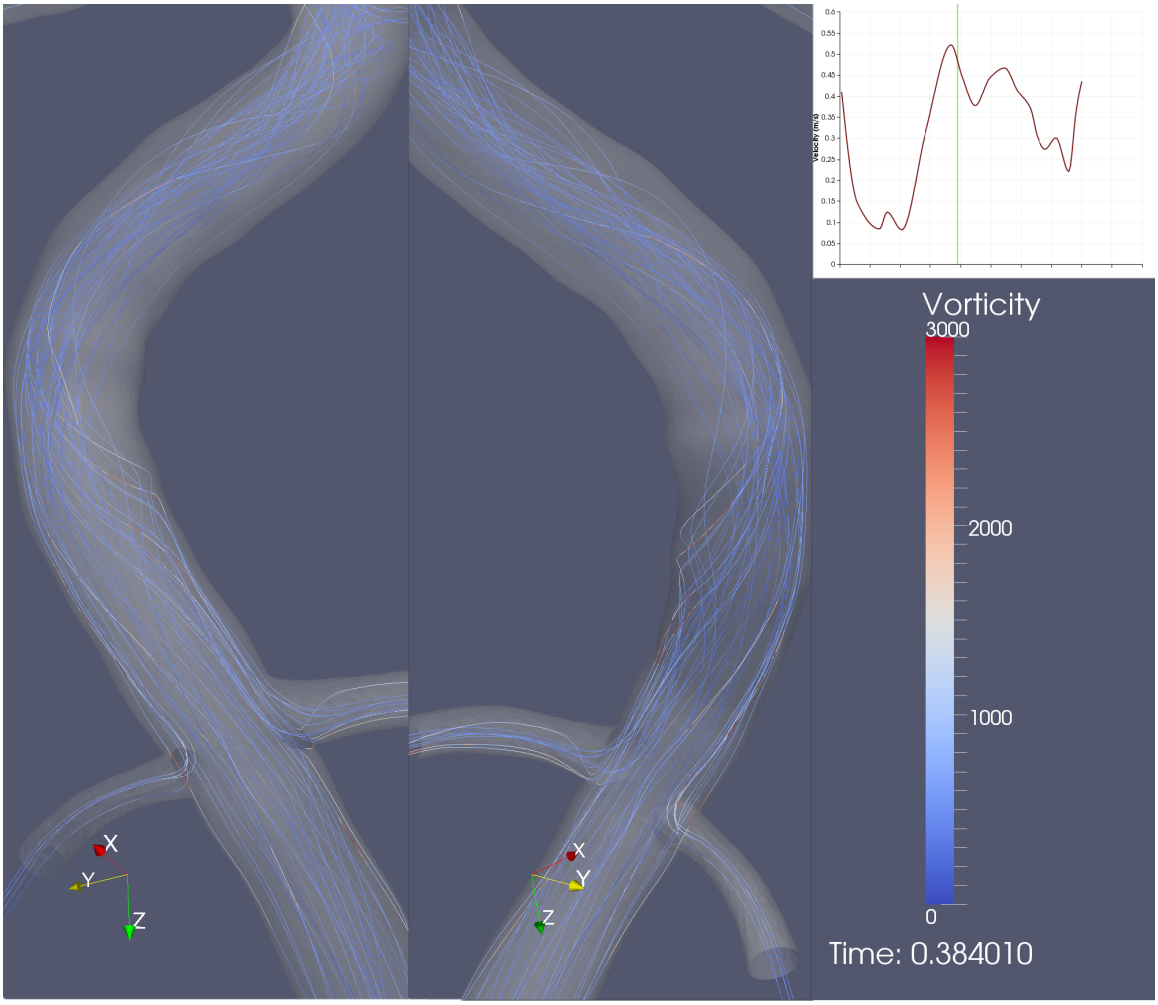


Figure 5.8: Transient helical flow structures: Occasional helical flow structures would appear at the site of plaque erosion when visualized by streamline analysis.

## *5.4 Discussion*

This initial modeling study suggests that flow does not seem to be a major factor in the localization of plaque erosion. In all three cases, neither the local flow environment nor the surround geometry were particularly remarkable. High wall shear stress, which we hypothesized would induce plaque erosion by damaging endothelium via shear, is not present in any of these patients at the site of thrombus formation. If anything, WSS tended to be low at these sites. Although we cannot rule out that very high WSS is sufficient to induce plaque erosion, we can conclude that it is not necessary.

Low WSS is known to be associated with increased apoptosis. However, this relationship is complex [86, 149, 150]. There were numerous other sites in each culprit vessel that also experienced low mean WSS, and yet no erosion occurred at those sites. Helical flow patterns were also present in the eroded regions during part of the cardiac cycle, but these too were present in segments without erosion. Thus, the relationship between plaque erosion and fluid mechanics is complex and possibly multifactorial, if one exists at all.

A major obstacle in most clinical plaque disruption research is the lack of data from before induction of thrombosis. In plaque erosion, a mural thrombus accumulates over a period of weeks [33], and during this time vascular remodeling may occur. If vasospasm induces plaque erosion, as has been hypothesized [34, 41], the fluid environment could well play a role, as it would lead to very high magnitudes of WSS resulting in denudation. However, vasospasm is a transient phenomenon [10]. No evidence of stenosis from such an event (or from vascular remodeling) was observed in our angiograms, but patients undergoing cardiac catheterization are given vasodilating drugs, so no evidence is expected. Ideal computation fluid dynamics modeling would simulate coronary flow based upon anatomies approximately two weeks before diagnosis of erosion, but such a dataset will continue to be nonexistent without prospective diagnostic criteria for erosion.

Other challenges when generating relevant vascular geometry include the possibility of thrombus in the angiogram. We used angiograms from the end of the procedure (or in one patient's case, a follow-up angiogram from several days later) when the thrombus had resolved. Because angiograms only resolve the lumen of vessels where flow is occurring, any residual mural thrombus would create a geometric artifact, artificially narrowing the lumen. We saw no such evidence of stenosis in

any of the images after thrombectomy, and if it would have occurred, our estimates of WSS should overestimate the true magnitude. Given that we computed relatively low WSS in regions of erosion, this possibility seems unlikely.

Geometric modeling assumptions could have affected our results as well. We simulated coronary vessels as rigid structures. In reality, arteries can both distend under pulsatile pressure as well as bend as the myocardium contracts and expands. This bending has been hypothesized as direct cause of plaque rupture [110, 151], and although moving walls like alters flow patterns, solid mechanical stresses from repeated bending do not appear to be a critical factor in plaque erosion (see Chapter 4). Still, future modeling using fluid-structure interaction (FSI) would alleviate some of these artifacts. Adding in patient-specific blood viscosity and using higher-order rheological models than a Newtonian fluid would further remove modeling assumptions.

Additionally, the software we used to generate 3D geometries from angiograms yields circular cross-sections for all vessels. In reality, vessel cross-sections are not perfectly symmetric and sometimes are rather elliptical, especially in the presence of atherosclerosis. Although more accurate geometry could be produced by considering vessel diameter in both views of biplane angiograms, previous research has shown that patterns of WSS are not significantly altered by assuming a circular cross section [152].

The opportunity to acquire both pre- and post-procedure biplane angiograms in conjunction with OCT in a case of plaque erosion is indeed very rare. Although our sample size of three patients is small, these are very unique data. This study is exploratory in nature but does rule out a very obvious flow-related etiology as being necessary for plaque erosion.

Our tallies indicate that anatomic features related to flow patterns do not appear associated with plaque erosion or rupture, although this initial work involves a small sample size and has not been evaluated statistically. We see the same trends in plaque erosion in both patient and autopsy angiograms: local curvature of the vessel segment is not associated with erosion, although this could alter flow patterns. The relationship between WSS and atherogenesis is especially apparent on the inner edge of curvatures and bifurcations, where low and oscillatory WSS occurs [78]. We do observe that many plaque erosions happen shortly downstream of vessel branching, but just the same, many erosions occur in regions without unusual geometry. For this reason, we suggest that

flow is not a direct modulator of plaque erosion and that biological or solid mechanical explanations may offer more promise for elucidating the exact mechanism of plaque erosion.

# CHAPTER VI

# CONCLUSIONS AND FUTURE DIRECTIONS

## *6.1 Summary*

In this dissertation, we aimed to investigate the role of biomechanics in endpoints of atherosclerosis, namely (putative) plaque rupture in mice and plaque erosion in humans. We used lesion-specific biomechanical modeling techniques to simulate solid and fluid stresses at sites of atherosclerosis, and we investigated how morphology and composition affect the likelihood of plaque rupture or erosion. These studies revealed how plaques in mice and plaques that have eroded experience unique distributions of stresses compared to plaque rupture. As such, neither of these situations is mechanically likely to rupture and should therefore be regarded as distinct phenotypes to which the standard risk factors for plaque rupture most likely do not apply.

The mouse model of atherosclerosis is a leading tool for studying the progression of atherosclerosis, but rupture in mice is elusive, if not entirely absent. In studies of murine plaques, researchers often describe plaques as "vulnerable" or "unstable" despite minimal evidence that mouse plaques rupture in the same way as in humans. Our biomechanical modeling has revealed that the distribution of solid mechanical stresses is completely different in mice than in humans. Whereas human "vulnerable" plaques experience local maxima of stress on the thin fibrous cap over a necrotic core, or on the shoulders of the plaque, murine plaques have the local maxima primarily on the media and adventitia where no plaque is available to rupture. Thus, descriptions of "vulnerable" plaques in mice are likely misnomers. If plaques can rupture in mice, they do not appear to do it at the stages of atherogenesis we studied, which we deliberately selected to represent a cross-section of available models in terms of time and severity.

The mechanics differ between mice in men at least in part due to differences in morphology and composition between the species. Plaques in mice are significantly more cellular and less fibrous than human thin-cap fibroatheromas. Acute models of plaque formation in mice do not form calcifications, either micro-scale or macro-scale, distal to the aortic leaflets within the timescale of these

models. Chronic models do form macrocalcifications and thus appear to be slightly more similar to human lesions, which form over a period of decades. However, the shape of atherosclerotic plaques is entirely different in mice than in humans, regardless of timescale. Murine plaques rarely cover the entire circumference of the vessel, whereas in humans some neointimal hyperplasia is nearly always observed on the full wall (with the consequence of redistributing mechanical stresses). The overall plaque burden is significantly lower in mice, and the complexity of lesions, with buried fibrous caps and multiple lipid pools, is often high in this species.

Mechanics, morphology, and composition differ within human lesions when comparing ruptured with eroded plaques, as well as with undisrupted plaques like thin-cap fibroatheromas and thick-cap fibroatheromas. However, the role of mechanics in differentiating human plaque phenotypes is more complex than simple distribution of stresses and strains. Using immunohistochemical detection of inflammatory markers within the lesions in tandem with solid mechanical modeling, we demonstrated that inflammation is positively associated with strain in ruptured and TCFA plaques, but not in eroded or ThCFA plaques. This suggests that inflammation is not the driving force in the progression of plaques to erosion, as well as suggests a novel pairing of varieties of atherothrombosis with "vulnerable" phenotypes for each. Whereas the link between plaque rupture and TCFAs is well-established, little is known about how plaques progress to erosion.

Although certainly not all ThCFA plaques will erode, so too is the fact that not all TCFAs will rupture. Thus, further research is necessary to understand the mechanism that initiates plaque erosion. Because inflammation is lower in eroded plaques than in ruptured and because it does not appear to be modulated by stress or strain like in ruptured plaques, it does not seem likely that inflammation is a primary modulator of this process. Therefore, clinical practice may need to be altered to treat these patients, as anti-inflammatory approaches to lesion management may not successfully mediate plaque erosion. Differences in media thickness and in the proportional composition of smooth muscle cells suggest that a different type of cell proliferation than inflammatory cells may be a possible target to manage these patients.

Initial modeling provided another biomechanical difference between plaque rupture and plaque erosion: flow. In plaque rupture, some studies suggest that patterns of shear stress on the endothelium could play a role in modulating the location of plaque rupture. Although our patient sample

size was small, our modeling did not reveal any obvious connection between flow patterns and plaque erosion. Erosion tended to happen in regions of low magnitude WSS without much oscillation, but these regions were not unique to the vessel and would not help identify plaque erosion location without additional factors. Geometric predictors like local curvature and vessel branching also did not help predict plaque erosion, which is noteworthy because rupture often occurs in regions of disturbed flow, particularly near branches. That flow does not seem to be associated with sites of plaque erosion further suggests that the processes resulting in plaque erosion are quite unique from those leading to plaque rupture.

### *6.2 Refinement of Research Methods*

Our mechanical modeling is based on a powerful, established technique to compute the distribution of solid mechanical stresses and strains from fixed histology specimens. However, several additions to this technique could minimize the effects of some of our assumptions. Here, we assume the magnitude of residual stresses is small relative to the incremental stresses in the wall from the pulse pressure. Although these magnitudes are likely small, their absence prevents us from estimating the magnitudes of stress and strain.

Several "inverse method" techniques have been developed that may be able to calculate residual stresses, given the geometry of fixed tissue [153–155]. These techniques are not currently part of the finite element software we use, and thus would require advanced computational approaches to incorporate them into our existing methodology. Such a process would be decidedly nontrivial to implement, and it would likely fail when used on specimens with histology artifacts. It would probably be best implemented on our mouse tissues perfused with vascular casting compound, as they contain the fewest artifacts.

Using an inverse method to calculate stresses would enable estimation of magnitude of stress and strain, a common concern we heard from reviewers and colleagues at conferences. Although none of the conclusions in the studies in this dissertation were affected by this detail, another benefit of being able to calculate the zero-stress conformation of tissues is that we could then apply nonlinear material properties in our model. It has been shown that the tissue components in coronary atherosclerosis can be closely approximated by bilinear material properties, which we implemented

in these studies [100]. However, prescribing nonlinear material properties would allow us to use material models described by other groups, including mouse-specific material properties. Again, implementing such methods come at the cost of great complexity (and their own set of assumptions) but are nonetheless an avenue worth future consideration.

Another material property factor not implemented in the current study is anisotropy of materials. Our reason for omitting this is straightforward: atherosclerotic lesions are far too complex to implement such details without knowledge of fiber directions. Anisotropic material properties are routinely described in vascular biomechanical literature where a blood vessel is approximated as a cylinder, but such a description fails to approximate patient-specific atherosclerotic lesions. Using registered high-resolution microscopy images of picrosirius red staining under polarized light, one may be able to derive primary fiber directions on a patient-specific basis. Such an approach would require advanced image-processing techniques to derive local fiber direction then apply it to the finite-element model.

Material property assumptions could be further refined by incorporating even more tissue types into our segmentation. Currently, we identify all tissue as being fibrous, cellular, lipid, or calcium. Although these describe all major components of lesions, some could be subdivided further to yield even more specific material properties. For example, Movat's pentachrome staining differentiates between collagen and proteoglycans, but we lump both tissue types together as "fibrous". With registered picrosirius red staining, we could even differentiate between Type I and Type IV collagen, which likely have different material properties as well. Taking these and other tissue types into account would improve accuracy of computational solid mechanics modeling.

Two major limitations to our histological techniques stand out that could be refined upon further analysis. First, our staining for apoptosis using the TUNEL assay does not conclusively identify apoptosis in all circumstances: regions of false positives are possible and could be confirmed using a second apoptosis assay such as staining for caspases or phosphotidylserine. The other histology limitation in this dissertation was our inability to use Movat's pentachrome stain in murine tissues. By identifying a different vascular casting compound that doesn't absorb the black stain in pentachrome, it's possible that we could have directly compared human to mouse tissue using the same stain. Sensitivity analysis showed that using this different stain did not affect our results, but a direct

comparison would nonetheless be more ideal. Unfortunately, even if a different vascular casting compound was identified, the entire study would need to be repeated in its entirety.

In our computational fluid dynamics models, the most physiologically relevant refinement we could make to our methods would be to include fluid-structure interaction (FSI) and eliminate our assumption of rigid walls. Such a task would add considerable complexity to our model: we would need to track the boundary of the coronary arteries across the entire cardiac cycle and, if we wanted to run full two-way FSI, apply material properties to the wall, even though we have neither thickness nor composition data for the arteries from our biplane angiograms. This task would be prohibitively difficult, which it why it was not included in this study. However, the fact remains that arteries move over the cardiac cycle, and future studies into coronary flow should take this motion into account. Other simplifying assumptions such as modeling blood as a Newtonian fluid could be removed by utilizing more complex rheological models.

### *6.3 Additional Experiments*

Additional endpoints could be considered to more thoroughly evaluate our conclusion that plaque rupture is mechanically unlikely in mice. We considered a range of mouse models encompassing some of the most severe models available, with the thinking that if rupture is unlikely in these models, it should be even less likely in more moderate models. However, we cannot rule out the possibility that other models may be strong candidates for rupture without performing similar analysis. Gender and age are two factors known to modulate the severity of atherosclerosis in mice that were not thoroughly investigated in our studies. We recommend incorporating female mice into future studies, as well as adding additional harvest time points in the chronic model of lesion formation, both shorter and longer than the 1 year time span we considered. Additionally, other mouse models such as ApoE$^{-/-}$ mice fed different formulations of diet, the ApoE*Leiden mouse, or hypertensive mice fed DOCA salt might be considered to include a wider cross-section of mouse models.

One might improve our solid mechanical modeling of plaque erosion study in a similar manner by considering additional histological markers to differentiate between plaque erosion and plaque rupture. We investigated MMP1 and MMP9 because they are well-established MMPs associated with plaque progression. However, there are dozens of additional MMPs and four families of tissue

inhibitors of metalloproteinases (TIMPs) that could be considered as well. Other inflammatory cell types such as leukocytes could additionally be stained for to derive an even more thorough understanding of the differences between plaque rupture and plaque erosion. A major limitation to wanton staining (besides the high cost of antibodies) is that our mechanical modeling is based on a single histological section, and each additional stain adds 500 microns to the distance from our Movat's pentachrome slide. Although morphological differences are small from slide to slide, this differences compound the farther one travels from the original slide. Thus, although staining for additional markers may be prudent to help elucidate the mechanism of plaque erosion, judicious selection of stains is necessary.

Another possibility for a future study would be a full 3D reconstruction of lesions from histology. By sectioning an entire lesion and digitally stacking the slides, one might recreate the entire lesion to provide additional mechanical insight beyond that of a single plane [156]. Such a task would be technically challenging and time-intensive to implement, but if carefully planned, it may yield important insights into lesion mechanics. With a full 3D model, one could not only simulate the solid mechanical stresses in the wall but also fluid mechanics as well by adding in FSI. This feature would significantly increase the comprehensiveness of the lesion-specific mechanical analysis.

Analysis of the role of flow in plaque erosion would be greatly strengthened with a larger patient sample. Unfortunately, such patients are not frequently identified in the cardiac catheterization laboratory, and thus the sample size for our present study was quite small. Of those that did arrive, not all had biplane angiograms acquired, a necessity for 3D reconstruction of vessels. By searching a longer time frame or by including additional institutions, one might improve the sample size of this study such that statistical differences between plaque erosion and plaque rupture might be identified.

One aspect not included in our study that should be considered in future CFD analysis of plaque erosion is comparison to patients with plaque rupture. Although such patients are common and datasets abound, careful consideration is necessary to design an appropriate study. The degree of stenosis from a lesion could be the single most important factor modulating the magnitude of wall shear stress, so careful matching of lesion stenosis is essential to the design of a good study. If wall shear stress is not a factor in plaque erosion, such consideration might be less critical, and an

expanded evaluation of the sites of rupture and erosion should be conducted.

Another factor that should be studied further is the pattern of blood swirling around the sites of lesions. We observed some helical flow structures at the sites of plaque erosion (as well as at sites away from plaque erosion) that could be further evaluated mathematically by computing the overall helicity. One factor that would improve the patient-specific accuracy of such analysis, besides FSI, would be application of patient-specific velocity profiles. Because all of the subjects in our study arrived in the cardiac catheterization laboratory in an emergency situation, no patient-specific flow waveform was acquired, as it was not clinically necessary. Future studies could perhaps follow up with such patients after they leave the cardiac catheterization laboratory to acquire a patient-specific waveform noninvasively, perhaps with techniques such as Doppler ultrasound.

### *6.4 Future Research Directions*

The long-term clinical goal of the research in this dissertation is to improve patient treatment by better understanding the mechanisms of plaque erosion and plaque rupture. The big picture right now is answering the question: why do some plaques progress to form a thrombus? The TCFA has been identified as the "vulnerable" phenotype for plaque rupture, but not all TCFAs progress to rupture. Similarly, this research suggests that ThCFAs are a family of plaques in which at least a subset are likely vulnerable to erosion. Not all ThCFAs progress to erosion either, so it is critical that future cardiovascular researchers better understand the mechanism that induces plaques to rupture or erode.

One key possibility for both types of plaques that was not included in this research is vasoreactivity, such as spasm. When this occurs, the mechanics of the media and intima change as the vessel contracts. So too does the pattern of WSS across the region change as a stenosis is induced. This shear force could have major consequences for the endothelium and might help explain plaque erosion. Contraction of the media will result in increased stress throughout a lesion, which could have great consequences for rupture. FSI modeling of vessels under vasospasm may yield important insights.

Given that our research has shown that inflammation is not likely the target for plaque erosion, the role of smooth muscle cells in the progression of ThCFAs into erosions seems another good

starting point for future studies. How do these cells leave the media, and what induces them to transition from a contractile to a synthetic phenotype? Do they play a role in signaling for endothelial apoptosis? If not smooth muscle cells, what causes this apoptosis? And, if apoptosis cannot explain denudation, what is the actual cause? An animal model of spontaneous plaque erosion would be a critical tool for studying means to identify and treat patients with erosion, but first these questions must be answered such that a physiologically-relevant model of erosion can be developed.

Our results indicate that current popular mouse models are not likely relevant for studying plaque rupture. The distribution of stresses is not on the lesion at all, and instead focuses primarily on the plaque-free media and adventitia. Although this finding may be disappointing for researchers seeking a mouse model of plaque rupture, this could indicate a new research direction for those studying aortic aneurysm formation. A number of approaches for inducing abdominal aortic aneurysms in mice exist, and each has benefits and weaknesses. Future research might take into account the distribution of stresses into the weak portion of the wall when developing new mouse models or studying existing ones and trying to reconcile how aneurysms in mice apply to those in humans.

Another finding in our studies of mice was the occurrence of micro-scale calcifications in lesions on the aortic leaflets. Even young mice under pro-atherogeneic conditions for 8 weeks formed these calcifications. Given recent studies suggesting a role for microcalcifications in rupture of the fibrous caps of human plaques as well as other studies suggesting a stabilizing role for macrocalcifications, the existence of these calcifications should be studied further. Why are they forming in lesions on the leaflets? Will they result in rupture? Will they stabilize the lesion? Will they progress to macrocalcifications or remain small? Are they even relevant to human microcalcifications? Are they relevant to studies of valvular heart disease? These are all questions that should be addressed through the intersection of computational solid mechanics and biological techniques.

Other phenotypes of plaque disruption should be studied biomechanically as well. Calcified nodules, although relatively rare, do exist and can result in fatal thrombus. Mechanical modeling could help identify plaques likely to progress to this stage and understand the function of calcification. Similarly, intraplaque hemorrhage is a phenomenon not well understood. Mechanics could

explain why microvessels leak, and biological studies are necessary to better understand the consequence of this phenomenon. The healing response to this phenomenon could have consequences for plaque remodeling and stability that could be studied using the lesion-specific modeling techniques in this dissertation.

A final research question at the intersection of biology and mechanics is the role of WSS in plaque progression. Atherogenesis is well-known to be associated with low magnitudes and oscillatory patterns of WSS, but those factors alone cannot explain plaque progression. Most lesions expand outward initially and preserve lumen diameter through Glagov remodeling, but when a lesion begins to remodel inward, it forms a stenosis. This stenosis typically experiences high magnitudes of WSS upstream but low magnitudes and oscillatory flow downstream, particularly as the severity of stenosis increases. This process would seem to form a positive feedback loop of perpetually-expanding lesion, but most people don't have extensive lesions like this process ought to create. There is more work yet to be done, especially with biomechanical techniques like those used in this dissertation, to better understand exactly how atherosclerosis begins, progresses, and leads to thrombosis.

### *6.5 Conclusion and Clinical Implications*

Overall, this dissertation research demonstrates that plaque rupture in humans is biomechanically unique when compared to plaque erosion and to plaque rupture in mice. We have shown that mouse models of atherosclerosis do not seem likely to experience plaque rupture and may not be physiologically relevant for studying the phenomenon. We have shown that inflammation is not modulated by mechanical strain in erosion as it is in rupture, which implies that clinical management of patients may need to be refined to account for a different etiology of thrombosis in erosion. Lastly, we have shown that erosion does not seem to be associated with flow, which implies that additional biological mechanisms should be considered to better understand the phenomenon.

# REFERENCES


[1] American Heart Association, "Women and Cardiovascular Diseases Statistics 2010," tech. rep., American Heart Association, 2010.

[2] Cockburn, E. and Reyman, T. A., *Mummies, Disease, & Ancient Cultures*. Cambridge: Cambridge University Press, 2, illustr ed., 1998.

[3] Stary, H. C., Chandler, A. B., Glagov, S., Guyton, J. R., Insull, W., Rosenfeld, M. E., Schaffer, S. A., Schwartz, C. J., Wagner, W. D., and Wissler, R. W., "A definition of initial, fatty streak, and intermediate lesions of atherosclerosis. A report from the Committee on Vascular Lesions of the Council on Arteriosclerosis, American Heart Association.," *Circulation*, vol. 89, pp. 2462–78, May 1994.

[4] Nissen, S. E., "The vulnerable plaque "hypothesis": promise, but little progress.," *JACC. Cardiovascular Imaging*, vol. 2, pp. 483–5, Apr. 2009.

[5] Hansson, G. K. and Heistad, D. D., "Two views on plaque rupture.," *Arteriosclerosis, Thrombosis, and Vascular Biology*, vol. 27, p. 697, Apr. 2007.

[6] Schwartz, S. M., Galis, Z. S., Rosenfeld, M. E., and Falk, E., "Plaque rupture in humans and mice.," *Arteriosclerosis, Thrombosis, and Vascular Biology*, vol. 27, pp. 705–13, Apr. 2007.

[7] Jackson, C. L., "Defining and defending murine models of plaque rupture.," *Arteriosclerosis, Thrombosis, and Vascular Biology*, vol. 27, pp. 973–7, Apr. 2007.

[8] Schwartz, S. M., DeBlois, D., and O'Brien, E. R., "The intima. Soil for atherosclerosis and restenosis.," *Circulation Research*, vol. 77, pp. 445–65, Sept. 1995.

[9] Ku, D. N., "Blood flow in Arteries," *Annual Reviews of Fluid Mechanics*, vol. 29, pp. 399–434, 1997.

[10] Fuster, V. and Chesebro, J. H., "Atherosclerosis - A. Pathogenesis: initiation, progression, acute coronary syndromes, and regression," in *Mayo Clinic Practice of Cardiology* (Giuliani, E., Gersh, B., McGoon, M., Hayes, D., and Schaff, H., eds.), ch. 28A, pp. 1056–1081, St. Louis: Mosby, 3 ed., 1996.

[11] Maiellaro, K. and Taylor, W. R., "The role of the adventitia in vascular inflammation.," *Cardiovascular Research*, vol. 75, pp. 640–8, Sept. 2007.

[12] Holzapfel, G. A. and Weizsäcker, H. W., "Biomechanical behavior of the arterial wall and its numerical characterization.," *Computers in Biology and Medicine*, vol. 28, pp. 377–92, July 1998.

[13] Wootton, D. M. and Ku, D. N., "Fluid Mechanics of Vascular Systems, Diseases, and Thrombosis," *Annual Reviews of Biomedical Engineering*, vol. 1, pp. 299–329, 1999.

[14] Stary, H. C., Chandler, A. B., Dinsmore, R. E., Fuster, V., Glagov, S., Insull, W., Rosenfeld, M. E., Schwartz, C. J., Wagner, W. D., and Wissler, R. W., "A definition of advanced types of atherosclerotic lesions and a histological classification of atherosclerosis. A report from the Committee on Vascular Lesions of the Council on Arteriosclerosis, American Heart Association.," *Arteriosclerosis, Thrombosis, and Vascular Biology*, vol. 15, pp. 1512–31, Sept. 1995.

[15] Virmani, R., Kolodgie, F. D., Burke, A. P., Farb, A., and Schwartz, S. M., "Lessons from sudden coronary death: a comprehensive morphological classification scheme for atherosclerotic lesions.," *Arteriosclerosis, Thrombosis, and Vascular Biology*, vol. 20, no. 5, pp. 1262–75, 2000.

[16] Mertens, A. and Holvoet, P., "Oxidized LDL and HDL: antagonists in atherothrombosis.," *FASEB Journal : Official Publication of the Federation of American Societies for Experimental Biology*, vol. 15, pp. 2073–84, Oct. 2001.

[17] Virmani, R., Burke, A. P., Farb, A., and Kolodgie, F. D., "Pathology of the vulnerable plaque.," *Journal of the American College of Cardiology*, vol. 47, no. 8 Suppl, pp. C13–8, 2006.

[18] Salvayre, R., Auge, N., Benoist, H., and Negre-Salvayre, A., "Oxidized low-density lipoprotein-induced apoptosis.," *Biochimica et Biophysica Acta*, vol. 1585, pp. 213–21, Dec. 2002.

[19] Tabas, I., "Macrophage apoptosis in atherosclerosis: consequences on plaque progression and the role of endoplasmic reticulum stress.," *Antioxidants & Redox Signaling*, vol. 11, pp. 2333–9, Sept. 2009.

[20] Maetzler, W., Stünitz, H., Bendfeldt, K., Vollenweider, F., Schwaller, B., and Nitsch, C., "Microcalcification after excitotoxicity is enhanced in transgenic mice expressing parvalbumin in all neurones, may commence in neuronal mitochondria and undergoes structural modifications over time.," *Neuropathology and Applied Neurobiology*, vol. 35, pp. 165–77, Apr. 2009.

[21] Burke, A. P., Farb, A., Malcom, G. T., Liang, Y. H., Smialek, J., and Virmani, R., "Coronary risk factors and plaque morphology in men with coronary disease who died suddenly.," *The New England Journal of Medicine*, vol. 336, pp. 1276–82, May 1997.

[22] Finet, G., Ohayon, J., and Rioufol, G., "Biomechanical interaction between cap thickness, lipid core composition and blood pressure in vulnerable coronary plaque: impact on stability or instability.," *Coronary Artery Disease*, vol. 15, pp. 13–20, Feb. 2004.

[23] Ohayon, J., Finet, G., Gharib, A. M., Herzka, D. A., Tracqui, P., Heroux, J., Rioufol, G., Kotys, M. S., Elagha, A., and Pettigrew, R. I., "Necrotic core thickness and positive arterial remodeling index: emergent biomechanical factors for evaluating the risk of plaque rupture.," *American Journal of Physiology. Heart and Circulatory Physiology*, vol. 295, pp. H717–27, Aug. 2008.

[24] Davies, M. J. and Thomas, A. C., "Plaque fissuring–the cause of acute myocardial infarction, sudden ischaemic death, and crescendo angina.," *British Heart Journal*, vol. 53, pp. 363–73, Apr. 1985.

[25] Fishbein, M. C., "The vulnerable and unstable atherosclerotic plaque.," *Cardiovascular Pathology : the Official Journal of the Society for Cardiovascular Pathology*, vol. 19, pp. 6–11, Sept. 2008.

[26] Richardson, P. D., "Biomechanics of plaque rupture: progress, problems, and new frontiers.," *Annals of Biomedical Engineering*, vol. 30, pp. 524–36, Apr. 2002.

[27] Shah, P. K., "Inflammation and plaque vulnerability.," *Cardiovascular Drugs and Therapy / sponsored by the International Society of Cardiovascular Pharmacotherapy*, vol. 23, pp. 31–40, Feb. 2009.

[28] Mallat, Z. and Tedgui, A., "Current Perspective on the Role of Apoptosis in Atherothrombotic Disease," *Circulation Research*, vol. 88, pp. 998–1003, May 2001.

[29] Dimmeler, S., Haendeler, J., and Zeiher, A. M., "Regulation of endothelial cell apoptosis in atherothrombosis.," *Current Opinion in Lipidology*, vol. 13, pp. 531–6, Oct. 2002.

[30] Farb, A., Burke, A. P., Tang, A. L., Liang, T. Y., Mannan, P., Smialek, J., and Virmani, R., "Coronary plaque erosion without rupture into a lipid core. A frequent cause of coronary thrombosis in sudden coronary death.," *Circulation*, vol. 93, pp. 1354–63, Apr. 1996.

[31] Arbustini, E., Dal Bello, B., Morbini, P., Burke, A. P., Bocciarelli, M., Specchia, G., and Virmani, R., "Plaque erosion is a major substrate for coronary thrombosis in acute myocardial infarction.," *Heart (British Cardiac Society)*, vol. 82, pp. 269–72, Sept. 1999.

[32] Insull, W., "The pathology of atherosclerosis: plaque development and plaque responses to medical treatment.," *The American Journal of Medicine*, vol. 122, pp. S3–S14, Jan. 2009.

[33] Kramer, M. C. A., Rittersma, S. Z. H., de Winter, R. J., Ladich, E. R., Fowler, D. R., Liang, Y.-H., Kutys, R., Carter-Monroe, N., Kolodgie, F. D., van der Wal, A. C., and Virmani, R., "Relationship of thrombus healing to underlying plaque morphology in sudden coronary death.," *Journal of the American College of Cardiology*, vol. 55, pp. 122–32, Jan. 2010.

[34] van der Wal, A. C., Becker, A. E., van der Loos, C. M., and Das, P. K., "Site of intimal rupture or erosion of thrombosed coronary atherosclerotic plaques is characterized by an inflammatory process irrespective of the dominant plaque morphology.," *Circulation*, vol. 89, pp. 36–44, Jan. 1994.

[35] Wootton, D. M., Markou, C. P., Hanson, S. R., and Ku, D. N., "A Mechanistic Model of Acute Platelet Accumulation in Thrombogenic Stenoses," *Annals of Biomedical Engineering*, vol. 29, pp. 321–329, Apr. 2001.

[36] Kolodgie, F. D., Burke, A. P., Wight, T. N., and Virmani, R., "The accumulation of specific types of proteoglycans in eroded plaques: a role in coronary thrombosis in the absence of rupture.," *Current Opinion in Lipidology*, vol. 15, pp. 575–82, Oct. 2004.

[37] Durand, E., Scoazec, A., Lafont, A., Boddaert, J., Al Hajzen, A., Addad, F., Mirshahi, M., Desnos, M., Tedgui, A., and Mallat, Z., "In vivo induction of endothelial apoptosis leads to vessel thrombosis and endothelial denudation: a clue to the understanding of the mechanisms of thrombotic plaque erosion.," *Circulation*, vol. 109, pp. 2503–6, June 2004.

[38] Sugiyama, S., Kugiyama, K., Aikawa, M., Nakamura, S., Ogawa, H., and Libby, P., "Hypochlorous acid, a macrophage product, induces endothelial apoptosis and tissue factor expression: involvement of myeloperoxidase-mediated oxidant in plaque erosion and thrombogenesis.," *Arteriosclerosis, Thrombosis, and Vascular Biology*, vol. 24, pp. 1309–14, July 2004.

[39] Lindstedt, K. A., Leskinen, M. J., and Kovanen, P. T., "Proteolysis of the pericellular matrix: a novel element determining cell survival and death in the pathogenesis of plaque erosion and rupture.," *Arteriosclerosis, Thrombosis, and Vascular Biology*, vol. 24, pp. 1350–8, Aug. 2004.

[40] Mäyränpää, M. I., Heikkilä, H. M., Lindstedt, K. a., Walls, A. F., and Kovanen, P. T., "Desquamation of human coronary artery endothelium by human mast cell proteases: implications for plaque erosion.," *Coronary Artery Disease*, vol. 17, pp. 611–21, Dec. 2006.

[41] Gertz, S. D., Uretsky, G., Wajnberg, R. S., Navot, N., and Gotsman, M. S., "Endothelial cell damage and thrombus formation after partial arterial constriction: relevance to the role of coronary artery spasm in the pathogenesis of myocardial infarction.," *Circulation*, vol. 63, pp. 476–86, Mar. 1981.

[42] Malek, A. M., Alper, S. L., and Izumo, S., "Hemodynamic shear stress and its role in atherosclerosis.," *JAMA : the Journal of the American Medical Association*, vol. 282, pp. 2035–42, Dec. 1999.

[43] Shah, P. K., "Mechanisms of plaque vulnerability and rupture.," *Journal of the American College of Cardiology*, vol. 41, no. 4 Suppl S, pp. 15S–22S, 2003.

[44] Glagov, S., Weisenberg, E., Zarins, C. K., Stankunavicius, R., and Kolettis, G. J., "Compensatory enlargement of human atherosclerotic coronary arteries.," *The New England Journal of Medicine*, vol. 316, no. 22, pp. 1371–5, 1987.

[45] Birchall, D., Zaman, A., Hacker, J., Davies, G., and Mendelow, D., "Analysis of haemodynamic disturbance in the atherosclerotic carotid artery using computational fluid dynamics.," *European Radiology*, vol. 16, pp. 1074–83, May 2006.

[46] Bale-Glickman, J., Selby, K., Saloner, D., and SavaÅ, O., "Experimental flow studies in exact-replica phantoms of atherosclerotic carotid bifurcations under steady input conditions.," *Journal of Biomechanical Engineering*, vol. 125, pp. 38–48, Feb. 2003.

[47] Para, A., Bark, D., Lin, A., and Ku, D., "Rapid platelet accumulation leading to thrombotic occlusion.," *Annals of Biomedical Engineering*, vol. 39, pp. 1961–71, July 2011.

[48] Li, M. X., Beech-Brandt, J. J., John, L. R., Hoskins, P. R., and Easson, W. J., "Numerical analysis of pulsatile blood flow and vessel wall mechanics in different degrees of stenoses.," *Journal of Biomechanics*, vol. 40, pp. 3715–24, Jan. 2007.

[49] Yim, P., Demarco, K., Castro, M. A., and Cebral, J., "Characterization of shear stress on the wall of the carotid artery using magnetic resonance imaging and computational fluid dynamics.," *Studies in Health Technology and Informatics*, vol. 113, pp. 412–42, Jan. 2005.

[50] Gilard, M., Rioufol, G., Zeller, M., Cottin, Y., Rochette, L., and Finet, G., "Reliability and limitations of angiography in the diagnosis of coronary plaque rupture: an intravascular ultrasound study.," *Archives of Cardiovascular Diseases*, vol. 101, pp. 114–20, Feb. 2008.

[51] Goubergrits, L., Wellnhofer, E., Kertzscher, U., Affeld, K., Petz, C., and Hege, H.-C., "Coronary artery WSS profiling using a geometry reconstruction based on biplane angiography.," *Annals of Biomedical Engineering*, vol. 37, pp. 682–91, Apr. 2009.

[52] Chatzizisis, Y. S., Coskun, A. U., Jonas, M., Edelman, E. R., Feldman, C. L., and Stone, P. H., "Role of endothelial shear stress in the natural history of coronary atherosclerosis and vascular remodeling: molecular, cellular, and vascular behavior.," *Journal of the American College of Cardiology*, vol. 49, pp. 2379–93, June 2007.

[53] Waxman, S., Dixon, S. R., L'Allier, P., Moses, J. W., Petersen, J. L., Cutlip, D., Tardif, J.-C., Nesto, R. W., Muller, J. E., Hendricks, M. J., Sum, S. T., Gardner, C. M., Goldstein, J. a., Stone, G. W., and Krucoff, M. W., "In vivo validation of a catheter-based near-infrared spectroscopy system for detection of lipid core coronary plaques: initial results of the SPECTACL study.," *JACC. Cardiovascular imaging*, vol. 2, pp. 858–68, July 2009.

[54] Maehara, A., Mintz, G. S., and Weissman, N. J., "Advances in intravascular imaging.," *Circulation. Cardiovascular interventions*, vol. 2, pp. 482–90, Oct. 2009.

[55] Feldman, C. L. and Stone, P. H., "Intravascular hemodynamic factors responsible for progression of coronary atherosclerosis and development of vulnerable plaque.," *Current Opinion in Cardiology*, vol. 15, pp. 430–40, Nov. 2000.

[56] Hallow, K. M., Taylor, W. R., Rachev, A., and Vito, R. P., "Markers of inflammation collocate with increased wall stress in human coronary arterial plaque.," *Biomechanics and Modeling in Mechanobiology*, Mar. 2009.

[57] Hallow, K. M., *Spatial Relationships Between Mechanical Stress and Markers of Inflammation in Diseased Human Coronary Arteries*. PhD thesis, Georgia Institute of Technology, 2007.

[58] Blythe, D., Hand, N. M., Jackson, P., Barrans, S. L., Bradbury, R. D., and Jack, A. S., "Use of methyl methacrylate resin for embedding bone marrow trephine biopsy specimens.," *Journal of Clinical Pathology*, vol. 50, pp. 45–9, Jan. 1997.

[59] Suri, J. S., Pattichis, C. S., Li, C., Macione, J., Yang, Z., Fox, M. D., Wu, D., and Laxminarayan, S., "Plaque imaging using ultrasound, magnetic resonance and computer tomography: a review.," *Studies in Health Technology and Informatics*, vol. 113, pp. 1–25, Jan. 2005.

[60] Clément-Guinaudeau, S. and Oshinski, J. N., "Cardiovascular Magnetic Resonance Imaging for the Biomedical Engineer," *Cardiovascular Engineering and Technology*, vol. 2, pp. 309–323, Oct. 2011.

[61] Ota, H., Yu, W., Underhill, H. R., Oikawa, M., Dong, L., Zhao, X., Polissar, N. L., Neradilek, B., Gao, T., Zhang, Z., Yan, Z., Guo, M., Zhang, Z., Hatsukami, T. S., and Yuan, C., "Hemorrhage and large lipid-rich necrotic cores are independently associated with thin or ruptured fibrous caps: an in vivo 3T MRI study.," *Arteriosclerosis, Thrombosis, and Vascular Biology*, vol. 29, pp. 1696–701, Oct. 2009.

[62] Li, Z.-Y., Howarth, S., Trivedi, R. A., U-King-Im, J. M., Graves, M. J., Brown, A., Wang, L., and Gillard, J. H., "Stress analysis of carotid plaque rupture based on in vivo high resolution MRI.," *Journal of Biomechanics*, vol. 39, pp. 2611–22, Jan. 2006.

[63] Ciesienski, K. L. and Caravan, P., "Molecular MRI of Thrombosis.," *Current Cardiovascular Imaging Reports*, vol. 4, pp. 77–84, Jan. 2010.

[64] Wake, A. K., Oshinski, J. N., Tannenbaum, A. R., and Giddens, D. P., "Choice of in vivo versus idealized velocity boundary conditions influences physiologically relevant flow patterns in a subject-specific simulation of flow in the human carotid bifurcation.," *Journal of Biomechanical Engineering*, vol. 131, p. 021013, Feb. 2009.

[65] van Ree, J. H., van den Broek, W. J., Dahlmans, V. E., Groot, P. H., Vidgeon-Hart, M., Frants, R. R., Wieringa, B., Havekes, L. M., and Hofker, M. H., "Diet-induced hypercholesterolemia and atherosclerosis in heterozygous apolipoprotein E-deficient mice.," *Atherosclerosis*, vol. 111, pp. 25–37, Nov. 1994.

[66] Zadelaar, S., Kleemann, R., Verschuren, L., de Vries-Van der Weij, J., van der Hoorn, J., Princen, H. M., and Kooistra, T., "Mouse models for atherosclerosis and pharmaceutical modifiers.," *Arteriosclerosis, Thrombosis, and Vascular Biology*, vol. 27, no. 8, pp. 1706–21, 2007.

[67] Russell, J. C. and Proctor, S. D., "Small animal models of cardiovascular disease: tools for the study of the roles of metabolic syndrome, dyslipidemia, and atherosclerosis.," *Cardiovascular Pathology : the Official Journal of the Society for Cardiovascular Pathology*, vol. 15, no. 6, pp. 318–30, 2006.

[68] Ni, M., Chen, W. Q., and Zhang, Y., "Animal models and potential mechanisms of plaque destabilisation and disruption.," *Heart (British Cardiac Society)*, vol. 95, pp. 1393–8, Sept. 2009.

[69] Weiss, D., Kools, J. J., and Taylor, W. R., "Angiotensin II-induced hypertension accelerates the development of atherosclerosis in apoE-deficient mice.," *Circulation*, vol. 103, pp. 448–54, Jan. 2001.

[70] Daugherty, A., Manning, M. W., and Cassis, L. a., "Angiotensin II promotes atherosclerotic lesions and aneurysms in apolipoprotein E-deficient mice.," *The Journal of Clinical Investigation*, vol. 105, pp. 1605–12, June 2000.

[71] Cheng, C., Tempel, D., van Haperen, R., van Der Baan, A., Grosveld, F., Daemen, M. J. A. P., Krams, R., and de Crom, R., "Atherosclerotic lesion size and vulnerability are determined by patterns of fluid shear stress.," *Circulation*, vol. 113, no. 23, pp. 2744–53, 2006.

[72] Willett, N. J., Long, R. C., Maiellaro-Rafferty, K., Sutliff, R. L., Shafer, R., Oshinski, J. N., Giddens, D. P., Guldberg, R. E., and Taylor, W. R., "An in vivo murine model of low-magnitude oscillatory wall shear stress to address the molecular mechanisms of mechanotransduction–brief report.," *Arteriosclerosis, Thrombosis, and Vascular Biology*, vol. 30, pp. 2099–102, Nov. 2010.

[73] Bentzon, J. F. and Falk, E., "Atherosclerotic lesions in mouse and man: is it the same disease?," *Current Opinion in Lipidology*, vol. 21, pp. 434–40, Oct. 2010.

[74] Jackson, C. L., "Ruptures of delight? A new mouse model of plaque rupture.," *Arteriosclerosis, Thrombosis, and Vascular Biology*, vol. 26, pp. 1191–2, June 2006.

[75] Rosenfeld, M. E., Averill, M. M., Bennett, B. J., and Schwartz, S. M., "Progression and disruption of advanced atherosclerotic plaques in murine models.," *Current Drug Targets*, vol. 9, pp. 210–6, Mar. 2008.

[76] Falk, E., Schwartz, S. M., Galis, Z. S., and Rosenfeld, M. E., "Putative murine models of plaque rupture.," *Arteriosclerosis, Thrombosis, and Vascular Biology*, vol. 27, pp. 969–72, Apr. 2007.

[77] Bond, A. R. and Jackson, C. L., "The fat-fed apolipoprotein E knockout mouse brachiocephalic artery in the study of atherosclerotic plaque rupture.," *Journal of Biomedicine & Biotechnology*, vol. 2011, p. 379069, Jan. 2011.

[78] Ku, D. N. and Giddens, D. P., "Pulsatile flow in a model carotid bifurcation.," *Arteriosclerosis (Dallas, Tex.)*, vol. 3, no. 1, pp. 31–9, 1983.

[79] DeBakey, M. E., Lawrie, G. M., and Glaeser, D. H., "Patterns of atherosclerosis and their surgical significance.," *Annals of Surgery*, vol. 201, pp. 115–31, Mar. 1985.

[80] Abad, C., Santana, C., Diaz, J., and Feijoo, J., "Arteriosclerotic histologic evaluation of the internal mammary artery in patients undergoing coronary artery bypass grafting.," *European Journal of Cardio-thoracic Surgery : official journal of the European Association for Cardiothoracic Surgery*, vol. 9, pp. 198–201, Jan. 1995.

[81] Ku, D. N., Giddens, D. P., Zarins, C. K., and Glagov, S., "Pulsatile flow and atherosclerosis in the human carotid bifurcation. Positive correlation between plaque location and low oscillating shear stress.," *Arteriosclerosis (Dallas, Tex.)*, vol. 5, no. 3, pp. 293–302, 1985.

[82] Friedman, M. H., Brinkman, a. M., Qin, J. J., and Seed, W. a., "Relation between coronary artery geometry and the distribution of early sudanophilic lesions.," *Atherosclerosis*, vol. 98, pp. 193–9, Jan. 1993.

[83] Traub, O. and Berk, B. C., "Laminar shear stress: mechanisms by which endothelial cells transduce an atheroprotective force.," *Arteriosclerosis, Thrombosis, and Vascular Biology*, vol. 18, no. 5, pp. 677–85, 1998.

[84] Slager, C. J., Wentzel, J. J., Gijsen, F. J. H., Schuurbiers, J. C. H., van Der Wal, A. C., van Der Steen, A. F. W., and Serruys, P. W., "The role of shear stress in the generation of rupture-prone vulnerable plaques.," *Nature Clinical Practice. Cardiovascular Medicine*, vol. 2, pp. 401–7, Aug. 2005.

[85] Li, Z.-Y., Howarth, S. P. S., Tang, T., and Gillard, J. H., "How critical is fibrous cap thickness to carotid plaque stability? A flow-plaque interaction model.," *Stroke; a Journal of Cerebral Circulation*, vol. 37, pp. 1195–9, May 2006.

[86] Tricot, O., Mallat, Z., Heymes, C., Belmin, J., Lesèche, G., and Tedgui, A., "Relation between endothelial cell apoptosis and blood flow direction in human atherosclerotic plaques.," *Circulation*, vol. 101, pp. 2450–3, May 2000.

[87] Taylor, C. a., Hughes, T. J., and Zarins, C. K., "Finite element modeling of three-dimensional pulsatile flow in the abdominal aorta: relevance to atherosclerosis.," *Annals of Biomedical Engineering*, vol. 26, no. 6, pp. 975–87, 1998.

[88] Moore, J. A., Steinman, D. A., Prakash, S., Johnston, K. W., and Ethier, C. R., "A numerical study of blood flow patterns in anatomically realistic and simplified end-to-side anastomoses.," *Journal of Biomechanical Engineering*, vol. 121, no. 3, pp. 265–72, 1999.

[89] Moore, J. A., Steinman, D. a., Holdsworth, D. W., and Ethier, C. R., "Accuracy of computational hemodynamics in complex arterial geometries reconstructed from magnetic resonance imaging.," *Annals of Biomedical Engineering*, vol. 27, no. 1, pp. 32–41, 1999.

[90] Holliday, C. J., Ankeny, R. F., Jo, H., and Nerem, R. M., "Discovery of shear- and side-specific mRNAs and miRNAs in human aortic valvular endothelial cells.," *American Journal of Physiology. Heart and Circulatory Physiology*, vol. 301, pp. H856–67, Sept. 2011.

[91] Moyle, K. R., Antiga, L., and Steinman, D. A., "Inlet conditions for image-based CFD models of the carotid bifurcation: is it reasonable to assume fully developed flow?," *Journal of Biomechanical Engineering*, vol. 128, pp. 371–9, June 2006.

[92] Lee, S.-W., Antiga, L., and Steinman, D. a., "Correlations among indicators of disturbed flow at the normal carotid bifurcation.," *Journal of Biomechanical Engineering*, vol. 131, p. 061013, June 2009.

[93] Panton, R. L., *Incompressible Flow*. Wiley, 3 ed., 2005.

[94] Lee, S.-W. and Steinman, D. A., "On the relative importance of rheology for image-based CFD models of the carotid bifurcation.," *Journal of Biomechanical Engineering*, vol. 129, pp. 273–8, Apr. 2007.

[95] Sutera, S. P. and Skalak, R., "The History of Poiseuille's Law," *Annual Review of Fluid Mechanics*, vol. 25, pp. 1–20, Jan. 1993.

[96] Womersley, J., "Method for the Calculation of Velocity, Rate of Flow and Viscous Drag in Arteries when the Pressure Gradient is Known," *Journal of Physiology*, vol. 127, no. 3, pp. 553–563, 1955.

[97] Campbell, I. C., Ries, J., Dhawan, S. S., Quyyumi, A. a., Taylor, W. R., and Oshinski, J. N., "Effect of inlet velocity profiles on patient-specific computational fluid dynamics simulations of the carotid bifurcation.," *Journal of Biomechanical Engineering*, vol. 134, p. 051001, May 2012.

[98] Groen, H. C., Gijsen, F. J. H., van der Lugt, A., Ferguson, M. S., Hatsukami, T. S., van Der Steen, A. F. W., Yuan, C., and Wentzel, J. J., "Plaque rupture in the carotid artery is localized at the high shear stress region: a case report.," *Stroke; a Journal of Cerebral Circulation*, vol. 38, pp. 2379–81, Aug. 2007.

[99] Fukumoto, Y., Hiro, T., Fujii, T., Hashimoto, G., Fujimura, T., Yamada, J., Okamura, T., and Matsuzaki, M., "Localized elevation of shear stress is related to coronary plaque rupture: a 3-dimensional intravascular ultrasound study with in-vivo color mapping of shear stress distribution.," *Journal of the American College of Cardiology*, vol. 51, pp. 645–50, Feb. 2008.

[100] Beattie, D., Xu, C., Vito, R., Glagov, S., and Whang, M. C., "Mechanical analysis of heterogeneous, atherosclerotic human aorta.," *Journal of Biomechanical Engineering*, vol. 120, pp. 602–7, Oct. 1998.

[101] Humphrey, J. D. and Rajagopal, K. R., "A constrained mixture model for growth and remodeling of soft tissues," *Mathematical Models and Methods in Applied Sciences*, vol. 12, no. 3, pp. 407–430, 2002.

[102] Holzapfel, G. A., Sommer, G., Gasser, C. T., and Regitnig, P., "Determination of layer-specific mechanical properties of human coronary arteries with nonatherosclerotic intimal thickening and related constitutive modeling.," *American Journal of Physiology. Heart and Circulatory Physiology*, vol. 289, pp. H2048–58, Nov. 2005.

[103] Baek, S., Gleason, R., Rajagopal, K., and Humphrey, J., "Theory of small on large: Potential utility in computations of fluidsolid interactions in arteries," *Computer Methods in Applied Mechanics and Engineering*, vol. 196, pp. 3070–3078, June 2007.

[104] Fung, Y., *Biomechanics: Mechanical Properties of Living Tissues*. Secaucus, NJ: Springer-Verlag, 2 ed., 1993.

[105] Cheng, G. C., Loree, H. M., Kamm, R. D., Fishbein, M. C., and Lee, R. T., "Distribution of circumferential stress in ruptured and stable atherosclerotic lesions. A structural analysis with histopathological correlation.," *Circulation*, vol. 87, pp. 1179–87, Apr. 1993.

[106] Arroyo, L. H. and Lee, R. T., "Mechanisms of plaque rupture: mechanical and biologic interactions.," *Cardiovascular Research*, vol. 41, pp. 369–75, Feb. 1999.

[107] Versluis, A., Bank, A. J., and Douglas, W. H., "Fatigue and plaque rupture in myocardial infarction.," *Journal of Biomechanics*, vol. 39, pp. 339–47, Jan. 2006.

[108] Varnava, A. M., Mills, P. G., and Davies, M. J., "Relationship between coronary artery remodeling and plaque vulnerability.," *Circulation*, vol. 105, pp. 939–43, Feb. 2002.

[109] Huang, H., Virmani, R., Younis, H., Burke, A. P., Kamm, R. D., and Lee, R. T., "The impact of calcification on the biomechanical stability of atherosclerotic plaques.," *Circulation*, vol. 103, pp. 1051–6, Mar. 2001.

[110] Loree, H. M., Kamm, R. D., Stringfellow, R. G., and Lee, R. T., "Effects of fibrous cap thickness on peak circumferential stress in model atherosclerotic vessels.," *Circulation Research*, vol. 71, pp. 850–8, Oct. 1992.

[111] Kilpatrick, D., Goudet, C., Sakaguchi, Y., Bassiouny, H. S., Glagov, S., and Vito, R., "Effect of plaque composition on fibrous cap stress in carotid endarterectomy specimens.," *Journal of Biomechanical Engineering*, vol. 123, pp. 635–8, Dec. 2001.

[112] Williamson, S. D., Lam, Y., Younis, H. F., Huang, H., Patel, S., Kaazempur-Mofrad, M. R., and Kamm, R. D., "On the sensitivity of wall stresses in diseased arteries to variable material properties.," *Journal of Biomechanical Engineering*, vol. 125, pp. 147–55, Feb. 2003.

[113] Vengrenyuk, Y., Carlier, S., Xanthos, S., Cardoso, L., Ganatos, P., Virmani, R., Einav, S., Gilchrist, L., and Weinbaum, S., "A hypothesis for vulnerable plaque rupture due to stress-induced debonding around cellular microcalcifications in thin fibrous caps.," *Proceedings of the National Academy of Sciences of the United States of America*, vol. 103, pp. 14678–83, Oct. 2006.

[114] Maldonado, N., Kelly-Arnold, A., Vengrenyuk, Y., Laudier, D., Fallon, J. T., Virmani, R., Cardoso, L., and Weinbaum, S., "A mechanistic analysis of the role of microcalcifications in atherosclerotic plaque stability: potential implications for plaque rupture.," *American Journal of Physiology. Heart and Circulatory Physiology*, vol. 303, pp. H619–28, Sept. 2012.

[115] Bäck, M., Ketelhuth, D. F. J., and Agewall, S., "Matrix metalloproteinases in atherothrombosis.," *Progress in Cardiovascular Diseases*, vol. 52, no. 5, pp. 410–28, 2010.

[116] Johnson, J. L., "Matrix metalloproteinases: influence on smooth muscle cells and atherosclerotic plaque stability.," *Expert Review of Cardiovascular Therapy*, vol. 5, pp. 265–82, Mar. 2007.

[117] Lehoux, S., Castier, Y., and Tedgui, A., "Molecular mechanisms of the vascular responses to haemodynamic forces.," *Journal of Internal Medicine*, vol. 259, pp. 381–92, Apr. 2006.

[118] Weiss, D., Sorescu, D., and Taylor, W. R., "Angiotensin II and atherosclerosis.," *The American Journal of Cardiology*, vol. 87, pp. 25C–32C, Apr. 2001.

[119] Rosenfeld, M. E., Polinsky, P., Virmani, R., Kauser, K., Rubanyi, G., and Schwartz, S. M., "Advanced atherosclerotic lesions in the innominate artery of the ApoE knockout mouse.," *Arteriosclerosis, Thrombosis, and Vascular Biology*, vol. 20, pp. 2587–92, Dec. 2000.

[120] Jin, S.-x., Shen, L.-h., Nie, P., Yuan, W., Hu, L.-h., Li, D.-d., Chen, X.-j., Zhang, X.-k., and He, B., "Endogenous renovascular hypertension combined with low shear stress induces plaque rupture in apolipoprotein E-deficient mice.," *Arteriosclerosis, Thrombosis, and Vascular Biology*, vol. 32, pp. 2372–9, Oct. 2012.

[121] Jawien, J., "The role of an experimental model of atherosclerosis: apoE-knockout mice in developing new drugs against atherogenesis.," *Current Pharmaceutical Biotechnology*, Jan. 2012.

[122] Calara, F., Silvestre, M., Casanada, F., Yuan, N., Napoli, C., and Palinski, W., "Spontaneous plaque rupture and secondary thrombosis in apolipoprotein E-deficient and LDL receptor-deficient mice.," *The Journal of Pathology*, vol. 195, pp. 257–63, Sept. 2001.

[123] Sasaki, T., Kuzuya, M., Nakamura, K., Cheng, X. W., Shibata, T., Sato, K., and Iguchi, A., "A simple method of plaque rupture induction in apolipoprotein E-deficient mice.," *Arteriosclerosis, Thrombosis, and Vascular Biology*, vol. 26, no. 6, pp. 1304–9, 2006.

[124] Shoelson, B., "clusterImg," 2006.

[125] Chodorowski, A., Mattsson, U., Langille, M., and Hamarneh, G., "Color Lesion Boundary Detection Using Live Wire," in *Proceedings of SPIE Medical Imaging: Image Processing, vol. 5747*, pp. 1589–1596, 2005.

[126] Yezzi, A. J. and Prince, J. L., "An Eulerian PDE approach for computing tissue thickness.," *IEEE Transactions on Medical Imaging*, vol. 22, pp. 1332–9, Oct. 2003.

[127] Saraff, K., Babamusta, F., Cassis, L. a., and Daugherty, A., "Aortic dissection precedes formation of aneurysms and atherosclerosis in angiotensin II-infused, apolipoprotein E-deficient mice.," *Arteriosclerosis, Thrombosis, and Vascular Biology*, vol. 23, pp. 1621–6, Sept. 2003.

[128] Suo, J., Ferrara, D. E., Sorescu, D., Guldberg, R. E., Taylor, W. R., and Giddens, D. P., "Hemodynamic shear stresses in mouse aortas: implications for atherogenesis.," *Arteriosclerosis, Thrombosis, and Vascular Biology*, vol. 27, pp. 346–51, Feb. 2007.

[129] Johnson, J., Carson, K., Williams, H., Karanam, S., Newby, A., Angelini, G., George, S., and Jackson, C., "Plaque rupture after short periods of fat feeding in the apolipoprotein E-knockout mouse: model characterization and effects of pravastatin treatment.," *Circulation*, vol. 111, pp. 1422–30, Mar. 2005.

[130] Broisat, A., Toczek, J., Mesnier, N., Tracqui, P., Ghezzi, C., Ohayon, J., and Riou, L. M., "Assessing low levels of mechanical stress in aortic atherosclerotic lesions from apolipoprotein E-/- mice–brief report.," *Arteriosclerosis, Thrombosis, and Vascular Biology*, vol. 31, pp. 1007–10, May 2011.

[131] Vengrenyuk, Y., Kaplan, T. J., Cardoso, L., Randolph, G. J., and Weinbaum, S., "Computational Stress Analysis of Atherosclerotic Plaques in ApoE Knockout Mice.," *Annals of Biomedical Engineering*, vol. 38, pp. 738–747, Jan. 2010.

[132] Ohayon, J., Mesnier, N., Broisat, A., Toczek, J., Riou, L., and Tracqui, P., "Elucidating atherosclerotic vulnerable plaque rupture by modeling cross substitution of ApoE-/- mouse and human plaque components stiffnesses.," *Biomechanics and Modeling in Mechanobiology*, vol. 11, pp. 801–13, July 2012.

[133] Tracqui, P., Broisat, A., Toczek, J., Mesnier, N., Ohayon, J., and Riou, L., "Mapping elasticity moduli of atherosclerotic plaque in situ via atomic force microscopy.," *Journal of Structural Biology*, vol. 174, pp. 115–23, Apr. 2011.

[134] Hayenga, H. N., Trache, a., Trzeciakowski, J., and Humphrey, J. D., "Regional atherosclerotic plaque properties in ApoE-/- mice quantified by atomic force, immunofluorescence, and light microscopy.," *Journal of Vascular Research*, vol. 48, pp. 495–504, Jan. 2011.

[135] Sumi, T., Yamashita, A., Matsuda, S., Goto, S., Nishihira, K., Furukoji, E., Sugimura, H., Kawahara, H., Imamura, T., Kitamura, K., Tamura, S., and Asada, Y., "Disturbed blood flow induces erosive injury to smooth muscle cell-rich neointima and promotes thrombus formation in rabbit femoral arteries.," *Journal of Thrombosis and Haemostasis : JTH*, vol. 8, pp. 1394–402, June 2010.

[136] Farb, A., Tang, A. L., Burke, A. P., Sessums, L., Liang, Y., and Virmani, R., "Sudden coronary death. Frequency of active coronary lesions, inactive coronary lesions, and myocardial infarction.," *Circulation*, vol. 92, pp. 1701–9, Oct. 1995.

[137] Timmins, L. H., Suever, J. D., Eshtehardi, P., McDaniel, M. C., Samady, H., Oshinski, J. N., and Giddens, D. P., "Correlation of Longitudinal Intravascular Ultrasound Data for the Clinical Assessment of Coronary Artery Disease Progression," in *ASME Summer Bioengineering Conference*, (Fajardo, Puerto Rico), ASME, 2012.

[138] Ridker, P. M., "Testing the inflammatory hypothesis of atherothrombosis: scientific rationale for the cardiovascular inflammation reduction trial (CIRT).," *Journal of Thrombosis and Haemostasis : JTH*, vol. 7 Suppl 1, pp. 332–9, July 2009.

[139] Ridker, P. M., Thuren, T., Zalewski, A., and Libby, P., "Interleukin-1$\beta$ inhibition and the prevention of recurrent cardiovascular events: rationale and design of the Canakinumab Anti-inflammatory Thrombosis Outcomes Study (CANTOS).," *American Heart Journal*, vol. 162, pp. 597–605, Oct. 2011.

[140] Ridker, P. M., MacFadyen, J., Cressman, M., and Glynn, R. J., "Efficacy of rosuvastatin among men and women with moderate chronic kidney disease and elevated high-sensitivity C-reactive protein: a secondary analysis from the JUPITER (Justification for the Use of Statins in Prevention-an Intervention Trial Evaluating ," *Journal of the American College of Cardiology*, vol. 55, pp. 1266–73, Mar. 2010.

[141] Rosenson, R. S., Hislop, C., Elliott, M., Stasiv, Y., Goulder, M., and Waters, D., "Effects of varespladib methyl on biomarkers and major cardiovascular events in acute coronary syndrome patients.," *Journal of the American College of Cardiology*, vol. 56, pp. 1079–88, Sept. 2010.

[142] Weber, M., Bhatt, D. L., Brennan, D. M., Hankey, G. J., Steinhubl, S. R., Johnston, S. C., Montalescot, G., Mak, K.-H., Fox, K. a. a., Easton, D. J., Topol, E. J., and Hamm, C. W., "High-sensitivity C-reactive protein and clopidogrel treatment in patients at high risk of cardiovascular events: a substudy from the CHARISMA trial.," *Heart (British Cardiac Society)*, vol. 97, pp. 626–31, Apr. 2011.

[143] Mäyränpää, M. I., Reséndiz, J. C., Heikkilä, H. M., Lindstedt, K. a., and Kovanen, P. T., "Improved identification of endothelial erosion by simultaneous detection of endothelial cells (CD31/CD34) and platelets (CD42b).," *Endothelium : Journal of Endothelial Cell Research*, vol. 14, no. 2, pp. 81–7, 2007.

[144] Lee, R. T., "Atherosclerotic lesion mechanics versus biology.," *Zeitschrift für Kardiologie*, vol. 89 Suppl 2, pp. 80–4, Jan. 2000.

[145] McDaniel, M. C., Galbraith, E. M., Jeroudi, A. M., Kashlan, O. R., Eshtehardi, P., Suo, J., Dhawan, S., Voeltz, M., Devireddy, C., Oshinski, J., Harrison, D. G., Giddens, D. P., and Samady, H., "Localization of culprit lesions in coronary arteries of patients with ST-segment elevation myocardial infarctions: relation to bifurcations and curvatures.," *American Heart Journal*, vol. 161, pp. 508–15, Mar. 2011.

[146] Fry, D. L., "Acute vascular endothelial changes associated with increased blood velocity gradients.," *Circulation Research*, vol. 22, pp. 165–97, Feb. 1968.

[147] Knot, H. J., Lounsbury, K. M., Brayden, J. E., and Nelson, M. T., "Gender differences in coronary artery diameter reflect changes in both endothelial Ca2+ and ecNOS activity.," *The American Journal of Physiology*, vol. 276, pp. H961–9, Mar. 1999.

[148] Yang, F., Minutello, R. M., Bhagan, S., Sharma, A., and Wong, S. C., "The impact of gender on vessel size in patients with angiographically normal coronary arteries.," *Journal of Interventional Cardiology*, vol. 19, pp. 340–4, Aug. 2006.

[149] Yoshizumi, M., Abe, J.-I., Tsuchiya, K., Berk, B. C., and Tamaki, T., "Stress and vascular responses: atheroprotective effect of laminar fluid shear stress in endothelial cells: possible role of mitogen-activated protein kinases.," *Journal of Pharmacological Sciences*, vol. 91, pp. 172–6, Mar. 2003.

[150] Brooks, A. R., Lelkes, P. I., and Rubanyi, G. M., "Gene expression profiling of vascular endothelial cells exposed to fluid mechanical forces: relevance for focal susceptibility to atherosclerosis.," *Endothelium : Journal of Endothelial Cell Research*, vol. 11, no. 1, pp. 45–57, 2004.

[151] McCord, B. N., *Fatigue of Atherosclerotic Plaque*. PhD thesis, Georgia Institute of Technology, 1992.

[152] Timmins, L. H., Suo, J., Eshtehardi, P., Dhawan, S. S., McDaniel, M. C., Oshinski, J. N., Samady, H., and Giddens, D. P., "Geometric and Hemodynamic Evaluation of 3-Dimensional Reconstruction Techniques for the Assessment of Coronary Artery Wall Shear Stress in the Setting of Clinical Disease Progression," in *ASME Summer Bioengineering Conference*, (Farmington, PA), ASME, 2011.

[153] Baldewsing, R. a., Danilouchkine, M. G., Mastik, F., Schaar, J. a., Serruys, P. W., and van der Steen, A. F. W., "An inverse method for imaging the local elasticity of atherosclerotic coronary plaques.," *IEEE Transactions on Information Technology in Biomedicine : a Publication of the IEEE Engineering in Medicine and Biology Society*, vol. 12, pp. 277–89, May 2008.

[154] Le Floc'h, S., Ohayon, J., Tracqui, P., Finet, G., Gharib, A. M., Maurice, R. L., Cloutier, G., and Pettigrew, R. I., "Vulnerable atherosclerotic plaque elasticity reconstruction based on a segmentation-driven optimization procedure using strain measurements: theoretical framework.," *IEEE Transactions on Medical Imaging*, vol. 28, pp. 1126–37, July 2009.

[155] Kim, Y.-H., Kim, J.-E., Ito, Y., Shih, A. M., Brott, B., and Anayiotos, A., "Hemodynamic analysis of a compliant femoral artery bifurcation model using a fluid structure interaction framework.," *Annals of Biomedical Engineering*, vol. 36, pp. 1753–63, Nov. 2008.

[156] Carnell, P. H., Vito, R. P., and Taylor, W. R., "Characterizing intramural stress and inflammation in hypertensive arterial bifurcations.," *Biomechanics and Modeling in Mechanobiology*, vol. 6, pp. 409–21, Nov. 2007.